NC STATE UNIVERSITY

CENTER
FOR
TRANSPORTATION
ENGINEERING
STUDIES

BOUNDARY CONDITIONS FOR BRIDGE SCOUR ANALYSIS

by

Margery F. Overton
Roger R. Grenier, Jr.
John S. Fisher

DEPARTMENT OF CIVIL ENGINEERING

BOUNDARY CONDITIONS FOR BRIDGE SCOUR ANALYSIS

by

Margery F. Overton
Roger R. Grenier, Jr.
John S. Fisher

March 1999

BOUNDARY CONDITIONS FOR BRIDGE SCOUR ANALYSIS

by

Margery F. Overton
Roger R. Grenier, Jr.
John S. Fisher

Research Project No. 23241-97-6

FINAL REPORT

in cooperation with

North Carolina Department of Transportation

CENTER FOR TRANSPORTATION ENGINEERING STUDIES

Department of Civil Engineering
North Carolina State University

March 1999

Technical Report Documentation Page

1. Report No.	2. Government Accession No.	3. Recipient's Catalog No.
FHWA/NC/98-002		

4. Title and Subtitle	5. Report Date
Boundary Conditions for Bridge Scour Analysis	March 1999
	6. Performing Organization Code
	8. Performing Organization Report No.
7. Author(s) Margery F. Overton, Roger R. Grenier, Jr., John S. Fisher	
9. Performing Organization Name and Address Center for Transportation Engineering Studies Department of Civil Engineering North Carolina State University Raleigh, NC 27695	10. Work Unit No. (TRAIS)
	11. Contract or Grant No. 23241-97-6
	13. Type of Report and Period Covered Final Report 7/1/96 - 6/30/98
12. Sponsoring Agency Name and Address North Carolina Department of Transportation P.O. Box 25201 Raleigh, NC 27611	14. Sponsoring Agency Code

15. Supplementary Notes

16. Abstract

The purpose of this study is to determine surge hydrographs which may be used in the analysis of proposed and existing highway structures along Albemarle-Pamlico Sounds. Historical data for tropical storms over the period 1886-1996 were collected and analyzed to identify storms proximate to the project study area. Application of the process models (CE Wind Model and ADCIRC Model) and statistical models (EST) resulted in predicted surge values at 25, 50 and 100 year return periods. These peaks were then incorporated into synthetic time series used to characterize the shape of the design hydrograph. The results of the surge modeling suggest that the simple exponential form of the hydrograph, recommended by the FHWA pooled fund study "Development of Hydraulic Computer Models to Analyze Tidal and Coastal Stream Hydraulic Conditions and Highway Structures", may be inadequate to characterize stations which experience periods of negative surge. An empirical approach based on a damped sine wave was developed as an alternative. The recommended procedure for implementing the results of the study suggests that both types of hydrographs be modeled, with design parameters based on the worst-case conditions.

17. Key Words	18. Distribution Statement
Storm surge hydrographs, Albemarle-Pamlico Sound, Empirical Simulation Technique, numerical surge model, ADCIRC, design hydrographs	No restrictions 125 copies of this document were printed at a cost of $2.10 per copy

19. Security Classif. (of this report)	20. Security Classif. (of this page)	21. No. of Pages	22. Price
Unclassified	Unclassified	70	

Form DOT F 1700.7 (8-72) Reproduction of completed page authorized

The contents of this report reflect the views of the authors who are responsible for the facts and the accuracy of the data presented herein. The contents do not necessarily reflect the official views or policies of the North Carolina Department of Transportation or the Federal Highway Administration. This report does not constitute a standard, specification or regulation.

TABLE OF CONTENTS

ABSTRACT

The purpose of this study is to determine surge hydrographs which may be used in the analysis of proposed and existing highway structures along Albemarle-Pamlico Sounds. The surge hydrographs were developed at multiple locations within the Sounds and are based on model simulations and statistical analysis of historical storm events.

Historical data for tropical storms over the period 1886-1996 were collected and analyzed to identify storms proximate to the project study area. A review of these data identified 87 storms, from which 36 storms were selected for model simulations. A statistical analysis of the selected storms suggests that the selected database, though quite similar to the original data, focuses on the strongest events which are closest in proximity and track to the Albemarle-Pamlico study area. The selected database of 36 historical events was augmented by including 3 hypothetical events which are considered meteorologically possible.

The numerical modeling of the selected events was performed using two separate process models: the CE Wind Model (Cardone et al., 1992) for simulation of the hurricane wind field and the ADCIRC Model (Luettich, et al., 1992) for simulation of the water level response. The modeling procedure consisted of first running the CE Wind model for each storm using input from the NWS Hurricane database. The wind fields generated by the CE Wind model were then used to force the surge calculations in ADCIRC. Comparisons of model results with measured wind fields and surge hydrographs suggest that the models are capable of producing peak surges and hydrograph shapes which reasonably approximate measured data.

The goal of the process modeling was to develop a set of peak surges at each station, which were then used to develop frequency of occurrence relationships computed from the Empirical Simulation Technique (EST). The EST is a statistical procedure for simulating time sequences of non-deterministic, multiparameter systems, and is based on a bootstrap resampling technique. In the present study the EST used storm characteristics and responses from the "training set" of 39 events to perform 50 simulations of a 200 year sequence of events. The only assumption is that the simulated population of events are statistically similar to events which have actually occurred.

Application of the EST resulted in predicted surge values at 25, 50 and 100 year return periods. These peaks were then incorporated into synthetic time series used to characterize the shape of the design hydrograph. The results of the surge modeling suggest that the simple exponential form of the hydrograph, recommended by the FHWA pooled fund study "Development of Hydraulic Computer Models to Analyze Tidal and Coastal Stream Hydraulic Conditons and Highway Structures", may be inadequate to characterize stations which experience periods of negative surge. An empirical approach based on a damped sine wave was developed as an alternative. The recommended procedure for implementing the results of the study suggests that both types of hydrographs be modeled, with design parameters based on the worst-case conditions.

ACKNOWLEDGEMENTS

The research documented in this report has been sponsored by the North Carolina Department of Transportation through the Center for Transportation Engineering Studies. Sincere appreciation is extended to the NCDOT Technical Advisory Committee, which included Mr. Archie Hankins, Mr. Mike Stanley and Mr. Don Idol of the NCDOT, and Mr. Paul Simon of the Federal Highway Administration's North Carolina Division office.

Special thanks go to Rick Luettich and Jim Hench of the University of North Carolina Institute of Marine Sciences for technical suggestions regarding the hurricane wind and surge models. Crystal Williams, research technician at UNC-IMS, deserves special mention for her diligence in generating and refining the finite element grid.

Some of the methods applied herein build upon the previous efforts of researchers in coastal hydraulics and risk assessment. The suggestions of Billy L. Edge of Texas A&M University were particularly valuable with regard to hydrograph development, while Norm Scheffner of the Coastal Hydraulics Lab, US Army Corps of Engineers provided invaluable assistance with the application of the empirical simulation technique. Will Brothers of the North Carolina Division of Emergency Management supplied important reference materials and useful background on previous modeling efforts in the state.

Data collection efforts were aided extensively by the efforts of students, including Courtney Garriga and Dwight Willie. Johnny Martin of Moffatt and Nichol Engineers also supplied a number of key reports. Finally, thanks are extended to Chris Landsea of the National Hurricane Center for his efforts in compiling the database of historical storm events.

LIST OF FIGURES

LIST OF TABLES

1. INTRODUCTION

1.1 Background

The analysis of foundation scour at highway structures has received increased attention in recent years. The FHWA pooled fund project "Development of Hydraulic Computer Models to Analyze Tidal and Coastal Stream Hydraulic Conditions and Highway Structures" was initiated to improve methods for determining design parameters for bridges, causeways and other hydraulic structures, with particular focus on flow-induced scour. The pooled fund project led to the selection of two computer models for assessing the dynamics of coastal waterways: UNET (HEC, 1996) and FESWMS–2DH (Froehlich, 1996).

Both of the selected models are suitable for use in advanced hydraulic analyses in areas where simplified methods cannot be employed. In applying these models, however, it is important to accurately account for the hydrodynamic forces of the system and to correctly specify boundary conditions at the ends of the model domain. The purpose of the present study is to determine surge hydrographs which may be used in the analysis of proposed and existing structures in the area of Albemarle-Pamlico Sound (Figure 1.1). The surge hydrographs were developed at multiple locations within the Sounds and are based on model simulations and statistical analysis of historical storm events.

1.2 Needs Statement

The design of highway structures located along the Albemarle-Pamlico Sounds system requires the development of surge hydrographs with specific frequencies of occurrence. At present, there is no systematic set of data available for determining these hydrographs at locations of proposed and existing structures. The goal of this study is to develop site-specific hydrographs at 25, 50 and 100 year return intervals which may be used as boundary conditions for localized applications of hydraulic models.

1.3 Scope

The scope of this study includes:

- Collection and analysis of historical data for storm events
- Development of a representative set of storms for use in model simulations
- Simulation of storms to develop surge hydrographs at multiple stations
- Statistical analysis of peak surge values
- Characterization of surge hydrographs at 25, 50 and 100 year recurrence intervals

1.4 Previous Research

The research presented herein builds upon the efforts of several previous research efforts, including the pooled fund project (Ayres Associates, 1997a,b) mentioned above. In particular, the present study employs the surge hydrograph calculation method developed during the pooled fund project as well as an alternate, empirical approach developed to characterize the hydrograph shapes observed in Albemarle-Pamlico Sound. The hydrographs developed as part of this study may be applied within the framework of the UNET and FESWMS-2DH hydraulic computer models.

The wind, surge and statistical analysis models applied during the course of this work are products of research programs sponsored by the US Army Corps of Engineers in cooperation with universities and private contractors. The Army Corps of Engineers (CE) wind model (Cardone et al., 1992) has been used extensively to provide tropical storm wind fields for input into surge models, including recent work by Blain, et al. (1994) in the Gulf of Mexico, Mark and Scheffner (1994) off the coast of Delaware and Scheffner and Butler (1996) near Long Island, NY. These studies also utilized the numerical surge model ADCIRC (Luettich, et al., 1992), which has been applied in both surge applications and large-scale tidal modeling efforts (Westerink et al., 1993). The frequency of occurrence procedure used in the present study, the Empirical Simulation Technique (EST), is under active development and has been applied in some of the studies mentioned above (see also Scheffner and Borgman, 1996). As a result of its demonstrated capability the EST has been adopted by the Army Corps of Engineers as the recommended approach in designing for storm-related impacts.

Each of these models is described in more detail in the following chapters. Consideration of previous synoptic, observational and modeling studies of the Albemarle-Pamlico Sound system (Pietrafesa et al., 1986, Pietrafesa and Janowitz, 1991, US Army Corps of Engineers, 1987), which provide insight and a basis for comparison, will be included in later chapters as well.

1.5 Organization

This report is organized as follows. Chapter 2 presents an analysis of the historical database of storms which have affected the Albemarle-Pamlico Sound study area. The discussion focuses on selection criteria for simulated storm events. A review of the hurricane wind field and surge models is presented in Chapter 3. Included in this review are comparisons of surge predictions with measured hydrographs and a summary of maximum predicted surges throughout the model domain. Frequency-of-occurrence relationships for surge height, computed from the Empirical Simulation Technique (EST), are described in Chapter 4. The 25, 50 and 100 year peak surge values are related to characteristic hydrograph shapes at each station using two different methods as outlined in Chapter 5. Chapter 5 also includes recommendations for implementation of the study findings. Chapter 6 contains a summary of the study results. References used in the study are contained in Chapter 7. Background data, including predicted peak surges and stage-frequency curves, are included as appendices.

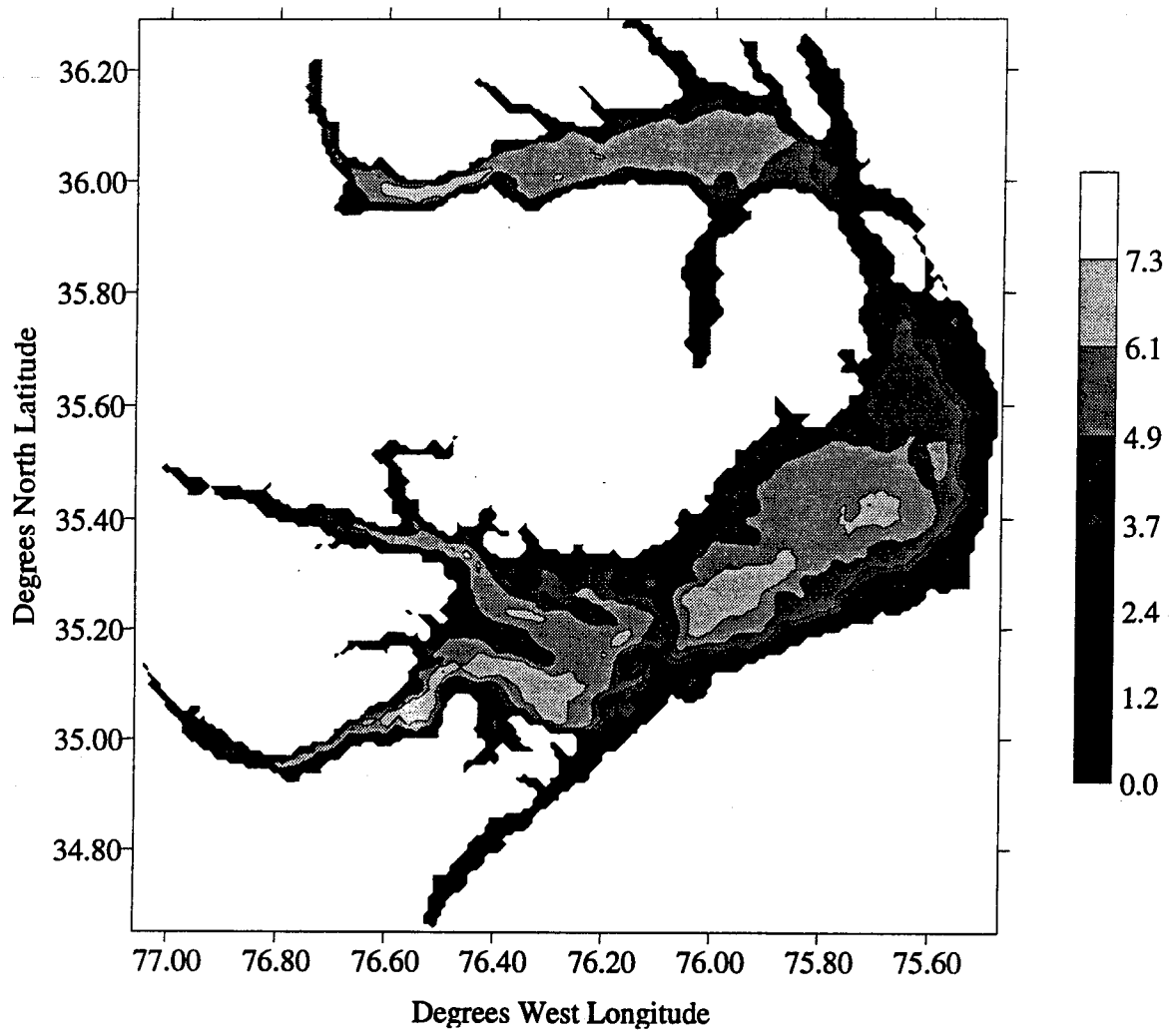

Figure 1.1 Albemarle-Pamlico Sound study area with bathymetry in meters (below msl).

2. ANALYSIS OF STORM EVENTS

2.1 Historical Data

A database of historical tropical storms proximate to the Albemarle-Pamlico Sounds study area is presented in Table 2.1 Data for these storms were compiled from the National Weather Service (NWS) by researchers at Colorado State University and are available from archives at Purdue University (http://wxp.atms.purdue.edu/hurricane/atlantic). The so-called "best track" information is based on NWS post-analysis of a variety of data sources, including ground measurements, reconnaissance flights and model data. The NWS data covers the period 1886-1996 and includes a time history of storm track, central pressure, 10m/1 minute sustained winds and storm status.

The storms included in Table 2.1 meet two main criteria: 1) the storm passed within 200 nautical miles (nm) of Cape Hatteras (36°16' N, 75°55' W) and 2) the storm was at least a minimal hurricane at some point within the 200nm radius. Tropical storms and hurricanes downgraded to tropical storms before reaching the 200nm radius were not included in the database. The 200nm criteria was selected to be much larger than the expected radius to maximum winds for hurricanes between 30°-40° latitude, which is typically between 9-45 nm (NWS, 1979).

The storms are described in terms of their wind speed category (i.e., category 1-5 based on wind speed only, not wind speed and central pressure as in the Saffir-Simpson scale), closest point of approach (CPA) to Cape Hatteras in nm, the date on which the storm first entered the 200 nm radius, the storm's bearing relative to Hatteras at the CPA, the wind speed in knots while within the 200nm radius and the track direction at the CPA.

An exception to the 200nm criteria was Hurricane Hugo, which passed well west and southwest of the project area and had minimal impact on water levels within the sounds. However, Hugo was included due to its size and strength and was used as a basis for hypothetical events which are discussed in more detail below.

2.2 Selection of Simulation Events

The data in Table 2.1 summarize a total of 87 storms from which a smaller number of storms was selected to form the "training set" for the statistical analysis discussed in Chapter 4. While a number of additional criteria where considered to reduce the database further, such as limiting the CPA to 150nm for all storms or to smaller distances (e.g., 50 or 100nm) for less intense hurricanes, it was decided that the final selection of storm events should be based on a review of each storm's track and intensity. One problem with an absolute criteria approach is that storms that could have a significant impact could be eliminated from consideration. For example, Hurricane Hazel (159nm CPA) would be eliminated under a 150nm CPA criteria. In addition, there may be smaller storms which could have significant, though localized, impacts.

Therefore, the "best track" data were reviewed along with plots of storm tracks to reduce the total number of historical events simulated to 36. In general, storms which were removed from consideration remained well offshore or tracked significantly west of the study area, had weak winds and were quickly downgraded to tropical storms after entering the 200m radius, were similar in track but lower in strength to storms already selected for simulation, or had insufficient data available to drive the wind model. Popular accounts of storm history (Barnes, 1995) were consulted in a number of cases to aid in the decision.

The storms selected for inclusion in the training set are summarized in Table 2.2. Tracks of these simulated storm are presented in Figure 2.1. The database includes recent events such as Emily (1993) and Gloria (1985), several storms from the intense activity between 1950-1960 and extreme early events (e.g., the "San Ciriaco' event of August, 1899).

In addition to these storms, 3 hypothetical events, patterned after Hurricane Hugo, were added to the training set. These "synthetic" events were added to account for storms which did not actually occur in the historical record but are considered meteorologically possible, i.e., storms which could be reasonably expected to have occurred. The tracks for these events, called Hugo1, Hugo2 and Hugo3, are shown in Figure 2.2. The speed and pressure data were translated in time to simulate near peak strength at time of landfall, the condition experienced in Charleston, SC in September, 1989. With the addition of these events, the total number of storms included in the training set is 39.

2.3 Statistical Summary of Training Set Events

In selecting the storms for inclusion in the training set it is important to ensure that the simulated events are statistically similar to the original database of 87 events. This is particularly important when applying the EST, as the primary assumption of the EST is that the extended population of events generated by the EST are statistically similar in magnitude and frequency to the training set.

Therefore, an analysis of the 36 historical training set storms was conducted in order to assess the composition of the simulated population of events. Comparisons with the original database were done on the basis of wind speed category, wind speed and track direction. The results are summarized in Figures 2.3-2.5.

Figure 2.3 presents a histogram of the percentage of storms falling within the defined wind speed categories: category 1, 65-82 knots, category 2, 82-95 knots, category 3, 95-113 knots, category 4, 113-135 knots and category 5:, 135 knots or greater. As shown in the figure, the percentage of storms in each category for both the original (dark shade) and selected (light shade) groups decreases as storm category increases. The selected database of events does, however, have a slight bias towards stronger events, as the combined percentage of wind speed category 4 and 5 storms in the selected database is approximately 13%. In contrast, only 7% of storms in the original database fall within these two categories. This slight bias is considered acceptable in light of the objective of identifying peak surge values.

A similar analysis is presented in Figure 2.4, in which wind speeds are divided into 7 bins. Each bin contains storms with winds less than or equal to the bin number down to the next lowest bin. The two data sets are again similar, as the percentage of total generally decreases with increasing wind speed. The selected database has a slight bias consistent with the results for wind speed category. For example, the selected database has approximately 40% of storms with wind speeds in the 95kn and105kn bins, as compared with 30% in the original database.

While the EST procedure will be discussed in more detail in Chapter 4 it is worth mentioning that in applying the EST the frequency of events, expressed in terms of the number of storms per year, will be less in the selected database than it would be if the entire original database were used as the training set. Therefore, the bias in the selected events is reduced by simulating fewer storms each year. Essentially this means that the analysis focuses on the more extreme events in the historical database, in effect "skipping" the weaker storms.

The final comparison, presented in Figure 2.5, shows the track direction in the two databases. The figure displays a direction rose, with axes plotted on a logarithmic scale. By observing the relative position of the symbols for the original storms (square) and the selected storms (triangle) the percentage of storms which tracked in a particular direction may be compared. For example, in both data sets approximately 40% of the storms tracked to the north-northeast (45% in the original and 38% in the selected) with another 25% headed east-northeast. The primary differences in the databases come in storms which tracked over the study area, where 24% of storms in the selected database tracked to the west-northwest, northwest and north-northwest, as compared to 17% of the original database of storms.

2.4 Summary

A review of available data on tropical storms identified 87 storms of interest to the study area, from which 36 storms were selected for model simulations. A statistical analysis of the selected storms suggests that the selected database, though quite similar to the original data, focuses on the strongest events which are closest in proximity and track to the Albemarle-Pamlico study area. The selected database of 36 historical events was augmented by including 3 hypothetical events which are considered meteorologically possible.

It should be noted that a review of data from severe extratropical storms suggests that peak surges are lower than those produced by tropical storm events. Moreover, the shape of the hydrograph in extratropical events is typically broader and flatter than those produced by hurricanes. This is significant for velocity computations, as the strongest velocities occur with shorter duration, sharply sloped hydrographs (Edge, et al., 1998). As result, the model simulations discussed in following chapters focused on tropical storm events.

	Name	Cat.[1]	Month[2]	Day	Year	CPA[3]	Bear.[4]	Wind[5]	DIR[6]
1	NOT NAMED	1	7	20	1886	89.2	SSW	70	ENE
2	NOT NAMED	2	8	24	1886	116.7	ESE	85	NNE
3	NOT NAMED	2	8	21	1887	86.7	SSW	90	ENE
4	NOT NAMED	3	8	24	1887	108.9	SSE	105	ENE
5	NOT NAMED	2	11	26	1888	114.3	ESE	85	NNE
6	NOT NAMED	1	5	21	1889	153.7	ESE	75	ENE
7	NOT NAMED	2	8	26	1889	161.9	ESE	85	NNE
8	NOT NAMED	2	10	12	1891	73.1	ESE	85	NNE
9	NOT NAMED	3	8	21	1893	162.4	ESE	105	NNE
10	NOT NAMED	2	8	23	1893	90.8	ENE	85	NNW
11	NOT NAMED	1	10	13	1893	185.3	WNW	80	NNE
12	NOT NAMED	1	9	29	1894	51.5	NNW	80	NE
13	NOT NAMED	1	10	10	1894	96.6	WNW	65	ENE
14	NOT NAMED	1	9	30	1896	194.1	WNW	65	NNE
15	NOT NAMED	2	10	11	1896	100.2	ESE	85	NE
16	NOT NAMED	3	8	17	1899	13.0	WSW	105	NW
17	NOT NAMED	1	10	31	1899	141.0	WSW	70	NNE
18	NOT NAMED	2	7	11	1901	37.5	WNW	85	SSW
19	NOT NAMED	2	9	16	1903	129.0	ENE	85	NNW
20	NOT NAMED	1	10	10	1903	105.2	ESE	70	NNW
21	NOT NAMED	1	9	15	1904	124.2	WNW	65	NE
22	NOT NAMED	2	6	19	1906	169.3	ESE	90	ENE
23	NOT NAMED	4	9	17	1906	129.9	SSW	120	WNW
24	NOT NAMED	2	7	31	1908	23.4	WNW	85	ENE
25	NOT NAMED	1	10	6	1912	127.4	SSE	80	WSW
26	NOT NAMED	1	11	23	1912	136.6	ESE	65	NNE
27	NOT NAMED	1	9	3	1913	39.1	WSW	80	WNW
28	NOT NAMED	2	7	20	1916	125.4	ESE	95	NNE
29	NOT NAMED	1	9	23	1920	146.1	WSW	70	WNW
30	NOT NAMED	3	8	26	1924	52.4	SSE	110	NNE
31	NOT NAMED	1	12	3	1925	26.0	WNW	65	NNE
32	NOT NAMED	3	8	24	1927	132.1	ENE	100	NNE
33	NOT NAMED	1	9	12	1930	59.6	SSE	75	ENE
34	NOT NAMED	3	8	23	1933	27.3	ESE	100	NW
35	NOT NAMED	3	9	16	1933	24.4	WSW	105	NNE
36	NOT NAMED	1	9	8	1934	71.9	NNE	75	NNE
37	NOT NAMED	1	9	6	1935	94.8	WNW	65	ENE
38	NOT NAMED	1	11	2	1935	151.0	SSE	70	WSW
39	NOT NAMED	2	9	18	1936	22.5	ESE	95	NNW
40	NOT NAMED	3	9	21	1938	120.4	ESE	110	NNE
41	NOT NAMED	1	9	1	1940	46.8	ESE	70	NNE
42	NOT NAMED	1	7	17	1944	172.2	SSE	80	ENE
43	NOT NAMED	2	9	14	1944	52.8	SSW	95	NNE
44	NOT NAMED	1	7	7	1946	50.4	NNE	65	ENE
45	NOT NAMED	2	8	31	1948	119.3	ESE	85	ENE
46	NOT NAMED	2	8	24	1949	53.3	ENE	95	ENE
47	ABLE	4	8	20	1950	59.2	SSE	120	NNE
48	DOG	2	9	11	1950	160.0	ESE	85	NNE

Table 2.1. Hurricanes Passing within 200nm of Cape Hatteras, NC since 1886.

Table 2.1. (continued)

	Name	Cat.[1]	Month[2]	Day	Year	CPA[3]	Bear.[4]	Wind[5]	DIR[6]
49	ABLE	3	5	21	1951	67.0	SSE	100	NNE
50	HOW	2	10	4	1951	65.6	ESE	95	ENE
51	BARBARA	2	8	14	1953	32.7	NNW	95	NNE
52	CAROL	2	8	31	1954	69.8	SSW	85	NNE
53	EDNA	3	9	11	1954	47.9	SSE	105	NNE
54	HAZEL	1	10	15	1954	158.3	WNW	80	NNE
55	CONNIE	2	8	12	1955	29.7	WNW	90	NNE
56	DIANE	1	8	17	1955	134.3	WSW	80	NNW
57	IONE	3	9	19	1955	50.6	WNW	100	ENE
58	BETSY	1	8	17	1956	190.9	ESE	80	NNE
59	DAISY	3	8	28	1958	82.0	ESE	110	NNE
60	HELENE	4	9	28	1958	30.8	SSW	115	ENE
61	DONNA	2	9	12	1960	68.3	WSW	95	NNE
62	ESTHER	4	9	20	1961	111.8	ESE	120	NNE
63	ALMA	1	8	28	1962	13.0	ESE	75	ENE
64	GINNY	2	10	21	1963	69.8	SSE	85	ESE
65	GLADYS	1	9	23	1964	155.0	ENE	75	NNE
66	ISBELL	1	10	16	1964	47.4	WSW	65	NNW
67	ALMA	1	6	11	1966	94.7	SSE	70	E
68	DORIA	1	9	17	1967	37.5	WNW	70	SSW
69	GLADYS	1	10	20	1968	48.6	ENE	75	ENE
70	GERDA	2	9	9	1969	56.5	ENE	85	NNE
71	KARA	1	10	12	1969	180.9	ESE	65	SSE
72	GINGER	2	9	30	1971	65.9	WSW	90	WNW
73	DAWN	1	9	9	1972	55.1	ENE	70	SSE
74	BELLE	3	8	9	1976	67.0	SSE	105	NNE
75	DENNIS	1	8	20	1981	22.0	ENE	65	ENE
76	DIANA	4	9	14	1984	29.7	WNW	115	ENE
77	JOSEPHINE	1	10	13	1984	193.1	ENE	70	NNW
78	GLORIA	2	9	27	1985	14.0	NNE	90	NNE
79	CHARLEY	1	8	17	1986	32.8	WNW	70	NNE
80	*HUGO	5	9	22	1989	258.5	WSW	140	NNW
81	LILI	1	10	13	1990	166.1	ESE	65	NNE
82	BOB	3	8	19	1991	42.1	SSE	100	NNE
83	EMILY	3	9	1	1993	37.5	ENE	100	NNE
84	GORDON	1	11	18	1994	94.7	SSW	75	SSW
85	FELIX	1	8	17	1995	130.0	ENE	70	N
86	BERTHA	2	7	13	1996	95.9	WNW	90	NNE
87	FRAN	3	9	6	1996	134.0	WSW	100	NNW

Data courtesy of Chris Landsea , Colorado State University via the weather server at Purdue University

Notes:
1. maximum storm category (based on wind speed only) while within 200nm radius
2. date on which storm first reached 200nm of Hatteras
3. closest point of approach to Hatteras in nautical miles (nm)
4. direction of storm relative to Hatteras at CPA
5. maximum wind speed in knots while within 200nm radius
6. storm path at CPA

Name	Date	CPA (nm)	Wind (knots)	Speed (mph)	DIR
NOT NAMED	Sep 1894	51.5	80	7	NE
NOT NAMED	Aug 1899	13.0	105	4	NW
NOT NAMED	Jul 1901	37.5	85	4	SSW
NOT NAMED	Sep 1906	129.9	120	18	WNW
NOT NAMED	Jul 1908	23.4	85	14	ENE
NOT NAMED	Sep 1913	39.1	80	6	WNW
NOT NAMED	Aug 1924	52.4	110	22	NNE
NOT NAMED	Sep 1930	59.6	75	17	ENE
NOT NAMED	Aug 1933	27.3	100	12	NW
NOT NAMED	Sep 1933	24.4	105	17	NNE
NOT NAMED	Sep 1935	94.8	65	22	ENE
NOT NAMED	Sep 1936	22.5	95	8	NNW
NOT NAMED	Sep 1944	52.8	95	33	NNE
NOT NAMED	Jul 1946	50.4	65	15	ENE
ABLE	Aug 1950	59.2	120	29	NNE
BARBARA	Aug 1953	32.7	95	15	NNE
CAROL	Aug 1954	69.8	85	40	NNE
HAZEL	Oct 1954	158.3	80	49	NNE
CONNIE	Aug 1955	29.7	90	12	NNE
IONE	Sep 1955	50.6	100	14	ENE
HELENE	Sep 1958	30.8	115	27	ENE
DONNA	Sep 1960	68.3	95	33	NNE
ALMA	Jun 1962	13.0	75	26	ENE
DORIA	Sep 1967	37.5	70	10	SSW
GLADYS	Oct 1968	48.6	75	30	ENE
GINGER	Sep 1971	65.9	90	5	WNW
DAWN	Sep 1972	55.1	70	7	SSE
DENNIS	Aug 1981	22.0	65	23	ENE
DIANA	Sep 1984	29.7	115	16	ENE
GLORIA	Sep 1985	14.0	90	35	NNE
CHARLEY	Aug 1986	32.8	70	13	NNE
*HUGO	Sep 1989	258.5	140	31	NNW
BOB	Aug 1991	42.1	100	23	NNE
EMILY	Sep 1993	37.5	100	12	NNE
BERTHA	Jul 1996	95.9	90	20	NNE
FRAN	Sep 1996	134.0	100	20	NNW

Table 2.2 Storms selected for simulations.

Figure 2.1. Hurricane tracks included in storm database.

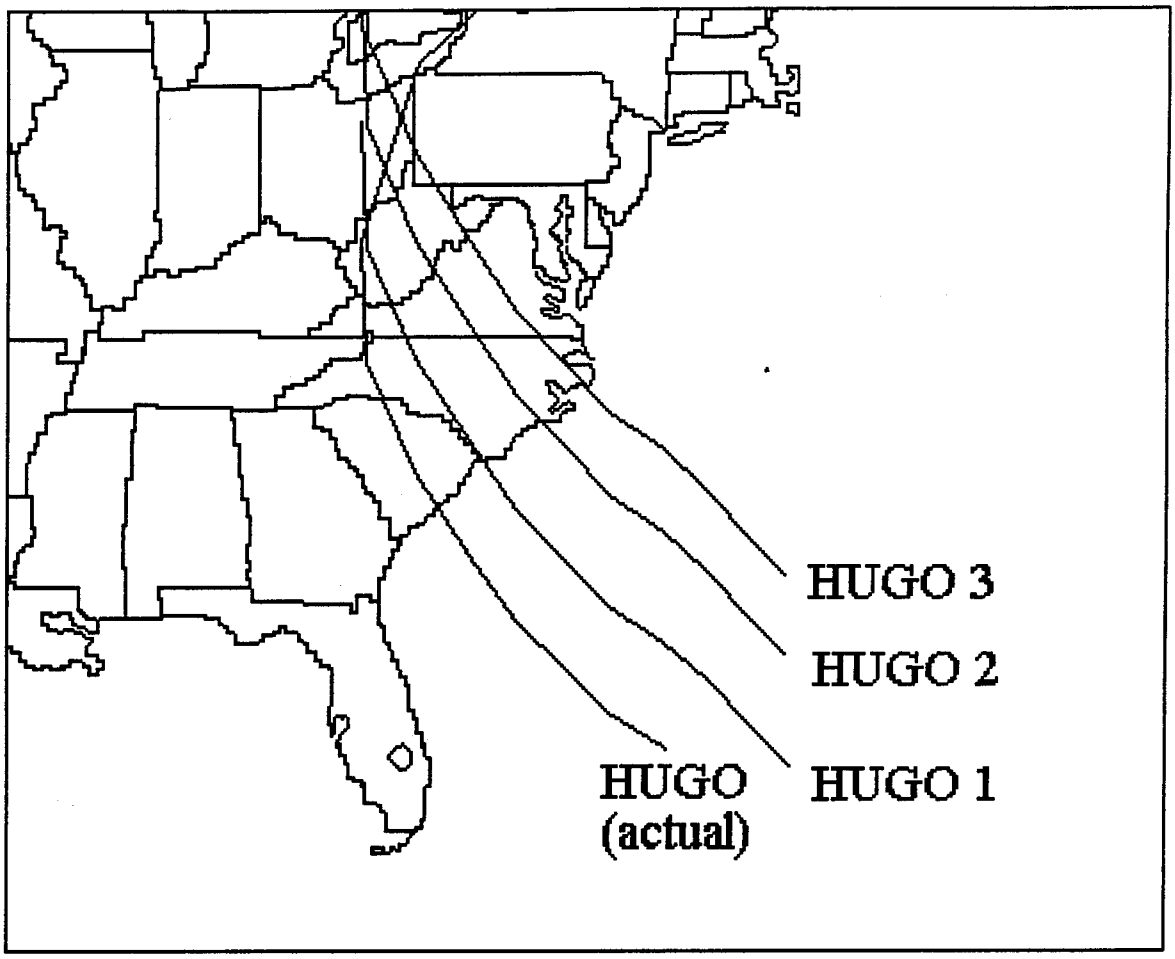

Figure 2.2. Hypothetical Hurricane Hugo tracks.

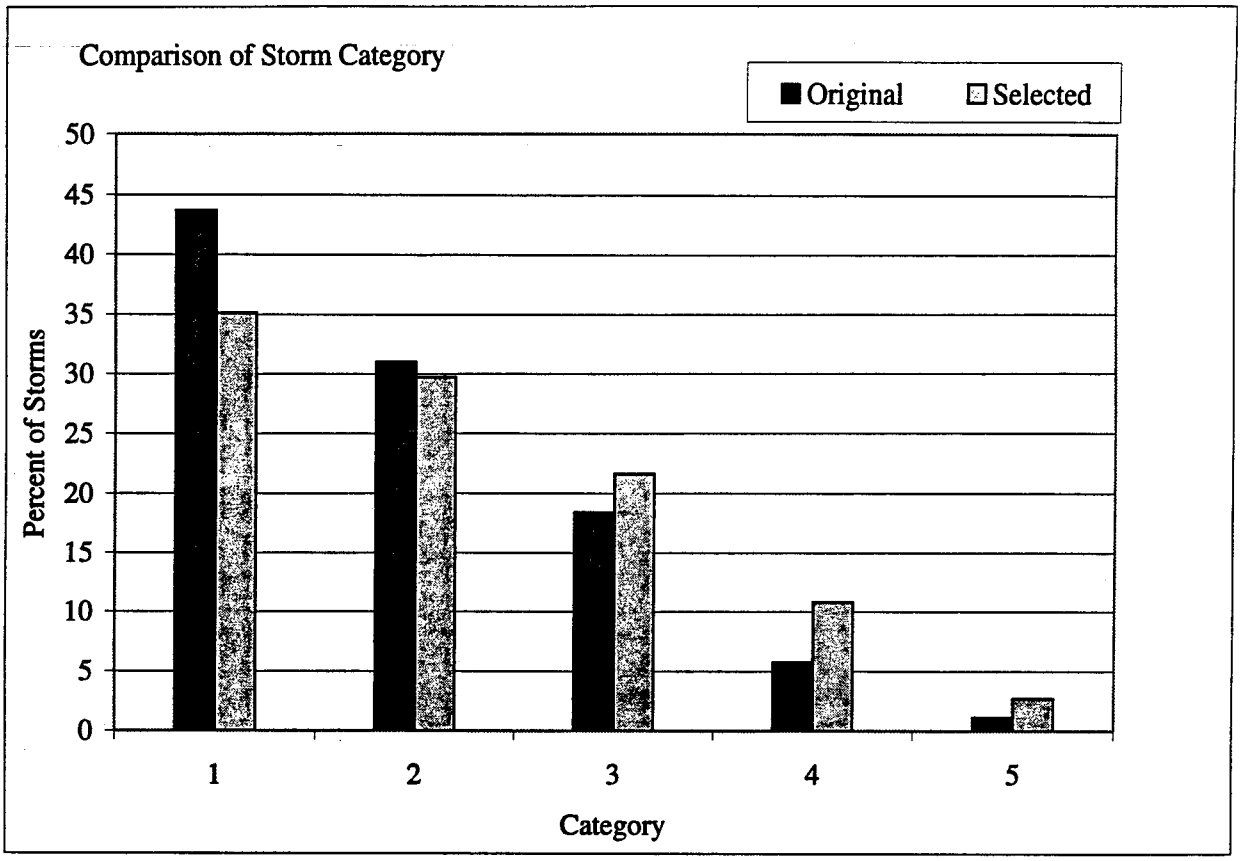

Figure 2.3 Comparison of storms by wind speed category.

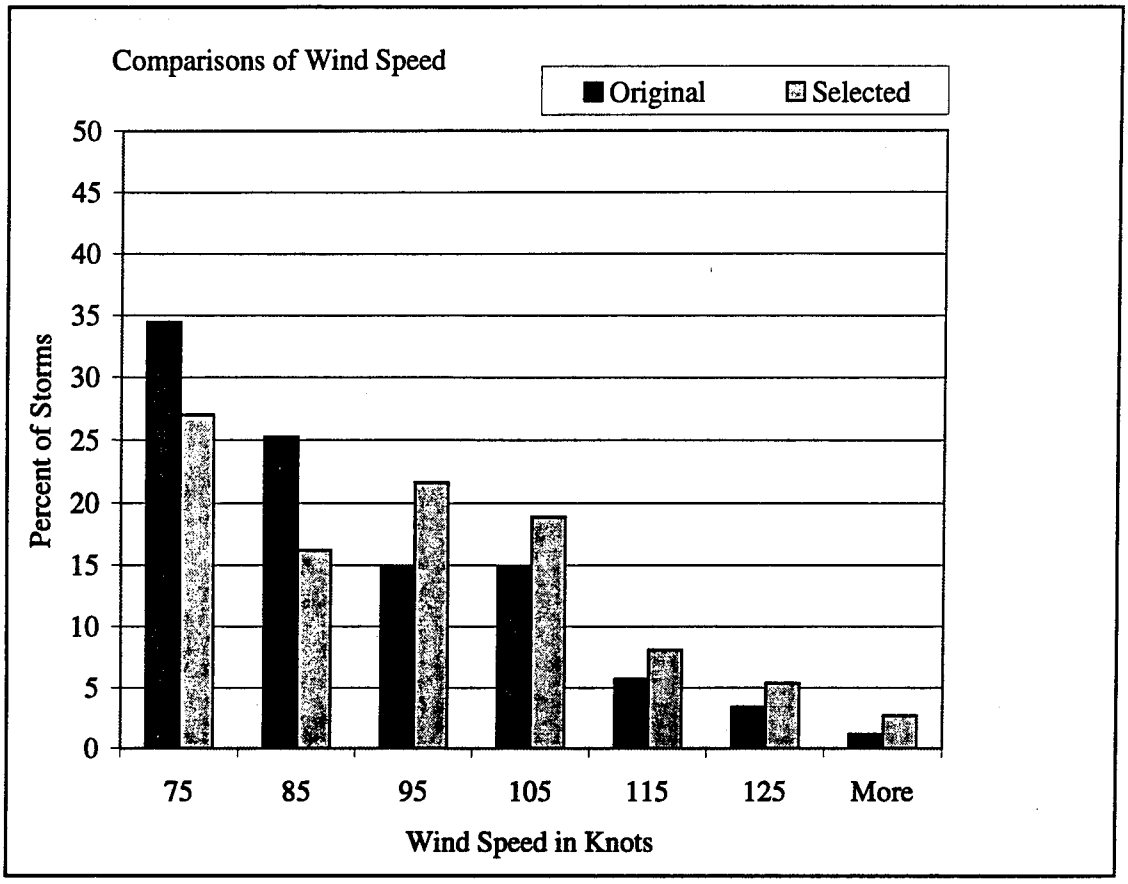

Figure 2.4 Comparison of storms by maximum wind speed.

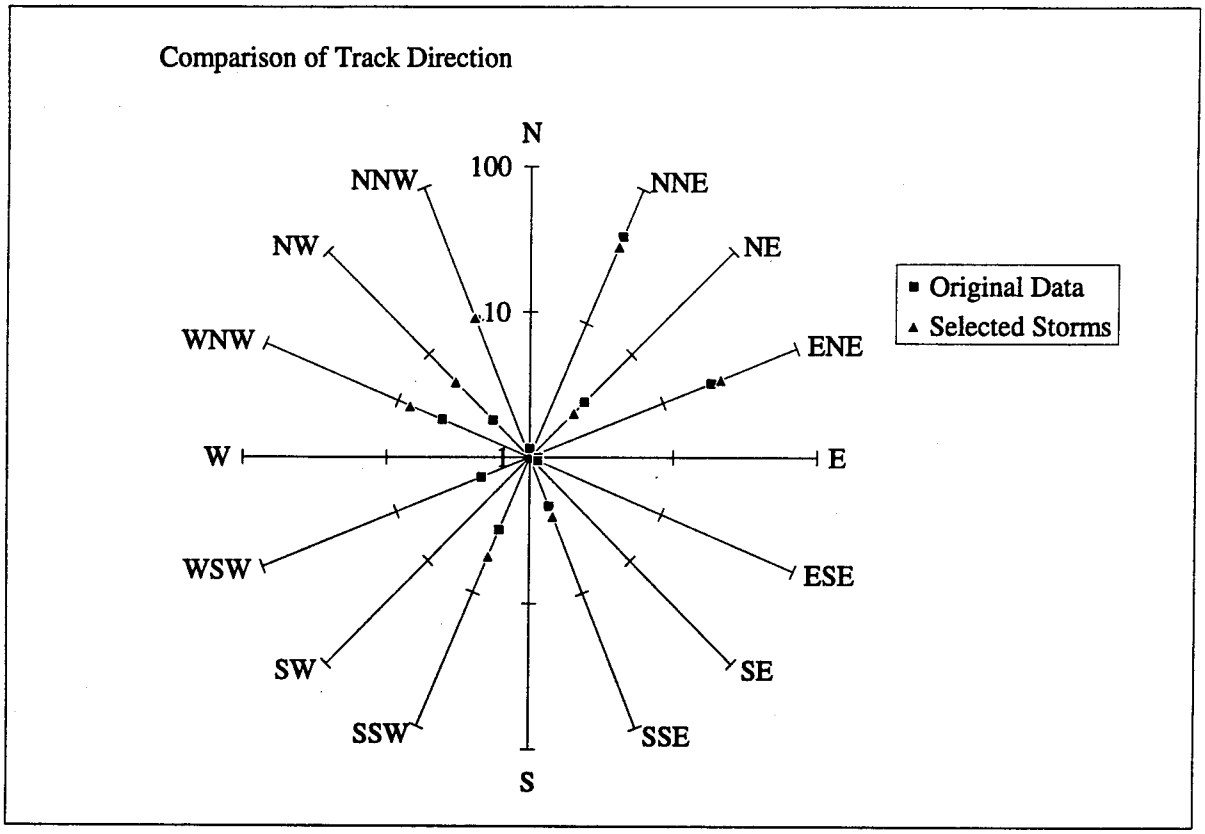

Figure 2.5 Comparison of storms by track direction.

3. NUMERICAL MODELING

3.1 Setting

The Albemarle-Pamlico Sound study area (Figure 3.1) is the largest barrier island estuarine system in the United States. Pamlico Sound, the larger of the two main areas, is oriented along an axis running from southwest to northeast and is approximately 85 miles (140km) long by 15-30 miles (25-55km) wide. Albemarle Sound, located to the north, is aligned west to east extending approximately 50 miles (85km). Albemarle Sound varies in width from approximately 12 miles (20km) in the east to less than 5 miles (8km) at its western end (Pietrafesa and Janowitz, 1991).

Albemarle and Pamlico Sounds are connected to each other by two narrow passages, Croatan and Roanoke Sounds, which are separated by Roanoke Island. Croatan Sound is the larger of the two and provides the most important link between the main basins. In addition, the southernmost part of the study area includes Core Sound, a much smaller estuary with a southwest to northeast orientation. Of the two main areas only Pamlico Sound has a direct connection to the Atlantic Ocean via Oregon, Hatteras and Ocracoke Inlets. Core Sound connects to the Atlantic Ocean via Drum Inlet.

A plot of the study area bathymetry, shown previously in Figure 1.1, depicts a broad, shallow estuarine system. Shoaling areas exist near the mouths of rivers, adjacent to inlets and along the back side of the barrier island boundaries. Depths in these shoaling areas are often less than 5 feet. The deepest regions of Pamlico Sound reach 25 feet, while depths along the axis of Albemarle Sound are usually less than 20 feet.

The entire area receives drainage from a number of rivers. Major sources of drainage to Pamlico Sound include the Neuse River and Pamlico River, located to the west. Albemarle Sound, which begins at the mouth of the Chowan River, is fed by several smaller rivers including the Roanoke and Alligator Rivers.

The effect of storm surge on water levels within these rivers is of major importance to the objective of the present study. As a result, a total of 26 stations were selected throughout the study area at which hydrographs were computed. The station locations, shown in Figure 3.1, were developed based on the distribution of actual and proposed NCDOT highway structure projects. The stations were chosen to be downstream of or adjacent to the locations of these structure projects. Actual locations and depths of these stations are included in Table 3.1.

3.2 Modeling Background

The numerical modeling of events listed in Table 2.2 was performed using two separate process models: the CE Wind Model (Cardone et al., 1992) for simulation of the hurricane wind field and the ADCIRC Model (Luettich, et al., 1992) for simulation of the water level response. The modeling procedure consisted of first running the CE Wind model for each

storm using input from the NWS Hurricane database. The wind fields generated by the CE Wind model were then used to force the surge calculations in ADCIRC. Following is a brief background of each model and the assumptions employed in the model applications.

3.2.1 Wind Model. As mentioned above the CE Wind model has been used to provide wind fields for a number of surge and wave modeling applications. The CE Wind model solves the momentum equations for a vertically integrated boundary layer flow and predicts the wind velocities and atmospheric pressures associated with a moving hurricane. The model equations are solved on a nested, translating grid which is centered on the hurricane eye and which follows the storm path. The nested grid system provides for a varying degree of resolution and allows for a minimum grid spacing of 3 miles (5km).

Input to the model is provided in the form of a series of "snapshots" which define the state of the storm throughout its duration. These 6-hour snapshots indicate the storm's position, track direction , forward speed, radius to maximum winds, central pressure, and geostrophic wind velocity. The radius to maximum winds is approximated using a function which accounts for wind speed and central pressure deficit (Jelesnianski and Taylor, 1973). Background pressure was assumed to be 1013 millibars. The snapshots are interpolated to an hourly time series to produce a smooth transition from one snapshot to the next, and the hourly wind and pressure fields generated by the model are then interpolated to the surge model grid and saved to input files for use in the surge calculations.

3.2.2 Surge Model. Previous studies directed towards understanding the physical processes affecting the sounds (e.g., Pietrafesa et al, 1986) suggest that the sounds may be characterized, generally speaking, as wind-dominated and vertically well mixed with a tidal influence that decreases substantially with distance from the inlets. Previous modeling studies (Pietrafesa and Janowitz, 1991, Xie and Pietrafesa, 1995) have confirmed this general characterization and also demonstrated the importance of Croatan Sound in providing a link between the two main basins. Therefore, in applying the surge model the sounds were assumed to be homogenous, and forcing from the tides (both internally and at the boundary) was ignored. The latter assumption simplifies the simulation of historical events and is consistent with the approach adopted by the pooled fund study, in which the design hydrograph is a superposition of the surge and tide hydrographs.

The three-dimensional version of ADCIRC was used to simulate each storm event. ADCIRC is a finite element, long-wave hydrodynamic model which solves the generalized wave-continuity equation for surface elevation and horizontal momentum equations for x and y velocity components. In addition, the model solves a separate equation for the vertical profile of stress at each horizontal grid point. The stress profile may then be integrated to recover the vertical velocities. This novel approach, known as the direct stress solution technique (DSS) has the advantage of requiring less grid resolution than the standard velocity-based method because stress profiles tend to vary less rapidly than velocity profiles over the depth (Luettich et al., 1994).

The use of a three-dimensional model, in contrast to a two-dimensional, depth integrated model, provides for a more realistic treatment of the dynamics of wind-driven flow in shallow, enclosed basins. In the latter model, the bottom stress is parameterized to oppose the depth averaged velocity. However, in reality the bottom stress opposes the near-bottom velocity, which may be in the opposite direction and significantly different in magnitude from the profile average. Therefore, the two-dimensional approach can lead to errors in the computed bottom stress which result in underpredicted surface slopes. In certain conditions this error can approach 50% (Hearn and Hunter, 1990). Pietrafesa et al. (1991) found differences of up to 33% between two-dimensional and three-dimensional models of Pamlico Sound.

The ADCIRC grid of the study area consists of over 8000 elements and 5000 nodes and has a resolution of approximately 0.6 miles (1km). The vertical grid, which employs a bottom-following (sigma) coordinate system, consists of 5 nodes. As shown in the figure, the domain extends westward into the Neuse, Pamlico and Chowan Rivers, with hydrograph stations located downstream of the ends to reduce boundary effects. The system is assumed to act as an enclosed basin during passage of a hurricane event, and thus the river boundaries and tidal inlets are closed. This assumption is consistent with the pooled fund study approach, as upland runoff is not included in the surge calculations, and reduces the size of the domain by eliminating offshore areas which would be necessary if the inlets were included. It is anticipated that including the inlets would have only minor, localized impacts on the peak water levels within the sounds.

Additional boundary conditions enforced on the model include a no-slip bottom boundary and a weir-type overtopping condition for boundary elements when the water surface at the boundary exceeds a specified elevation. The weir overtopping eliminates the physically unrealistic effect of a vertical wall at the model boundary and accounts for the possibility of overland flow, although the actual wetting and drying of land elements is not included. An estimated weir height of approximately 10 feet was used throughout the study area, a height considered to be realistic based upon a review of nearshore topography throughout the domain.

All of the model simulations employ a 60 second time step and a bottom roughness of 5cm. The vertical eddy viscosity scales on the shear velocity and was specified to increase linearly from the surface and bottom boundaries and approach a constant value in between. Actual model simulations start from mean sea level and were initiated generally 1-2 days before the storm arrival as the sounds tend to "spin-up" in response to wind forcing within 12-24 hours. Since areas of the model domain exhibited instabilities due to element drying (which is not addressed in ADCIRC) the model was run without including the finite amplitude component of the total depth. The effect of this assumption on interpretation of results is addressed in more detail below.

An initial series of model runs were conducted to compare the performance of the model with measured wind fields and surge hydrographs from a number of historical events. A discussion of these comparisons is presented below.

3.3 Data Comparisons

Comparisons of model predictions with measured data were performed for Hurricanes Emily (1993), Bertha (1996), Fran (1996) and Donna (1960). The measured data include water levels from gaging stations and high water mark surveys as well as wind speeds acquired from reconnaissance aircraft, surface meteorological stations, moored buoys and ship reports.

The first series of comparisons focused on the wind field model and used data collected and analyzed by NOAA following Hurricane Emily (Garcia, 1995). Emily tracked just to the east of Cape Hatteras on September 1, 1993, attaining peak wind speeds of 100knots while at its closest approach to land. The position of the peak winds relative to the Outer Banks resulted in water being forced up against the back of the barrier islands, causing extensive sound side flooding in the communities of Hatteras, Buxton and Avon. Three snapshots of Emily's wind field were compared with model results, corresponding to a 12 hour period beginning just prior to and ending just after the storm's closest approach to land. From initial comparisons with measured maximum wind speeds and radius to maximum winds it was apparent that the wind model underpredicted the size of the storm, resulting in lower wind speeds over Pamlico Sound and a reduction in surge levels along the back of the barrier islands.

In order to improve the model's performance an alternate method for determining the radius to maximum winds was developed and applied to storms such as Emily which remained offshore. The procedure, which is based on a regression analysis of measured data from 70 east coast hurricanes (Ho, et al., 1987), uses the wind speed, central pressure and forward speed from the best track data to estimate the radius to maximum winds. The revised procedure effectively produces slightly larger storms than those produced using the method of Jelesnianski and Taylor (1973), and in the case of Emily produced wind fields which more closely approximated measurements. Additional discussion of limitations to the wind model is presented below.

Comparisons of predicted water levels with a high water mark survey conducted after Hurricane Emily indicate that the model reliably produced the surge characteristics which led to sound side flooding in the areas of Hatteras, Buxton and Avon. Measured water marks ranged from approximately 7 feet in Hatteras and Avon and peaked over 10 feet in Buxton. Model predictions for these areas were slightly lower, ranging from 6 to 9 feet, but consistent with the assumption that high water marks include wave setup and swash not accounted for by the surge model.

A second set of comparisons was made using data from Hurricanes Fran and Bertha (1996). Both storms made landfall in the vicinity of Cape Fear and had their greatest impact to the south of the study area. However, comparisons with data measured at New Bern, NC, Figures 3.2, illustrate the model's performance. The model predicted the peak surges of both storms to within approximately 1 foot, and accurately reproduced the shape and timing of the hydrograph which was different for each storm.

A final group of model comparisons focused on data collected from Hurricane Donna, which also made landfall around Cape Fear but tracked to the northeast and moved directly over the Albemarle-Pamlico Sound study area. Surge data were available at 12 stations within the sounds, with snapshots of wind speed available for 4 locations (Davidson, 1961). Examples of model predictions are presented in Figure 3.3 for northern parts of the study area (Elizabeth City and Columbia) and in Figure 3.4 for central and southern regions (Belhaven and Engelhard). As shown in the figures, model predictions are again within a foot, and the model reproduces the shape and timing of the hydrographs quite well. It should be noted that the wind model, which used the radius to maximum winds calculation of Jelesnianski and Taylor (1973) (since Donna did not remain offshore) generally agreed with the snapshots of measured winds.

3.4 Applications and Results

The comparisons presented above suggest that the wind and surge models are capable of producing peak surges and hydrograph shapes which reasonably approximate measured data. Therefore, the models were applied to each of the storms given in Table 2.2. Three additional storms, patterned after Hurricane Hugo as discussed in section 2.2, were simulated as well. Peak surge elevations from these 39 simulated events were recorded at each of the 26 output stations (Figure 3.1). The model results are summarized in Figure 3.5.

Figure 3.5 shows the maximum surge predicted by the model at each of the output stations. It is interesting to note that while the figure includes results from the 3 synthetic Hugo-type events, the maximum surge values were produced by actual storms at 19 of the 26 stations. Moreover, the largest surge from an actual event was within a foot of the synthetic maximum at all but one of the remaining stations. Therefore, the inclusion of the synthetic events does not extend the population of expected surge values too far beyond what actually occurred, i.e., the synthetic Hugo events do not introduce significant bias into the results.

Histograms of predicted surge heights at each of the 26 output stations are included as Appendix A. In contrast to Figure 3.5, the results in Appendix A do not include the synthetic Hugo events; i.e., only results from the 36 actual hurricanes are included. The figures provide an indication of the distribution of events and illustrate how the maximum predicted surge value compares with the results for other storms at each station.

3.5 Discussion

The results presented above should be interpreted in light of the limitations of the process models. In general, predicted surge elevations are assumed to be within +/- 1 foot of actual peak surges. Discrepancies between model and actual surges are due to a number of factors:

- Sensitivity of the wind model to storm track – Simulations using the preliminary storm track for Hurricanes Fran and Bertha, produced shortly after the storm, and the post-processed data in the best track database suggest that model results may be quite sensitive

to even minor differences in storm position. The differences appeared to be greatest in upstream locations on the Neuse and Pamlico Rivers, where changes to the wind field near the mouth influenced the magnitude of the funneling effect observed upstream. In their simulation for Hurricane Emily, Xie and Pietrafesa (1995) also found the magnitude and location of maximum water levels were dependent on the storm track.

- Adjustment of wind speeds over land – The CE Wind model does not account for changes in wind speeds as the hurricane rotates over land, and as a result the wind speeds remain high and subsequent large negative surges can occur in areas adjacent to land. Output stations were generally moved far enough offshore to reduce this effect, although in a few instances predicted hydrographs show these large negative surges. However, the hydrographs used to produce the peak elevations at each station were free of this unrealistic effect.
- Treatment of overland flow – As mentioned above the 3D version of ADCIRC does not have the ability to handle areas of wetting and drying which would be necessary to accurately represent overland flow which occurs during more extreme events. The approach adopted instead was a weir-type boundary condition, which allows some overflow to occur. This simplification does not allow flow back into the system and more importantly is somewhat sensitive to the weir elevation. While the weir elevation (3m) chosen for the boundary is considered reasonable, output stations were moved away from boundaries where possible to reduce the influence of the assumed weir height. As demonstrated by the results above, the weir condition is encountered in a limited number of events.
- Resolution of hurricane wind field – The version of the CE Wind model available for use in the present study limits the finest resolution in the nested grid to 5km, which may be too coarse to accurately simulate tight storms. More recent versions of the model (Cardone et al, 1994) address this (and other) limitations to the wind field model.

Overall the model results appear to adequately represent the population of peak surges resulting from actual and hypothetical storm events. Comparisons with values presented by FEMA in Flood Insurance Studies and Hurricane Evacuation studies (see comparisons in Chapter 4) confirm that the results presented above are consistent with past modeling efforts. Therefore, the results are considered acceptable for input into the frequency of occurrence analyses which follow.

Station	Latitude (degrees N)	Longitude (degrees W)	Depth (meters)	Depth (feet)
1	35.44	76.85	3.8	12.4
2	34.99	76.90	4.0	13.0
3	35.40	76.72	4.6	15.1
4	35.51	76.60	3.9	12.7
5	35.36	76.54	5.2	17.0
6	35.18	76.49	5.0	16.3
7	35.04	76.58	6.9	22.6
8	34.84	76.38	2.9	9.4
9	34.93	76.27	1.6	5.2
10	35.17	75.91	3.2	10.4
11	35.48	75.94	3.4	11.3
12	35.54	75.83	4.3	14.2
13	35.49	75.65	5.2	17.1
14	35.66	75.72	2.5	8.2
15	35.74	75.62	2.0	6.4
16	35.80	76.03	3.2	10.6
17	35.91	75.74	4.4	14.6
18	35.94	75.66	2.3	7.7
19	36.04	75.76	2.0	6.5
20	36.12	75.90	4.9	16.0
21	35.97	75.97	3.8	12.4
22	35.08	76.38	4.4	14.3
23	36.17	76.04	3.5	11.6
24	36.10	76.28	4.4	14.4
25	35.99	76.48	7.2	23.7
26	36.02	76.67	5.9	19.3

Table 3.1 Locations and depths of selected output stations.

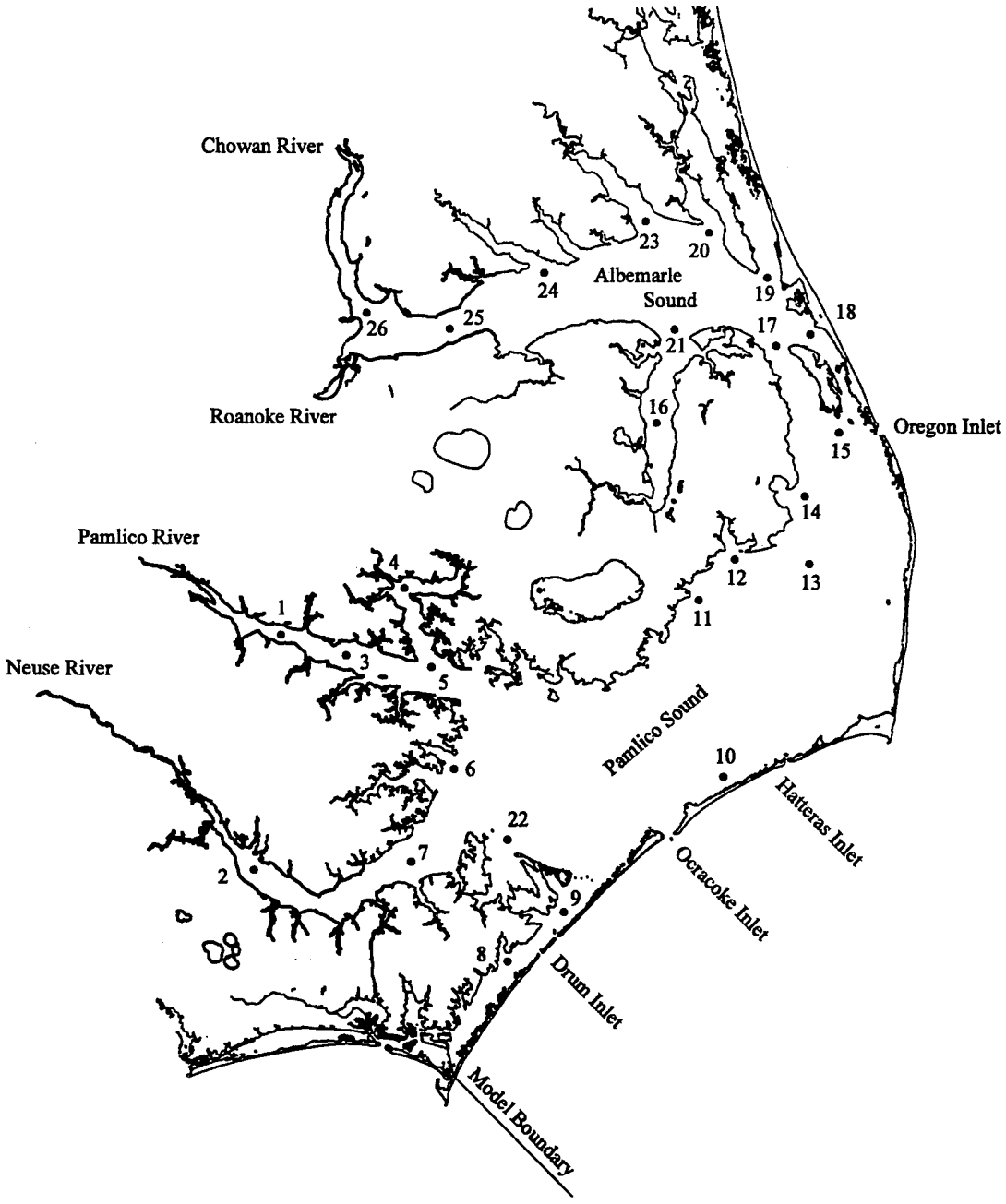

Figure 3.1 Study area with station numbers and locations. Station coordinates are presented in Table 3.1.

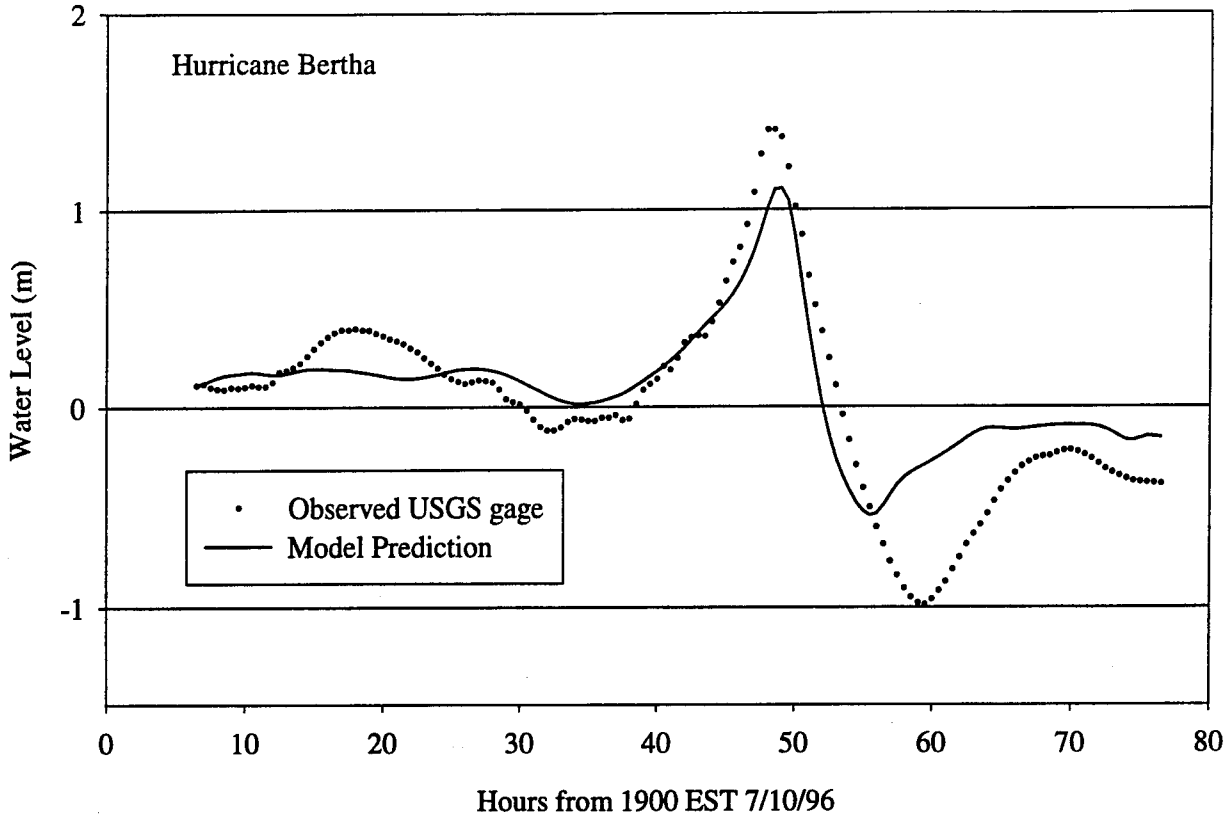

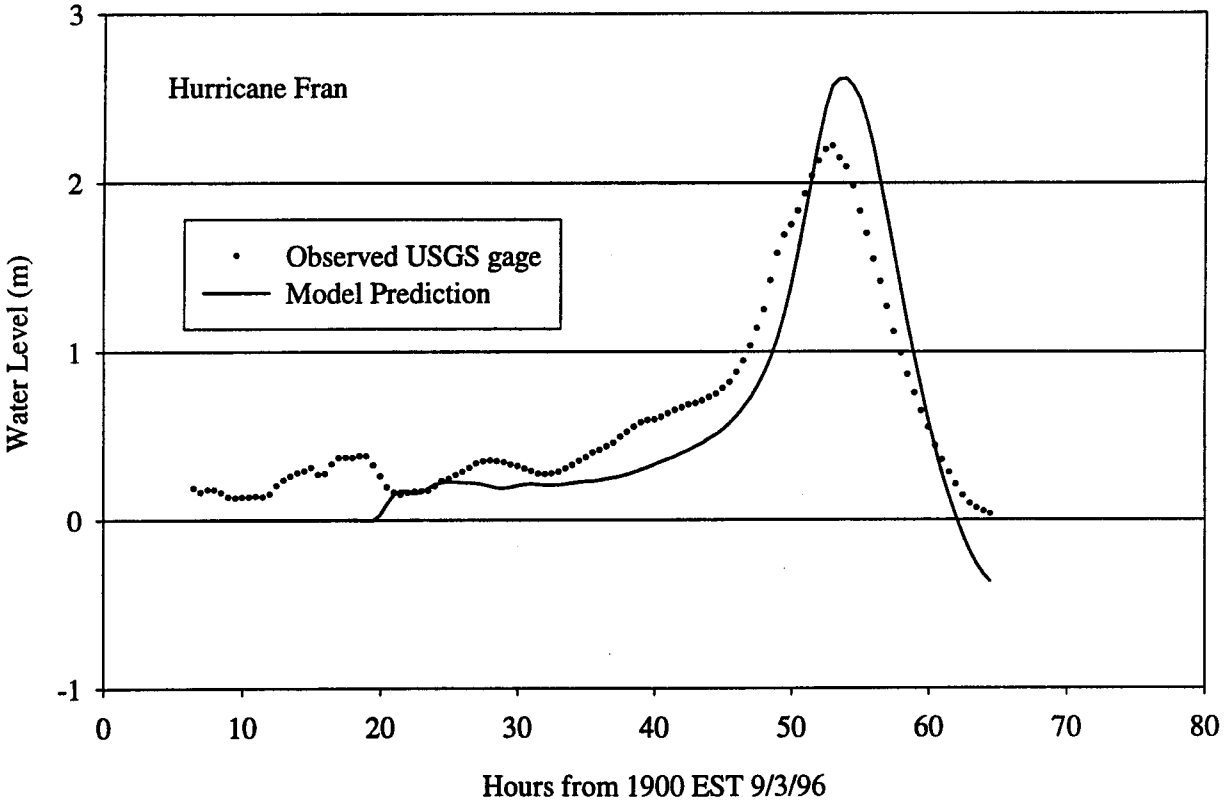

Figure 3.2 Model comparisons at New Bern, NC.

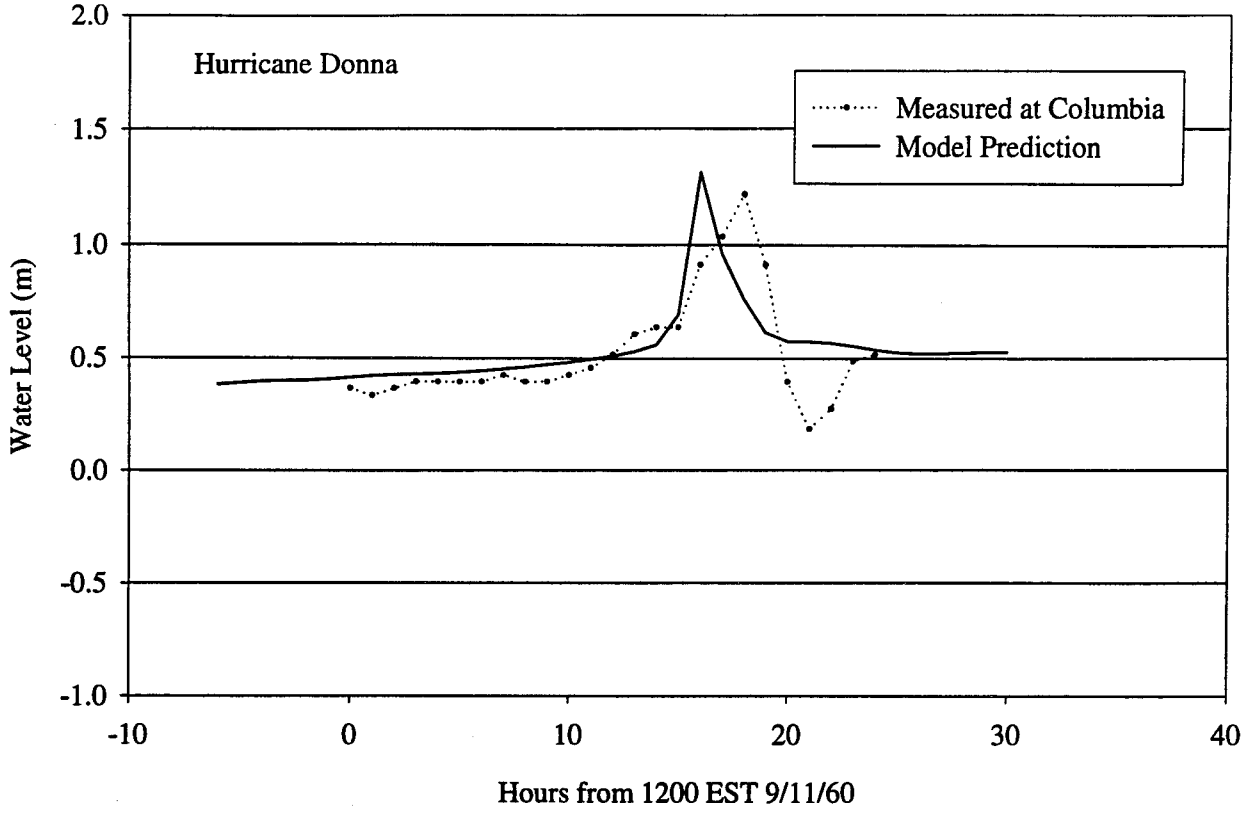

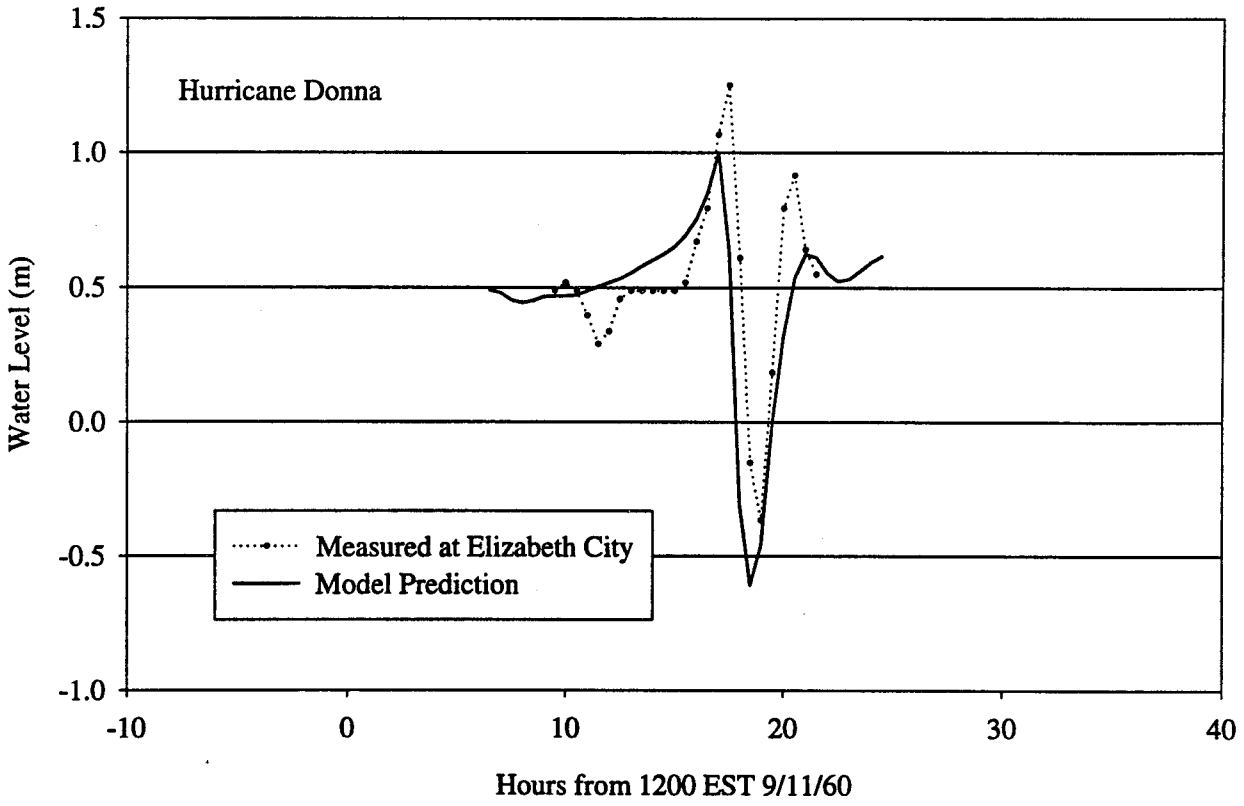

Figure 3.3 Model comparisons from Hurricane Donna.

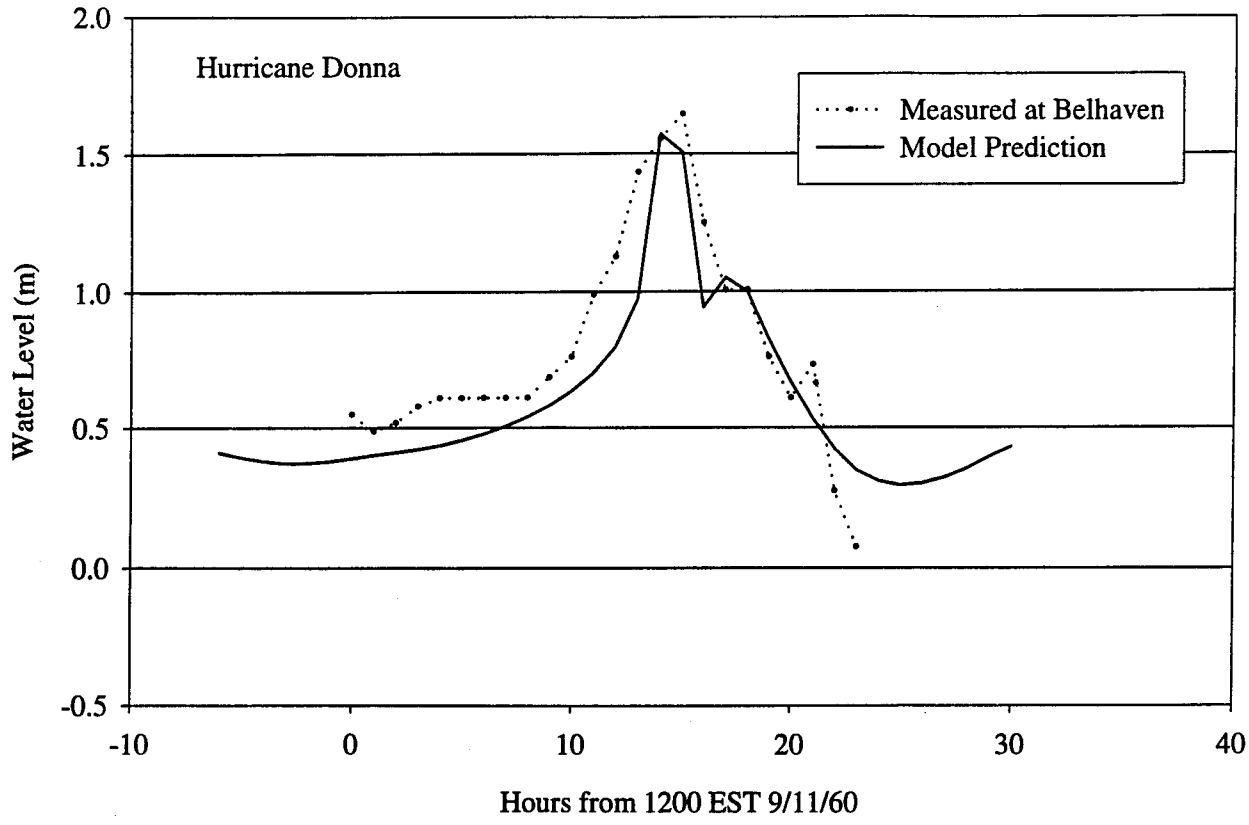

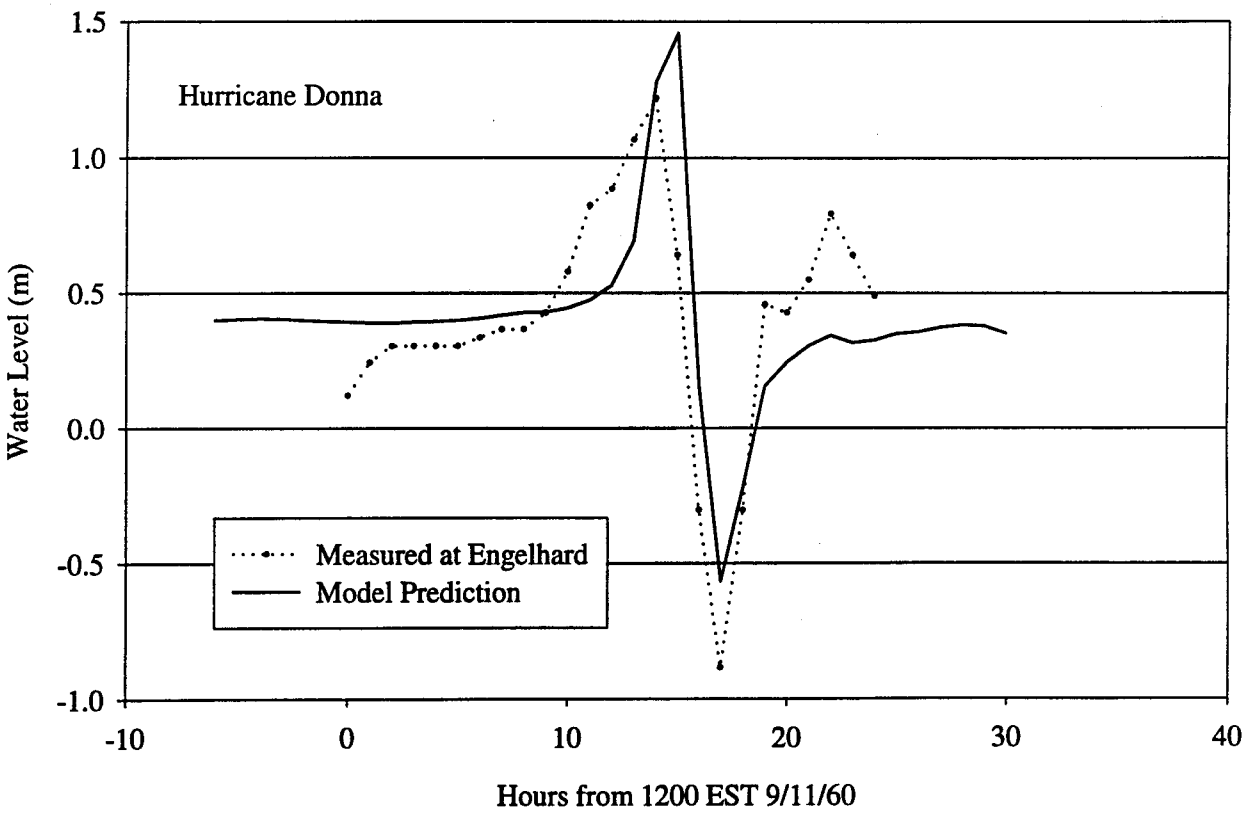

Figure 3.4 Model comparisons from Hurricane Donna.

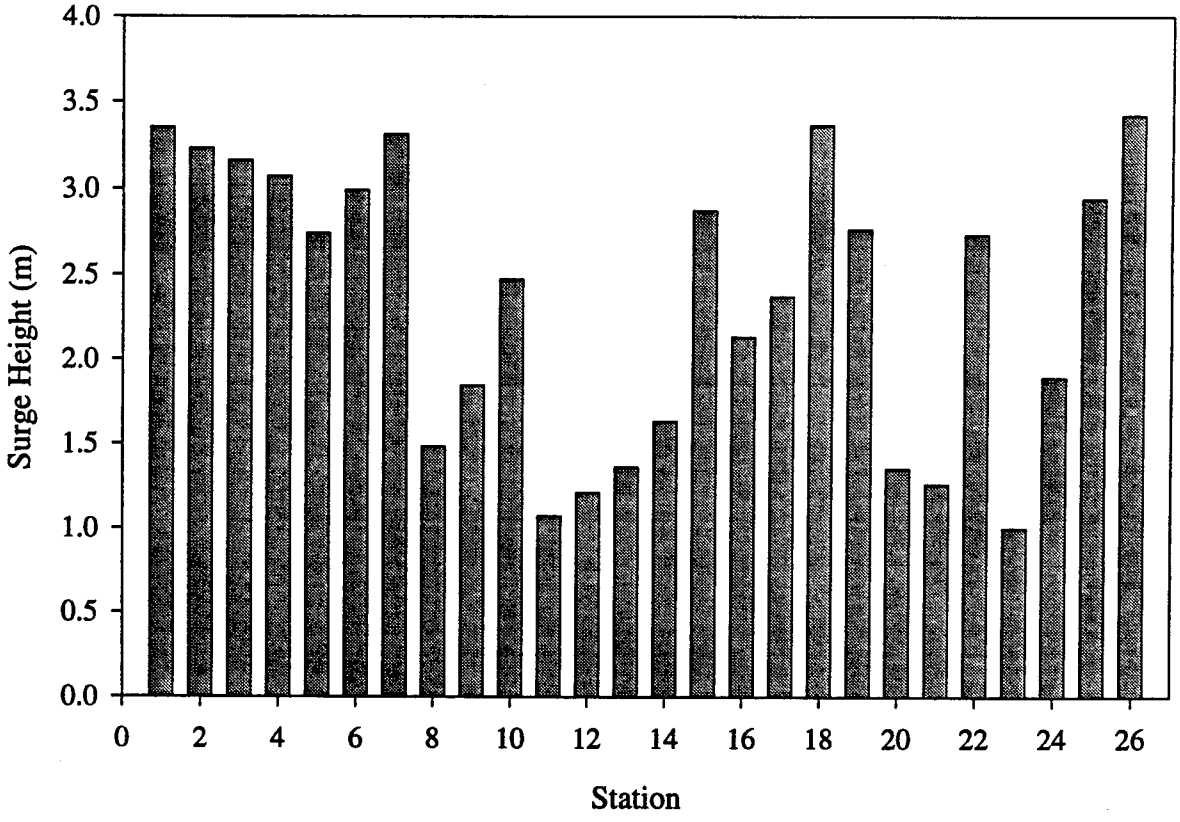

Figure 3.5 Maximum surge heights at output stations.

4. EMPIRICAL SIMULATION TECHNIQUE

4.1 Overview

Frequency of occurrence relationships for peak surge values were computed from the Empirical Simulation Technique (EST), a statistical procedure for simulating time sequences of non-deterministic, multiparameter systems. The EST is a general procedure which may be applied to estimate return periods ranging from days to years. Although the focus in the present case is peak surge values, recurrence rates for any result of a tropical storm, e.g., dune recession, could be estimated using the EST.

The EST is based on a bootstrap resampling technique, which uses storm characteristics and responses from a "training set" of events to generate N sets of a T-year sequence of events. The total population of events derived in this way are statistically similar, though not identical, to the original group of training set storms. This is because the training set storms are not simply resampled but rather are used to simulate a new population of events with a distribution of parameters which matches the training set storms.

Before discussing the EST in more detail it is useful to contrast the procedure with another common statistical technique, the Joint Probability Method (JPM). Until recently the JPM was commonly applied to problems of the current type, that is, estimating recurrence relationships for hurricane-induced surge. The basic assumptions in the JPM are that each storm may be characterized by a number of parameters (e.g., the radius to maximum winds, central pressure deficit, etc.) and that the probability of occurrence for each of these parameters may be described using an empirical relation. Furthermore, the JPM assumes that these parameters are independent, and thus the probability of an event is given by the product of the individual parameter probabilities as derived from the empirical relationships.

A number of difficulties arise with this technique. First, it requires a substantial number of simulations, as storms are derived from the convolution of all the storm parameters. This also raises the possibility that unrealistic events may be included in the storm simulations (e.g., a storm with large winds but low central pressure deficit). Second, the parameters are not truly independent but rather are related in a complicated way. Finally, the parameter probabilities are constant within a domain.

The EST addresses many of these concerns. The method requires simulations to be performed on only the training set storms and uses these results to "bootstrap" the frequency of occurrence simulations. Most importantly, the method makes no assumptions about how the parameters are related and further does not require empirical relationships to describe the probabilities (parameter probabilities are inherent in the database). The method may thus be described as "distribution free" and "non-parametric". In addition, the input parameters and hence results are site specific, and the multiple repetitions of sequences of events allows one to estimate the variability in the recurrence relationships.

Details of the EST and its implementation may be found in Scheffner et al., (1996) and Scheffner and Borgman (1997). The procedure is briefly outlined below.

4.2 Input and Response Vectors

The method relies on the specification of a set of input and response vectors, specific to each output station, which characterizes each storm in the training set. In the present study, the input vectors were derived from parameters of the storm at the closest point of approach (CPA) to each station. The input vectors included the 1) maximum wind speed, 2) central pressure deficit, 3) forward speed, 4) radius to maximum winds, 5)minimum distance from the eye to the station, 6) track direction and 7) bearing direction. The response vector for each event was the peak surge value predicted for the station.

The objective in selecting the training set events is to cover the parameter space of all historical events, such that the new population of events will be similar to storms which have actually occurred. Thus, removing storms from the training set which are similar to storms already in the training set is acceptable, as the removed storms are essentially redundant from the standpoint of the vector space. This was discussed previously in Chapter 2.

Each storm in the training set is assigned a segment of the total probability from 0 to 1. Hypothetical storms, such as the Hugo events included in the present study, may be included while assigning probabilities. The goal is to generate a probability distribution function similar to the historical events. In addition, probabilities are assigned such that storms near each other in parameter space have about equal probabilities. The parameters in the storm vectors are scaled (based on RMS values, with the exception of angles which are subjected to sine and cosine operations), and ranked in a "neighbor" table where the "nearness" of neighbors is determined from a weighted Euclidean distance. The neighbor table is the basis for the fundamental EST procedure described below.

4.3 EST Application

As noted above the EST program performs N simulations of a T year sequence of events. In the present study, N = 50 and T = 200. For each year, the simulation begins by selecting a random number from 0 to 1 to determine the number of storms specified to occur that year (n) based on a Poisson distribution:

$$P(s;\lambda) = \lambda^s \exp(-\lambda)/s! \qquad 4.1$$

where s = number of storms per year, λ = number of events/record length in years (= 0.35, or 36/102 in the present study) and P(s; λ) is the probability of experiencing s storms per year. Thus, in this study P(0;0.35) = 0.7047 and P(1;0.35) is 0.2466. Is the random number is less than P(0;0.35) then no storms occur; if it is between P(0;0.35) and P(0;0.35) + P(1;0.35) then one storm occurs, etc.

The program selects one of the n storms from the training set according to the probabilities assigned to the storms in the training set. The selected storm becomes the reference event. The simulated response for the current event starts from this reference event and incorporates a nearest neighbor interpolation technique as explained below:

> Let R_{ref} be the response for the reference event and $R_1, R_2, \ldots R_{numnay}$ be the responses for a variable number (numnay) of storms in the neighborhood of the reference event. The value of numnay equals the number of neighbors. The new simulated response is given by
>
> $$R = R_{ref} + \sum U_j(R_j - R_{ref}) \qquad 4.2$$
>
> where the summation runs from j to numnay (typically 3 or 4) and U_j is a normally distributed random number on the interval $-1/(2*numnay)$ to $1/(2*numnay)$. The procedure is repeated for each of the N years in the T year sequence.

The computation of frequency of occurrence for the responses is then performed. The cumulative probability distribution function for the response follows a Gumbel distribution:

$$P(X<X_r) = r/(n+1) \qquad 4.3$$

where r is the data rank (r = 1 is the smallest) and n = number of years (200). The probability for an n-year return event is given by

$$F(n) = 1 - (1/n) \qquad 4.4$$

where F(n) is the cumulative probability of occurrence for an event with a return period of n-years. The frequency of occurrence relationship of the response is obtained by linearly interpolating a response from Equation 4.3 which corresponds to the probability in Equation 4.4.

4.4 Results

The results for 25, 50 and 100 year return periods at each station are shown in Table 4.1 The EST results presented are mean values. EST results for all of the simulations, along with plots of the mean value and the mean +/- one standard deviation, are presented in Appendix B. The results are consistent with the peak surge values presented in Chapter 3; i.e., the largest values occur within the rivers and adjacent to model boundaries.

It is interesting to compare the EST results with results of the SLOSH model calculations performed for the Eastern North Carolina Hurricane Evacuation Study (USACE, 1987) Direct comparisons of the two models are difficult, as the SLOSH runs were performed for Category 1-5 Hurricanes (using parameters derived from the JPM) using assumed tracks (e.g., northeast, northwest, west, etc), while the EST are based on actual (or meteorologically

possible) storm events. Furthermore, the SLOSH results were estimated from contours adjacent to the 26 ADCIRC stations and are thus accurate to probably +/- 1 foot. However, as shown in Figure 4.1, a comparison of models yields several interesting observations:

- The distribution of surge in the two models is generally similar, as larger values occur near boundaries and small values occur in open water
- According to the EST analysis the SLOSH category 5 hurricanes appear to have a less than 100 year frequency of occurrence, which is expected from the historical record
- SLOSH category 3 hurricanes produce surge values on the order of the EST 50-year recurrence storms, also consistent with the historical record.
- SLOSH category 1 storms appear to occur more frequently than once in 25 years, on average.
- The two models produce surge values of approximately the same order of magnitude, with the exception of a few stations in Albemarle Sound. While an investigation of differences in the models is beyond the scope of the present work, these discrepancies may be related to 1) the coarse resolution in the SLOSH model grid over Albemarle Sound or 2) the influence of overland flow (simulated by SLOSH) in reducing surge values within the Sound.

The final step in producing the model boundary conditions is the characterization of the hydrographs based on the EST results. This topic is considered in Chapter 5.

Station	25 year		50 year		100 year	
	(feet)	(meters)	(feet)	(meters)	(feet)	(meters)
1	8.0	2.4	10.3	3.1	12.3	3.7
2	9.8	3.0	11.5	3.5	12.9	3.9
3	7.0	2.1	9.4	2.9	11.2	3.4
4	5.1	1.6	7.3	2.2	9.6	2.9
5	5.4	1.6	7.4	2.3	9.1	2.8
6	5.7	1.7	7.6	2.3	9.8	3.0
7	8.6	2.6	10.7	3.3	12.3	3.7
8	3.5	1.1	4.2	1.3	5.1	1.6
9	4.1	1.2	4.9	1.5	5.7	1.7
10	3.8	1.2	4.9	1.5	5.8	1.8
11	1.9	0.6	2.6	0.8	3.4	1.0
12	2.1	0.6	2.7	0.8	3.6	1.1
13	2.1	0.6	2.8	0.9	3.7	1.1
14	2.7	0.8	3.9	1.2	5.3	1.6
15	4.1	1.2	6.0	1.8	7.5	2.3
16	5.4	1.6	6.5	2.0	7.6	2.3
17	2.8	0.9	4.8	1.5	6.2	1.9
18	4.5	1.4	7.6	2.3	10.1	3.1
19	3.8	1.2	6.2	1.9	7.9	2.4
20	2.5	0.8	3.4	1.0	4.3	1.3
21	2.1	0.6	2.9	0.9	3.6	1.1
22	5.9	1.8	7.7	2.3	8.9	2.7
23	2.1	0.6	2.7	0.8	3.2	1.0
24	3.3	1.0	4.7	1.4	5.8	1.8
25	7.0	2.1	8.9	2.7	10.2	3.1
26	8.2	2.5	10.5	3.2	12.3	3.7

Table 4.1 Computed surge heights for 25, 50 and 100 year return periods.

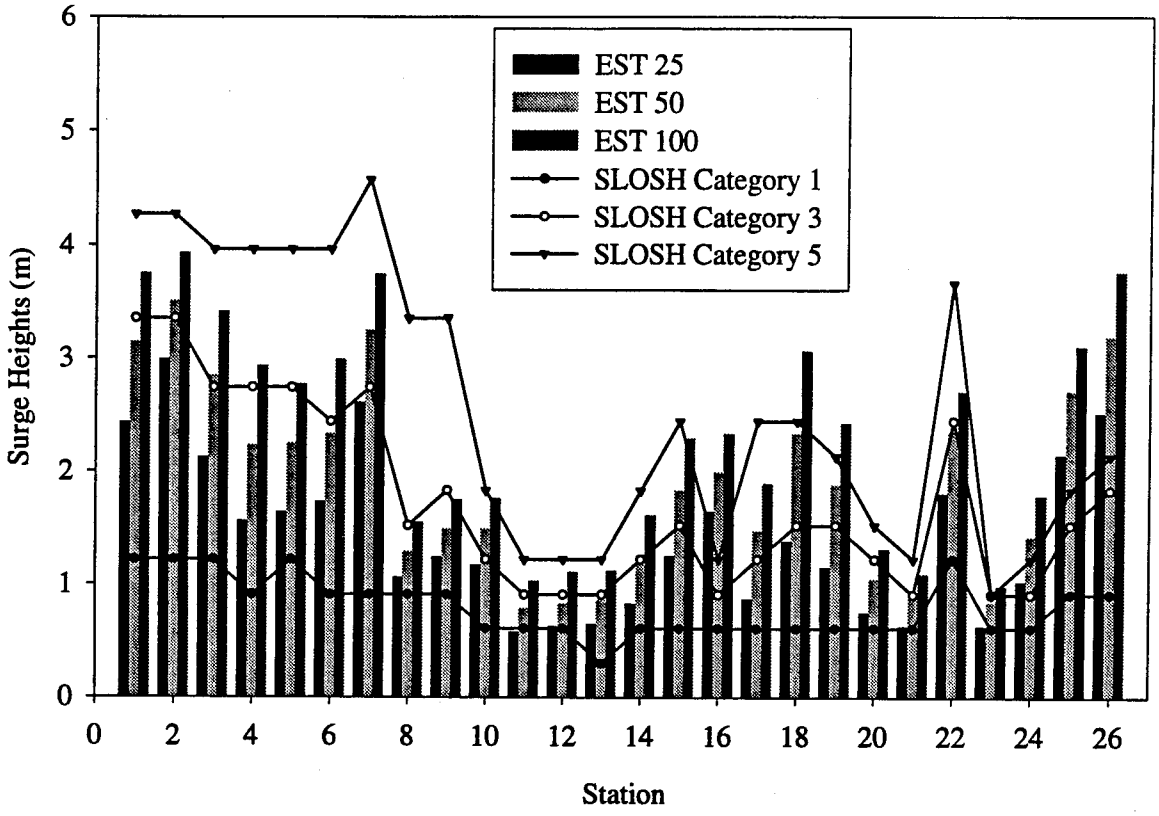

Figure 4.1 Comparisons of surge heights predicted with EST versus SLOSH model results. SLOSH results were estimated from contours closest to ADCIRC station locations for northwest storms.

5. CHARACTERIZATION OF DESIGN HYDROGRAPHS

5.1 Pooled-Fund Study Approach

When peak surge values are known for the recurrence interval of interest, the simplest method for developing the design hydrograph is to use a model equation. If it is assumed that a synthetic time series will suffice, an equation of the form:

$$S_t(t) = S_p(1-e^{-|D/t|}) \qquad 5.1$$

should be acceptable (Ayres Associates, 1997b). In 5.1, S_p is the peak surge value, D = R/f is the storm duration, R is the radius to maximum winds and f is the forward speed of the storm. The appropriate values of R and f can be derived from NWS data (Ho, et al, 1987). In the Pooled Fund Study, it was recommended that 50 percent values of these parameters be used; for Cape Hatteras, the 50 percent values of R (~30nm) and f (~15 kn) result in D~2 hours.

To incorporate the full effect of the storm surge, it is also suggested that the hydrograph in 5.1 be developed such that the peak is centered at hour 50:

$$S_t(t) = S_p(1-e^{-|D/(50-t)|}) \qquad 5.2$$

where it is recognized that $S_t(t) = S_p$ when t = 50 hours. Therefore, one approach for specifying boundary condition hydrographs would be to use 5.2 directly, with values of S_p taken from Table 4.1.

One difficulty with this approach is that 5.2 cannot represent periods of negative surge, and thus it may underestimate the slope of the hydrograph and hence the magnitude of the resulting current velocity at some locations. Figure 5.1 illustrates some examples. Four different stations from the Albemarle-Pamlico Sound study area are shown, with solid lines indicating the hydrographs predicted by the model for all of the training set storms. The diamonds depict the synthetic hydrograph shape described by 5.2.

As shown in Figure 5.1, the synthetic shape given by Equation 5.2 is probably adequate at Station 2 and possibly Station 25. At these stations, the synthetic shape (with no negative surge component) gives a reasonable approximation of most of the hydrographs predicted by the model. However, at the remaining two stations (16 and 17), significant negative peaks were predicted by the surge model prior to as well as after the positive peaks. The surface slope suggested by these curves could result in significant flood and/or ebb velocities which Equation 5.2 cannot reproduce.

Since a number of stations in the Albemarle-Pamlico study area exhibited negative peaks an attempt was made in the present study to address the potential inadequacy of 5.2. The approach is outlined below.

Before proceeding it should be noted that while in some instances the negative surges result from overpredicted wind speeds (see Chapter 3), there are measured hydrographs from actual events (e.g., Hurricane Donna and others) which confirm that large negative peaks can occur. In addition, popular accounts suggest that under certain circumstances areas of the sounds may become dry (Barnes, 1995). The spurious events are considered to be those in which the negative surge exceeds the water depth, a condition numerically possible when finite amplitude effects are ignored. In the analysis presented below consideration is given to the water depth at each station when developing the hydrograph shape.

5.2 Empirical Approach

The approach adopted is purely empirical, based on a nonlinear regression analysis via the Levenberg-Marquardt method. The method was developed by first fitting a damped sine wave:

$$S_t(t)= A\sin(Bt+C)*(1-e^{-|D/(50-t)|}) \qquad 5.3$$

to the 39 predicted hydrographs at each station, where A, B, C and D are parameters to be fit by the regression (and $S_t(t)= A\sin(Bt+C)$ for t=50). Next, "candidate" parameter sets were obtained at each station by eliminating parameters which produced correlation coefficients less than 0.75. Since many adjacent hydrographs exhibit similar shapes, candidate sets could be roughly grouped together. Finally, graphical comparisons of the synthetic and predicted hydrographs led to the selection of four "characteristic" curves which reasonably approximate the predicted hydrograph shapes.

These four characteristic curves, denoted as Type 1 through Type 4, are illustrated in Figure 5.2 by plotting them on the same stations used in Figure 5.1. As shown in the figure these curves provide a better fit to the predominant shape than the single curve given by 5.2. While each of these curves overestimates the curvature in the predicted shape, this was necessary in order to more closely approximate the hydrograph slope. The effect of the increased curvature is expected to be small. For comparison, the four empirically derived curves are replotted along with 5.2 in Figure 5.3.

Essentially this empirical approach is equivalent to using the predicted hydrographs for a particular storm as the design hydrograph. The approach presented here simply describes a characteristic hydrograph using a functional form, and has the advantage of producing a hydrograph with a peak corresponding to a particular recurrence interval. Table 5.1 contains the model equation, parameter values and applicable stations for these empirically derived shapes. The recommended application procedure is provided below.

5.3 Application Procedure

The following procedure is recommended when developing boundary condition hydrographs:

- The closest station to the area of interest is first selected from Figure 3.1 or Table 3.1. This is used for selecting both the peak surge value and the curve type for the synthetic hydrograph.
- The appropriate peak surge value for that station is obtained from Table 4.1.
- A 100 hour hydrograph is developed using Equation 5.4, the parameters included in Table 5.1, and the selected peak surge value.

$$S_t(t) = S_p * A\sin(Bt+C) * (1-e^{-|D/(50-t)|}) \qquad 5.4$$

- A second 100 hour hydrograph (consistent with the pooled fund approach) can also be determined using equation 5.2.
- Both hydrographs are used to determine worst-case velocity conditions to be used in the scour analysis.

Curve Type	A	B	C	D	Stations
1	-1.50	0.14	5.38	-9.07	1-9, 22
2	1.06	0.23	-4.18	4.46	16, 18, 19, 23
3	1.95	0.16	4.84	4.16	11-15, 17, 20, 21
4	-1.60	0.13	-0.89	-1.27	10, 24-26

Table 5.1 Parameter values and applicable stations for synthetic curve types 1 through 4.

Therefore, the recommended procedure involves creating two hydrographs, and then running the local hydraulic model using both hydrographs as boundary conditions to determine a worst case. In many cases the curve given by 5.2 may produce the largest velocities, as the hydrograph slope for this curve is generally steeper than the curves by Equation 5.4 and the parameters given in Table 5.1.

Although beyond the scope of the present study, consideration should also be given to the effect of wind stress on the water surface when applying local hydraulic models. This wind stress would apply a forcing in addition to the hydrographs developed herein and could have an impact on the predicted velocities at highway structures. The simplest approach would be to specify a wind stress along the axis of the river, in the same direction as the hydrograph induced flow, using wind speeds developed from hurricane data (e.g., Ho et al, 1987).

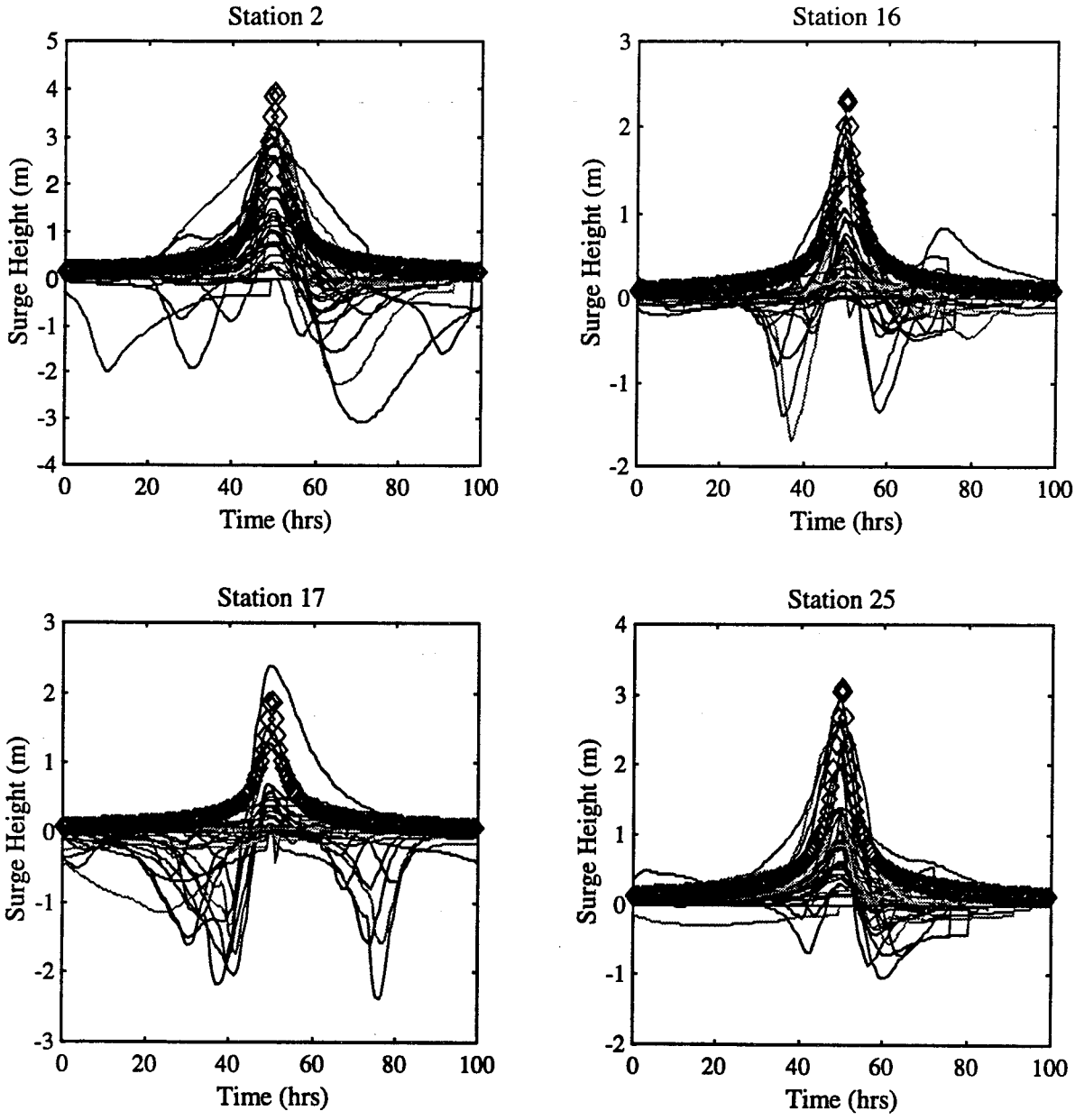

Figure 5.1 Comparisons of pooled fund synthetic hydrograh with predicted hydrographs at selected stations.

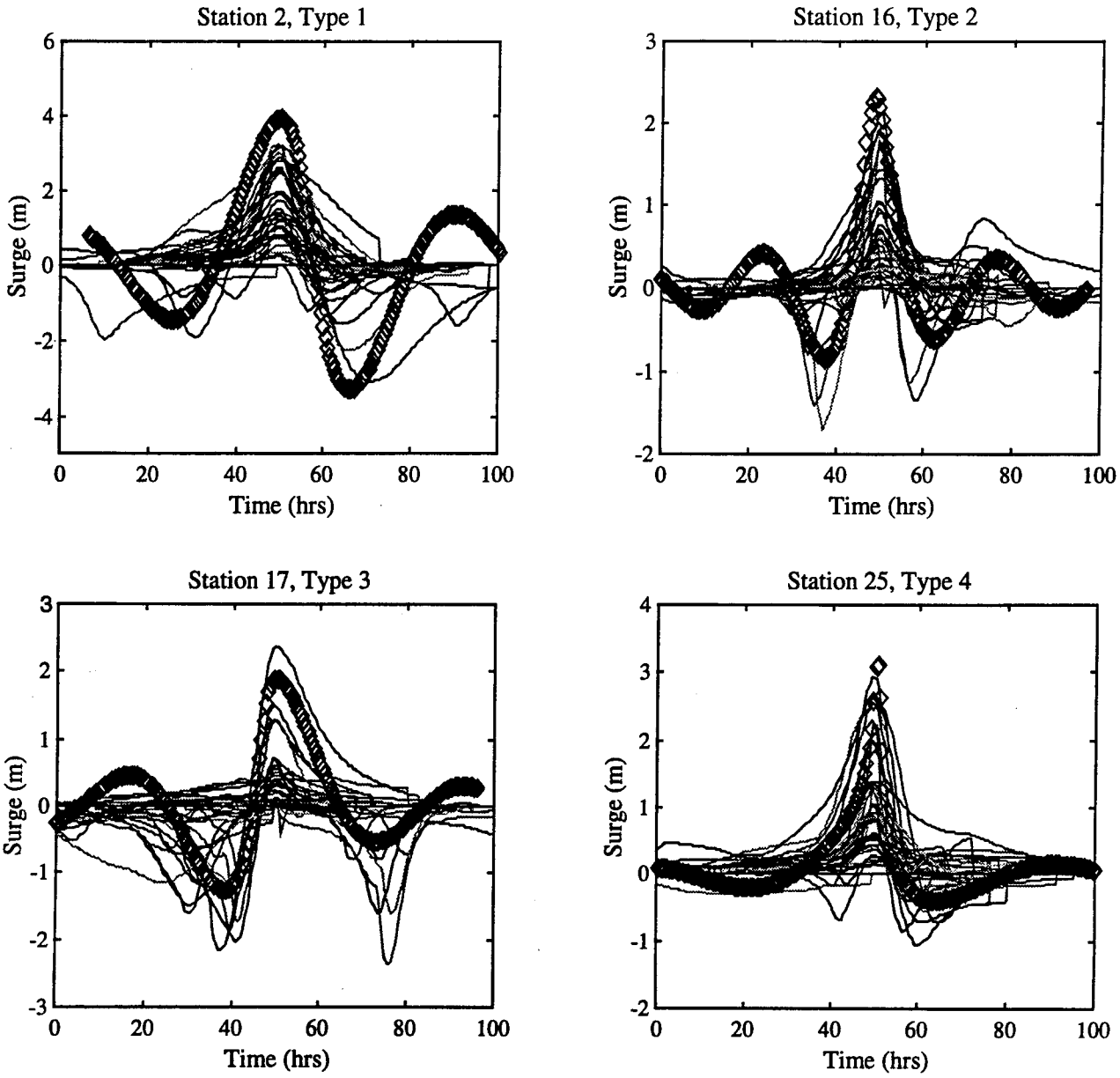

Figure 5.2 Comparisons of hydrograph curve types 1 through 4 with predicted hydrographs.

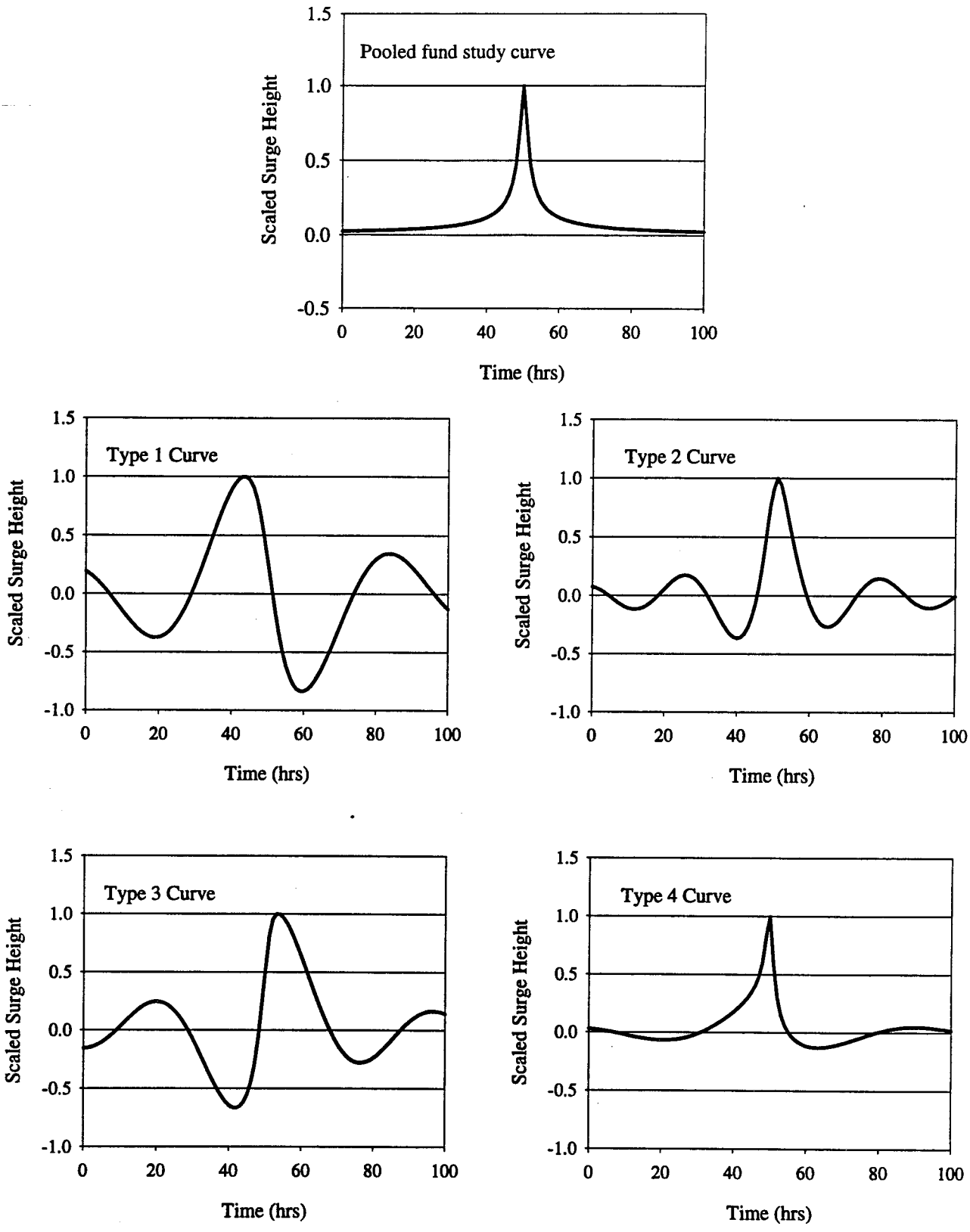

Figure 5.3 Pooled fund study synthetic hydrograph and curve types 1 through 4.

6 CONCLUSIONS

The purpose of this study is to determine surge hydrographs which may be used in the analysis of proposed and existing highway structures along Albemarle-Pamlico Sounds. The surge hydrographs were developed at multiple locations within the Sounds and are based on model simulations and statistical analysis of historical storm events.

Historical data for tropical storms over the period 1886-1996 were collected and analyzed to identify storms proximate to the project study area. A review of these data identified 87 storms, from which 36 storms were selected for model simulations. A statistical analysis of the selected storms suggests that the selected database, though quite similar to the original data, focuses on the strongest events which are closest in proximity and track to the Albemarle-Pamlico study area. The selected database of 36 historical events was augmented by including 3 hypothetical events which are considered meteorologically possible.

The numerical modeling of the selected events was performed using two separate process models: the CE Wind Model (Cardone et al., 1992) for simulation of the hurricane wind field and the ADCIRC Model (Luettich, et al., 1992) for simulation of the water level response. The modeling procedure consisted of first running the CE Wind model for each storm using input from the NWS Hurricane database. The wind fields generated by the CE Wind model were then used to force the surge calculations in ADCIRC. Comparisons of model results with measured wind fields and surge hydrographs suggest that the models are capable of producing peak surges and hydrograph shapes which reasonably approximate measured data.

The goal of the process modeling was to develop a set of peak surges at each station, which were then used to develop frequency of occurrence relationships computed from the Empirical Simulation Technique (EST). The EST is a statistical procedure for simulating time sequences of non-deterministic, multiparameter systems, and is based on a bootstrap resampling technique. In the present study the EST used storm characteristics and responses from the "training set" of 39 events to perform 50 simulations of a 200 year sequence of events. The only assumption is that the simulated population of events are statistically similar to events which have actually occurred.

Application of the EST resulted in predicted surge values at 25, 50 and 100 year return periods. These peaks were then incorporated into synthetic time series used to characterize the shape of the design hydrograph. The results of the surge modeling suggest that the simple exponential form of the hydrograph, recommended by the pooled fund study, may be inadequate to characterize stations that experience periods of negative surge. An empirical approach based on a damped sine wave was developed as an alternative. The recommended procedure for implementing the results of the study suggests that both types of hydrographs be modeled, with design parameters based on the worst-case conditions.

7. REFERENCES

Ayres Associates, 1997a. "Development of Hydraulic Computer Models to Analyze Tidal and Coastal Stream Hydraulic Conditions at Highway Structures," Phase II for the Pooled Fund Study SPR-3(22), FHWA Report: FHWA/SC97/04, South Carolina Department of Transportation, Columbia, South Carolina.

Ayres Associates, 1997b. "Tidal Hydraulic Modeling for Bridges Users Manual" Pooled Fund Study HPR552, Development of Hydraulic Computer Models to Analyze Tidal and Coastal Stream Hydraulic Conditions and Highway Structures, Phase II. Fort Collins, CO.

Barnes, J.T. 1995. North Carolina's Hurricane History, University of North Carolina Press, Chapel Hill, NC.

Cardone, V.J., Greenwood, C.V. and Greenwood, J.A., 1992. "Unified Program for the Specification of Hurricane Boundary Layer Winds over Surfaces of Specified Roughness," Contract Report CERC-92-1, US Army Engineer Waterways Experiment Station, Vicksburg, MS.

Cardone, V. J., Cox A.T., Greenwood A.J., and Thompson E.F., 1994. "Upgrade of Tropical Cyclone Surface Wind Field Model," Miscellaneous Paper CERC-94-14, US Army Engineer Waterways Experiment Station, Vicksburg, MS.

Davidson, R.P., 1961. "Report on the Tropical Hurricane of September 1960 (Donna)," US Army Corps of Engineers Wilmington District, Wilmington, NC.

Edge, B.L., Scheffner, N.S. and Fisher, J.S., 1998. "Determination of Velocity in Estuary for Bridge Scour Computations," *Journal of Hydraulic Engineering, 124*, 619-628.

Froehlich, D.C., 1996. "Finite Element Surface Water Modeling System: Two-Dimensional Flow in a Horizontal Plane," FESWMS-2DH Version 2 Users' Manual, US Department of Transportation, Federal Highway Administration, Research, Development and Technology, Turner-Fairbank Highway Research Center, McLean, VA.

Garcia, A. W., 1995. "Surface Wind Analyses and Storm-Surge Effects of Hurricane Emily on the Outer Banks of North Carolina," Miscellaneous Paper CERC-95-9, US Army Engineer Waterways Experiment Station, Vicksburg, MS.

Hearn, C.J., and Hunter, J.R., 1990. "A Note on the Equivalence of Some Two- and Three-Dimensional Models of Wind-Driven Barotropic Flow in Shallow Seas," *Applied Mathematical Modeling,* 140, 553-556.

HEC, 1996. "UNET-One-dimensional Unsteady Flow Through a Full Network of Open Channels" Users' Manual, CPD-66 Version 3.1, US Army Corps of Engineers, Hydraulic Engineering Center , Davis, CA.

Ho, F.P., Su, J.C., Hanerich, K.L. and Smith, R.J., 1987. "Hurricane Climatology for the Atlantic and Gulf Coasts of the United States," NOAA Technical Report NWS-38. National Weather Service, US Department of Commerce, Washington, DC.

Jelesnianski, C.P. and Taylor, A.D., 1973. "A Preliminary View of Storm Surges Before and After Storm Modifications", NOAA Technical Memorandum ERL WMPO-3. Weather Modification Program Office, Boulder, CO.

Luettich, R.A., Westerink, J.J., and Scheffner, N.W., 1992. "ADCIRC: An Advanced Three-Dimensional Circulation Model for Shelves, Coasts and Estuaries; Report 1, Theory and Methodology of ADCIRC 2DDI and ADCIRC 3D-L", Technical Report DRP-92-6, US Army Engineer Waterways Experiment Station, Vicksburg, MS.

Luettich, R.A., Jr., Hu, S. and Westerink, J.J., 1994. "Development of the Direct Stress Solution Technique for Three-Dimensional Hydrodynamic Models Using Finite Elements," *International Journal for Numerical Methods in Fluids,* 19, 295-319.

Mark, D. J., and Scheffner, N.W., 1994. "Validation of a Continental-Scale Storm Surge Model for the Coast of Delaware," *Estuarine and Coastal Modeling, Proceedings, 3rd International Conference*, 249-263.

National Weather Service, 1979. "Meteorological Criteria for Standard Project Hurricane and Probable Maximum Hurricane Windfields, Gulf and East Coasts of the United States," NOAA Technical Report NWS 23, Washington D.C.

Pietrafesa, L.J., and Janowitz, G.S., 1991. "The Albemarle Pamlico Coupling Study," Final Report, Pamlico Estuarine Study Project 90-13, NCSU, Raleigh, North Carolina.

Pietrafesa, L.J., Janowitz, G.S., Chao, T.-Y., Weisberg, R.H., Askari, F. and Noble, E., 1986. "The Physical Oceanography of Pamlico Sound," Sea Grant Pub. UNC-WP-86-5, NCSU, Raleigh.

Scheffner, N.W., Borgman, L.E. and Mark, D.J., 1996. "Empirical Simulation Technique Based Storm Surge Frequency Analyses," *Journal of Waterway, Port, Coastal, and Ocean Engineering,* 122, 93-101.

Scheffner, N.W., and Butler, H.L., 1996. "Storm Surge Frequency Computations for Long Island, NY: A Comparison of Methodologies," *Estuarine and Coastal Modeling, Proceedings, 4th International Conference*, 80-91.

Scheffner, N.W. and Borgman, L.E., 1997. "Users' Guide to the Use and Application of the Empirical Simulation Technique", Draft Technical Report CHL-97-00, US Army Engineer Waterways Experiment Station, Vicksburg, MS.

US Army Corps of Engineers, 1987. "Eastern North Carolina Hurricane Evacuation Study", Technical Data Report prepared for the North Carolina Division of Emergency Management. US Army Corps of Engineers Wilmington District, Wilmington, NC.

Westerink, J.J., Luettich, R.A., and Scheffner, N.W., 1993. "ADCIRC: An Advanced Three-Dimensional Circulation Model for Shelves, Coasts, and Estuaries, Report 3, Development of a Tidal Constituent Database for the Western North Atlantic and Gulf of Mexico" Technical Report DRP-92-6, US Army Engineer Waterways Experiment Station, Vicksburg, MS.

Xie, L., and Pietrafesa, L.J., 1995. "Modeling the Flooding Around the Pamlico-Albemarle Sounds Caused by Hurricanes, Part II: Predicting the Flooding Caused by Emily," *21st Conference on Hurricanes and Tropical Meteorology,* American Meteorological Society, Miami, FL.

APPENDIX A

Histograms of Surge Heights

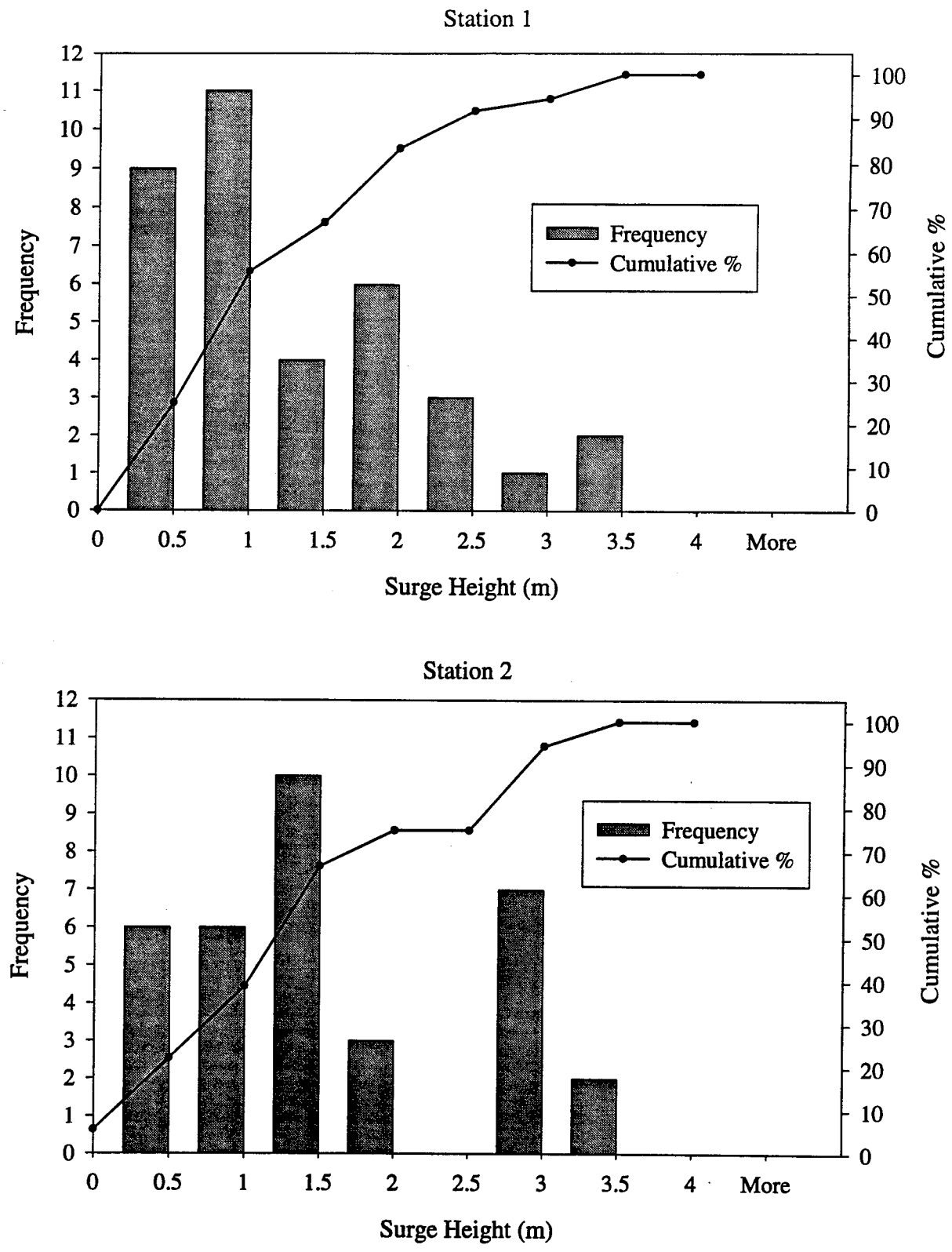

Figure A.1 Histograms of Surge Heights, Stations 1 and 2.

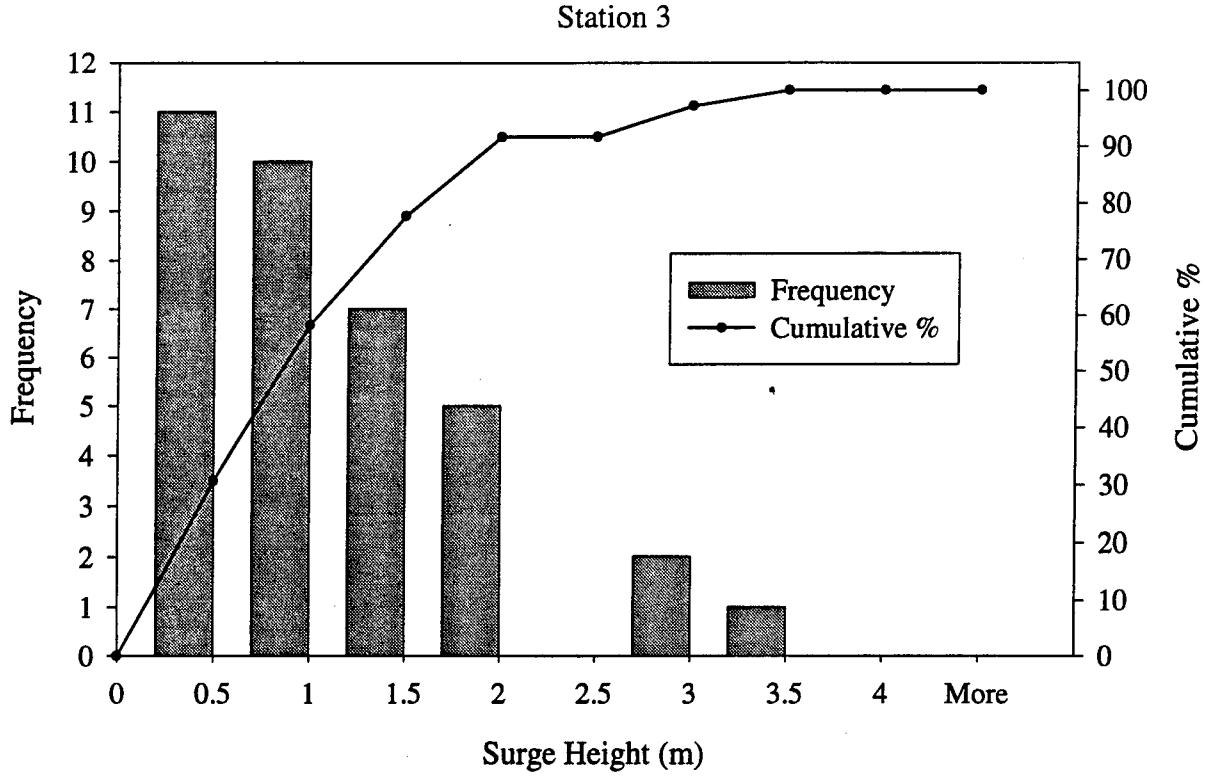

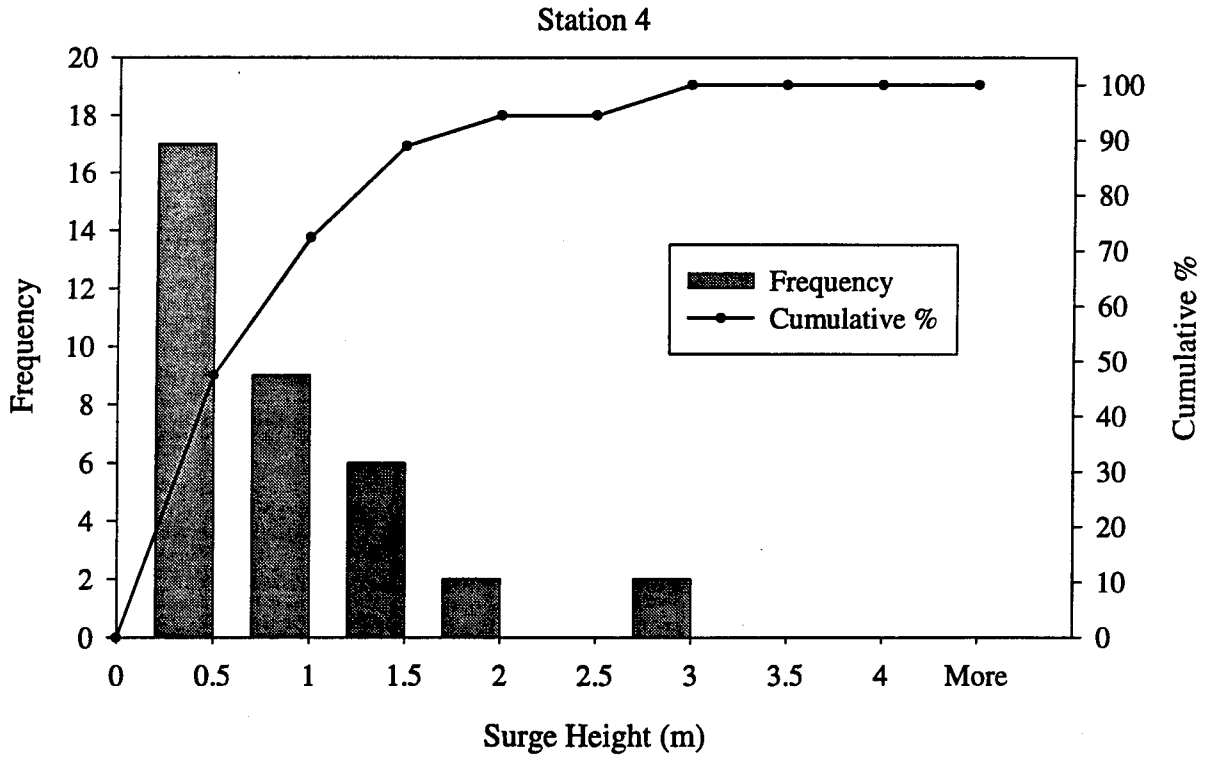

Figure A.2 Histograms of Surge Heights, Stations 3 and 4.

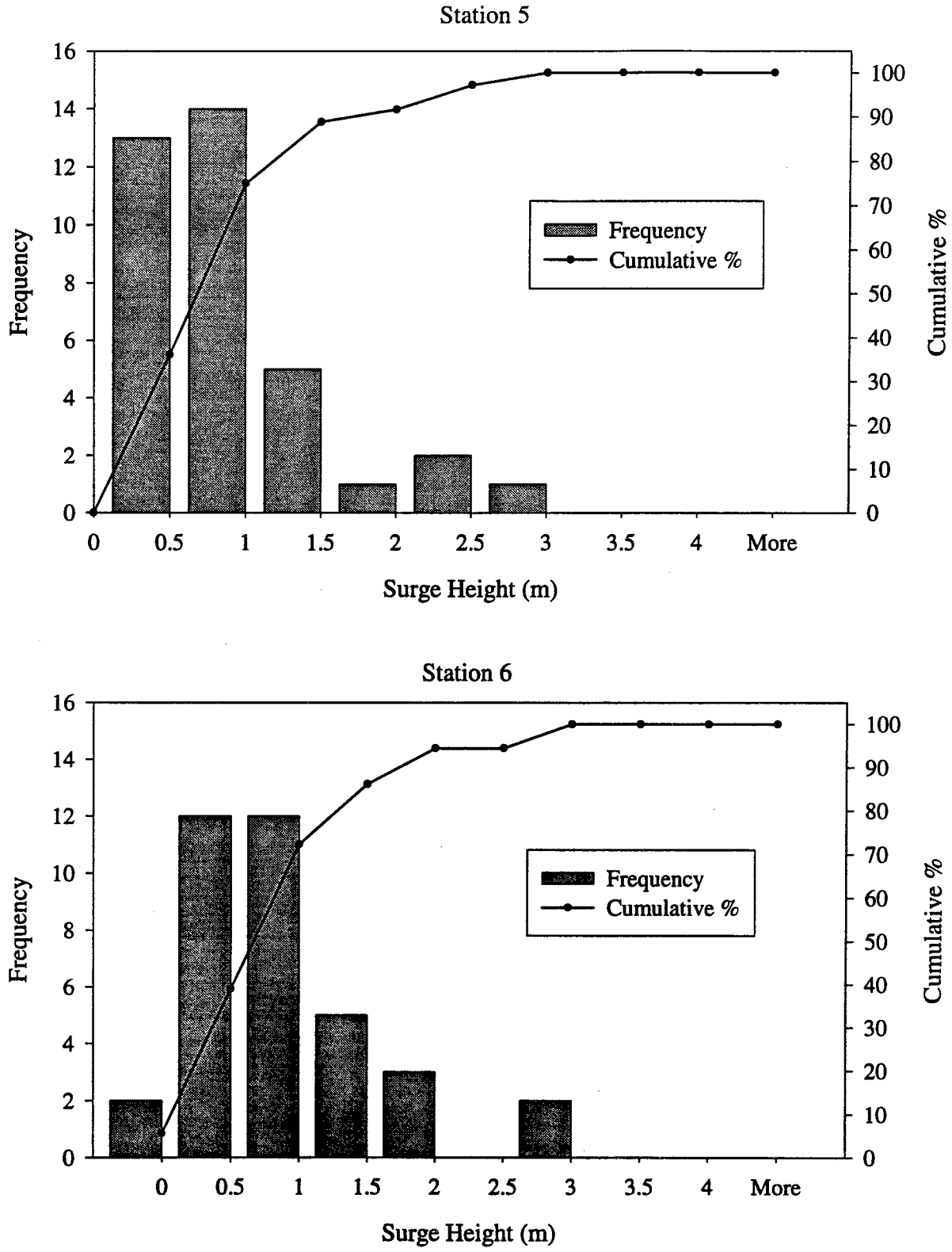

Figure A.3 Histograms of Surge Heights, Stations 5 and 6.

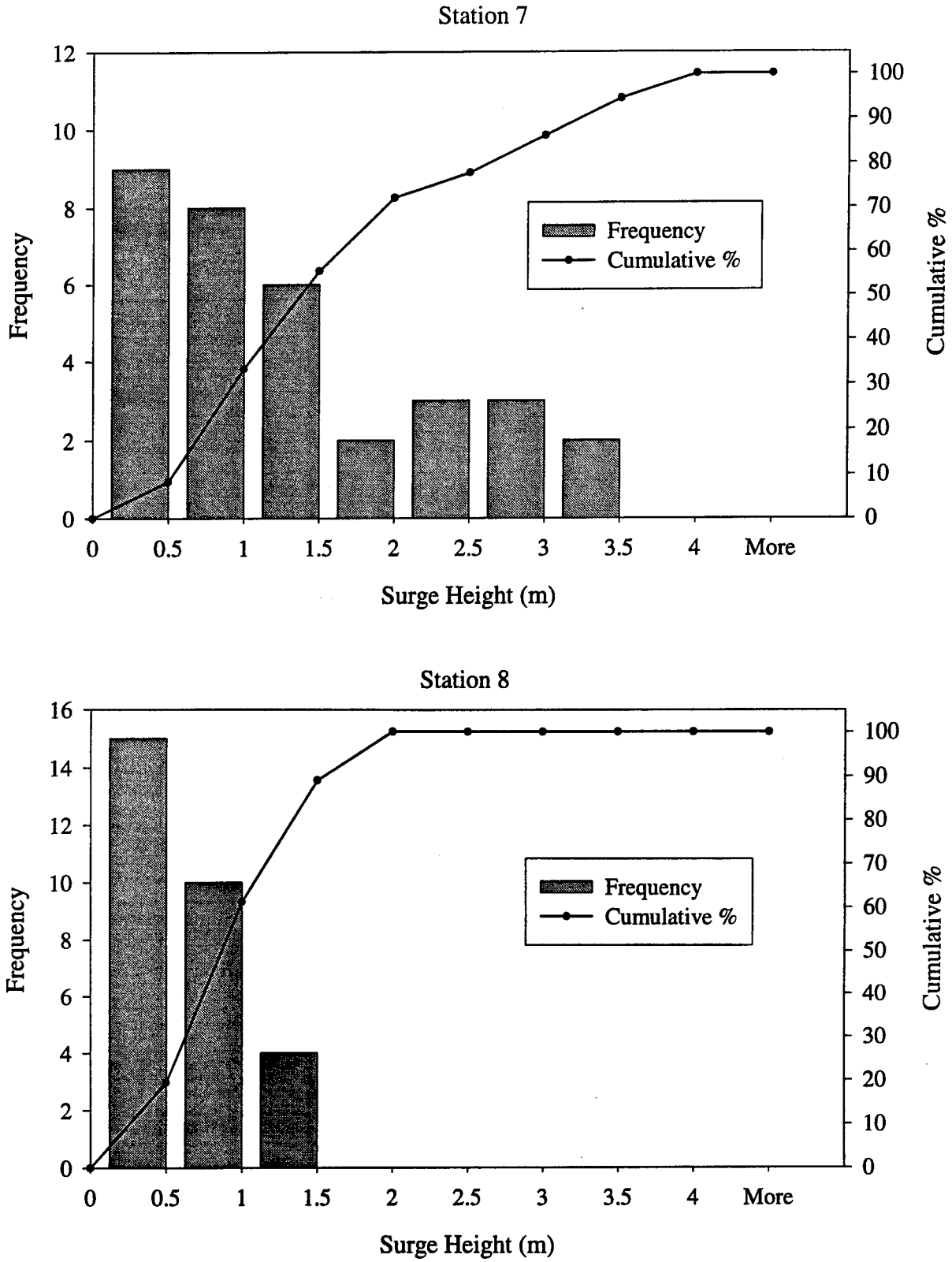

Figure A.4 Histograms of Surge Heights, Stations 7 and 8.

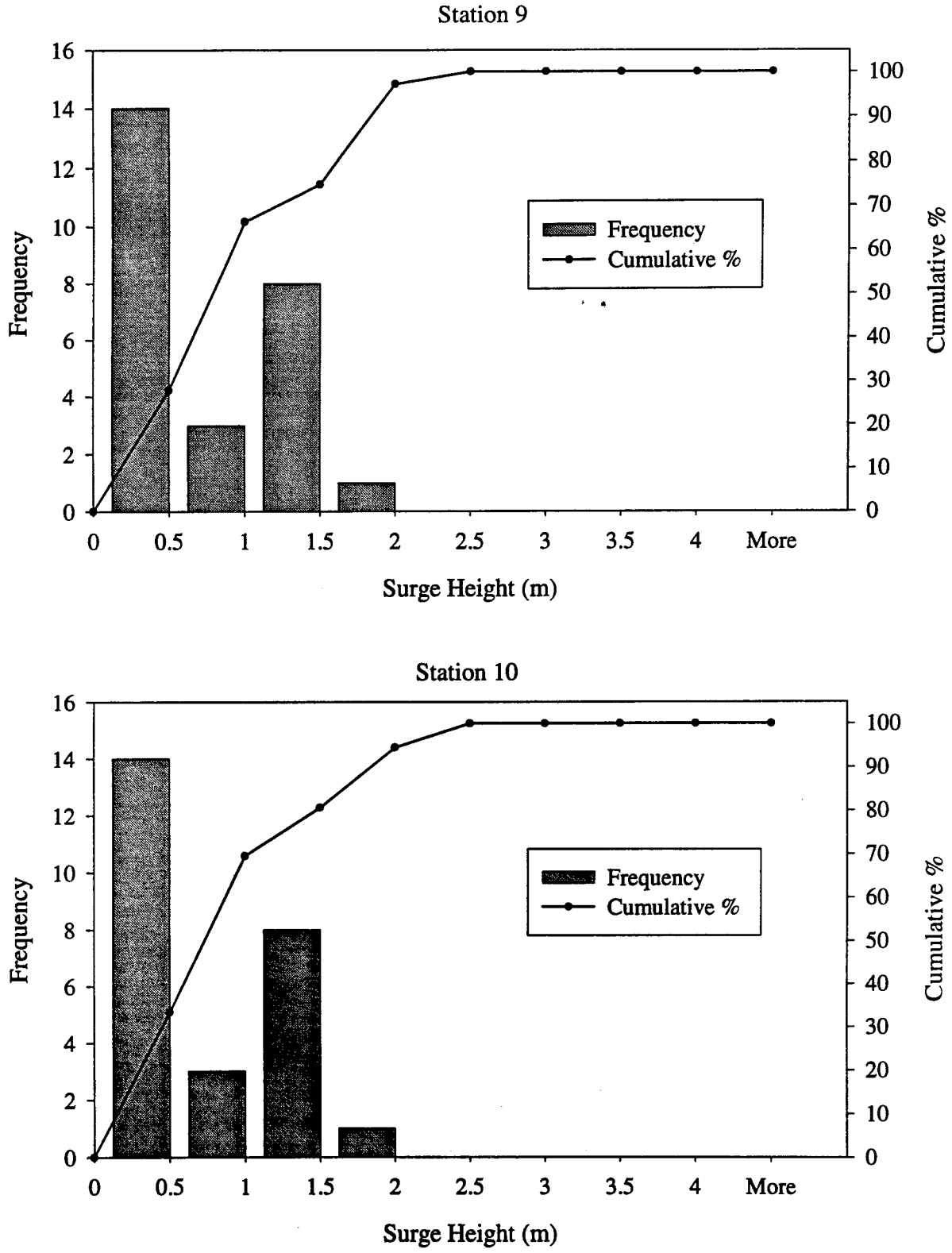

Figure A.5 Histograms of Surge Heights, Stations 9 and 10.

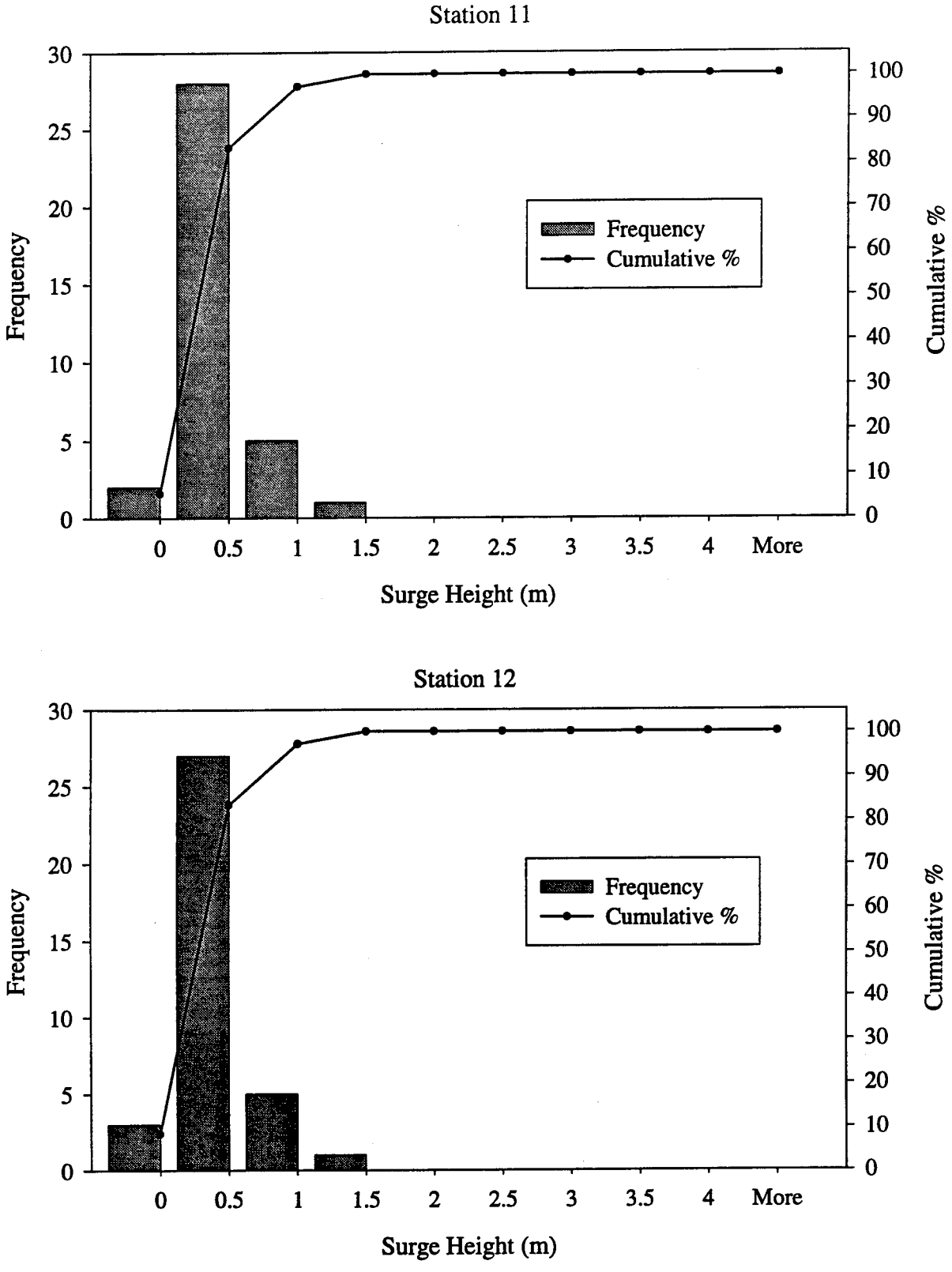

Figure A.6 Histograms of Surge Heights, Stations 11 and 12.

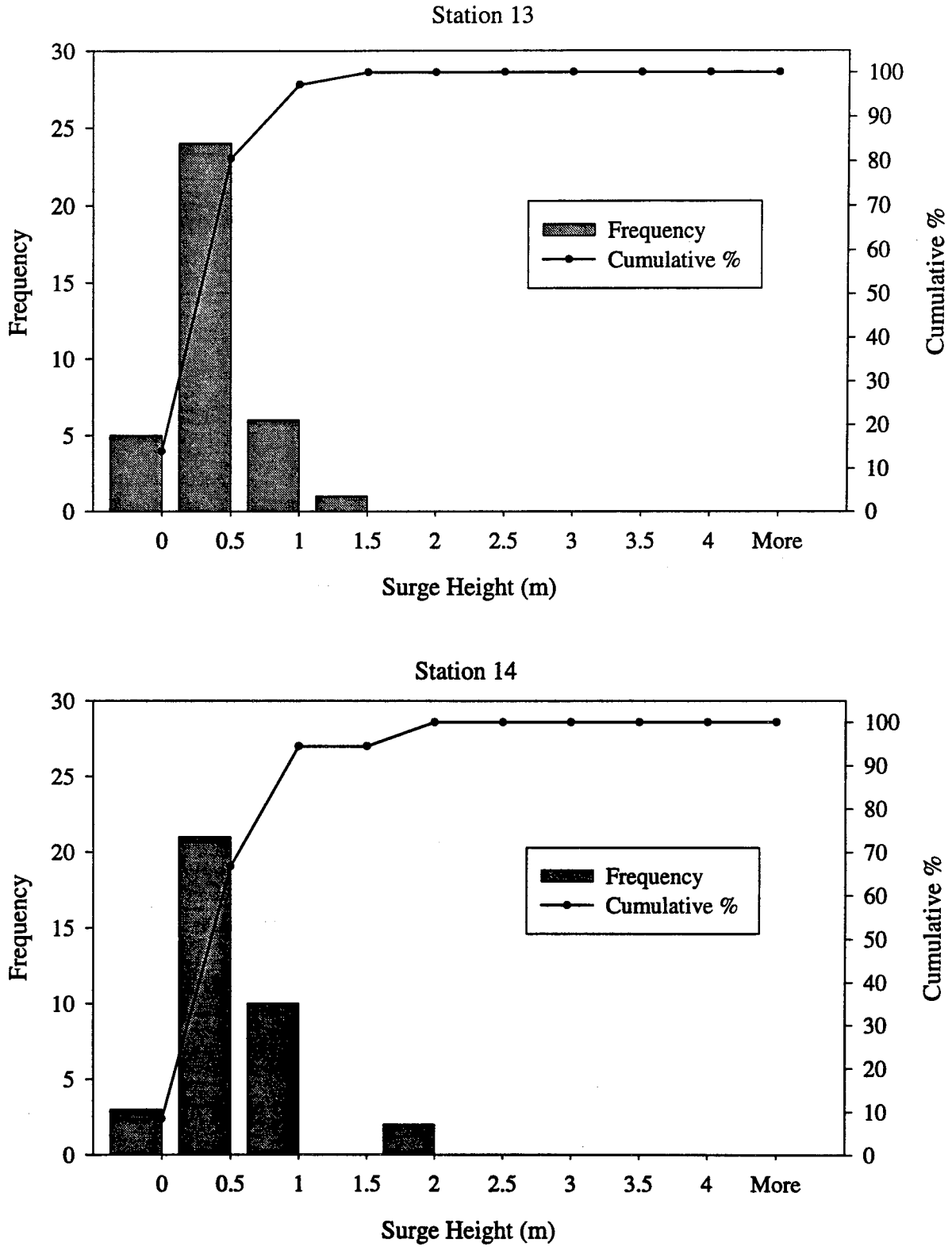

Figure A.7 Histograms of Surge Heights, Stations 13 and 14.

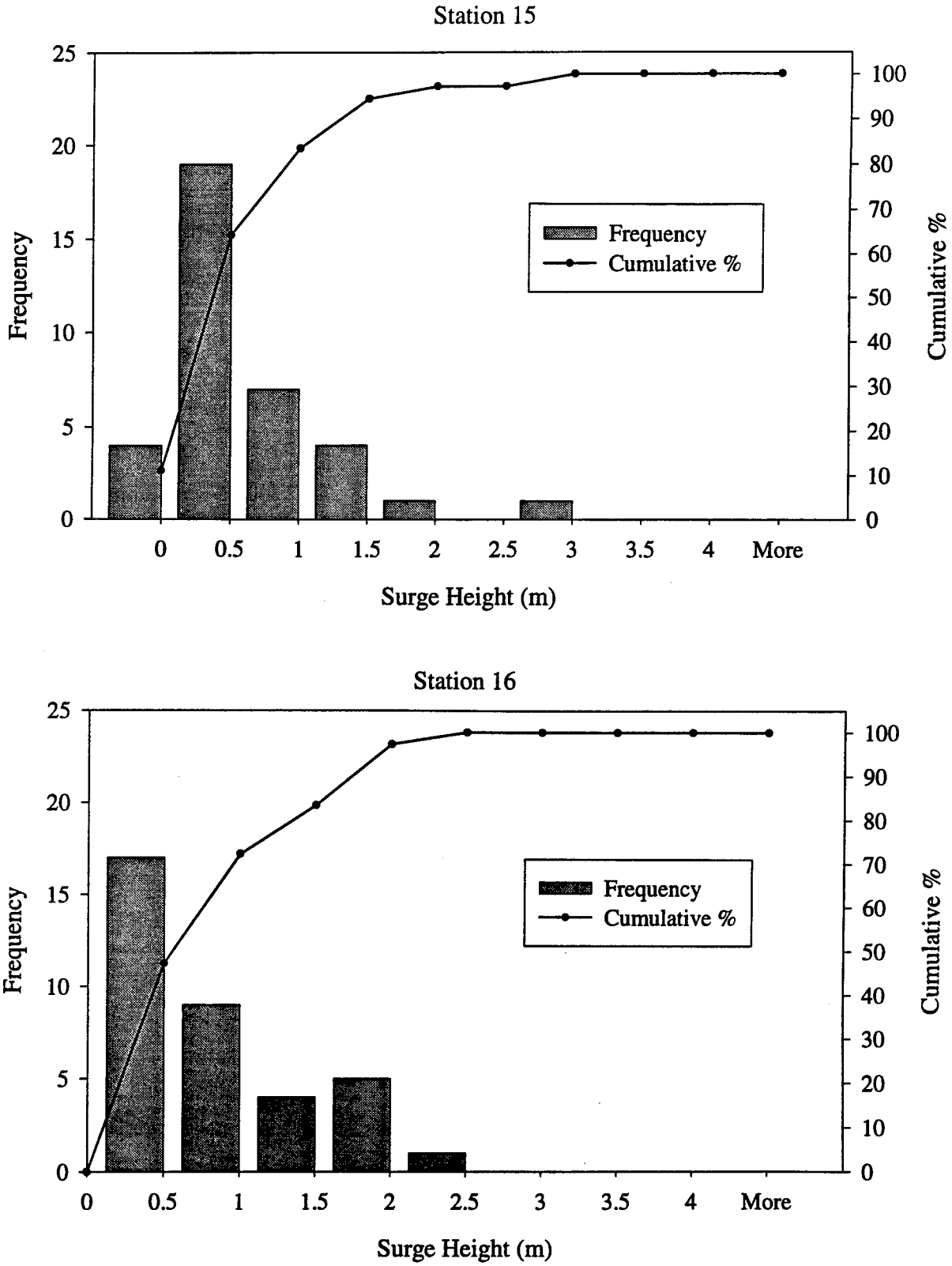

Figure A.8 Histograms of Surge Heights, Stations 15 and 16.

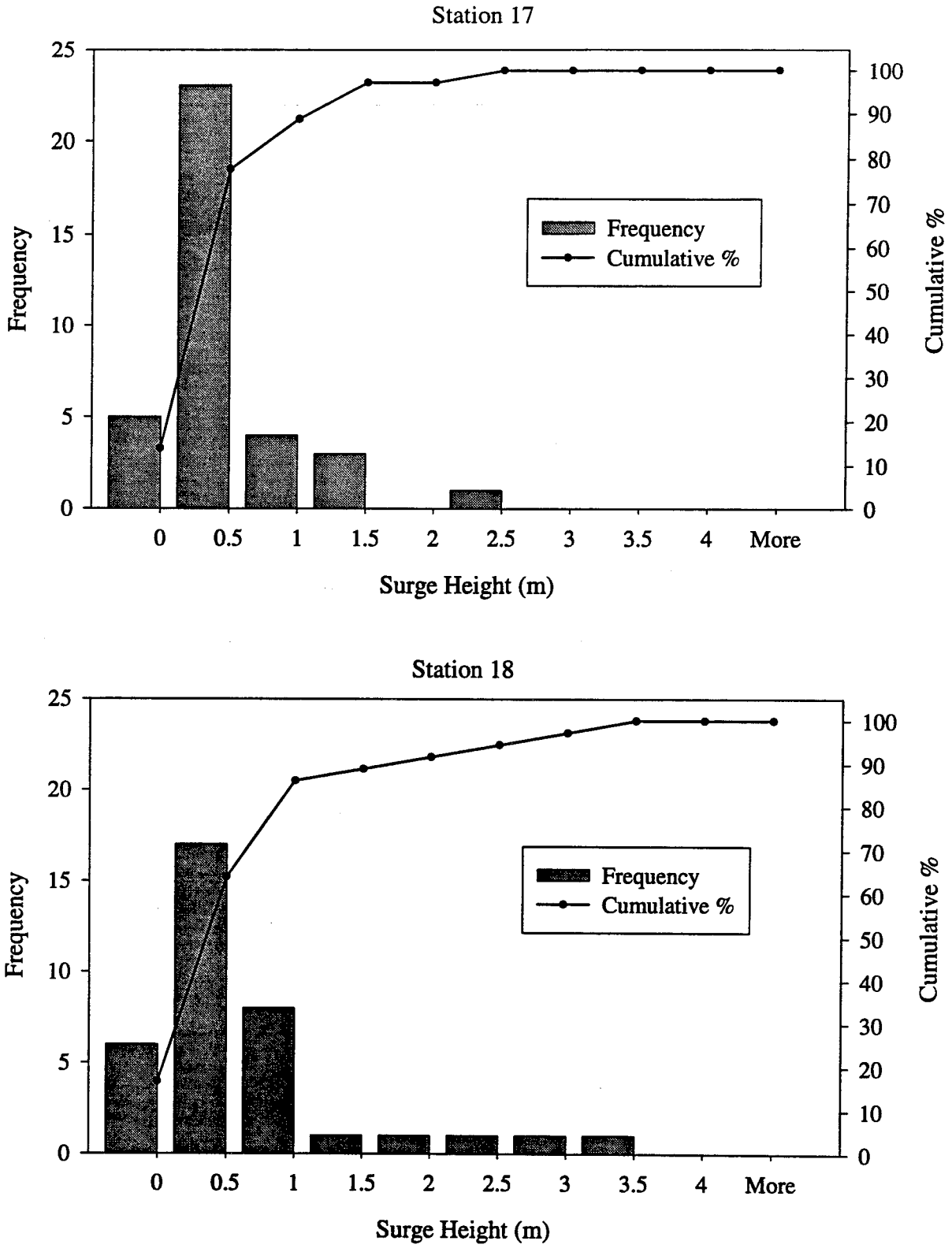

Figure A.9 Histograms of Surge Heights, Stations 17 and 18.

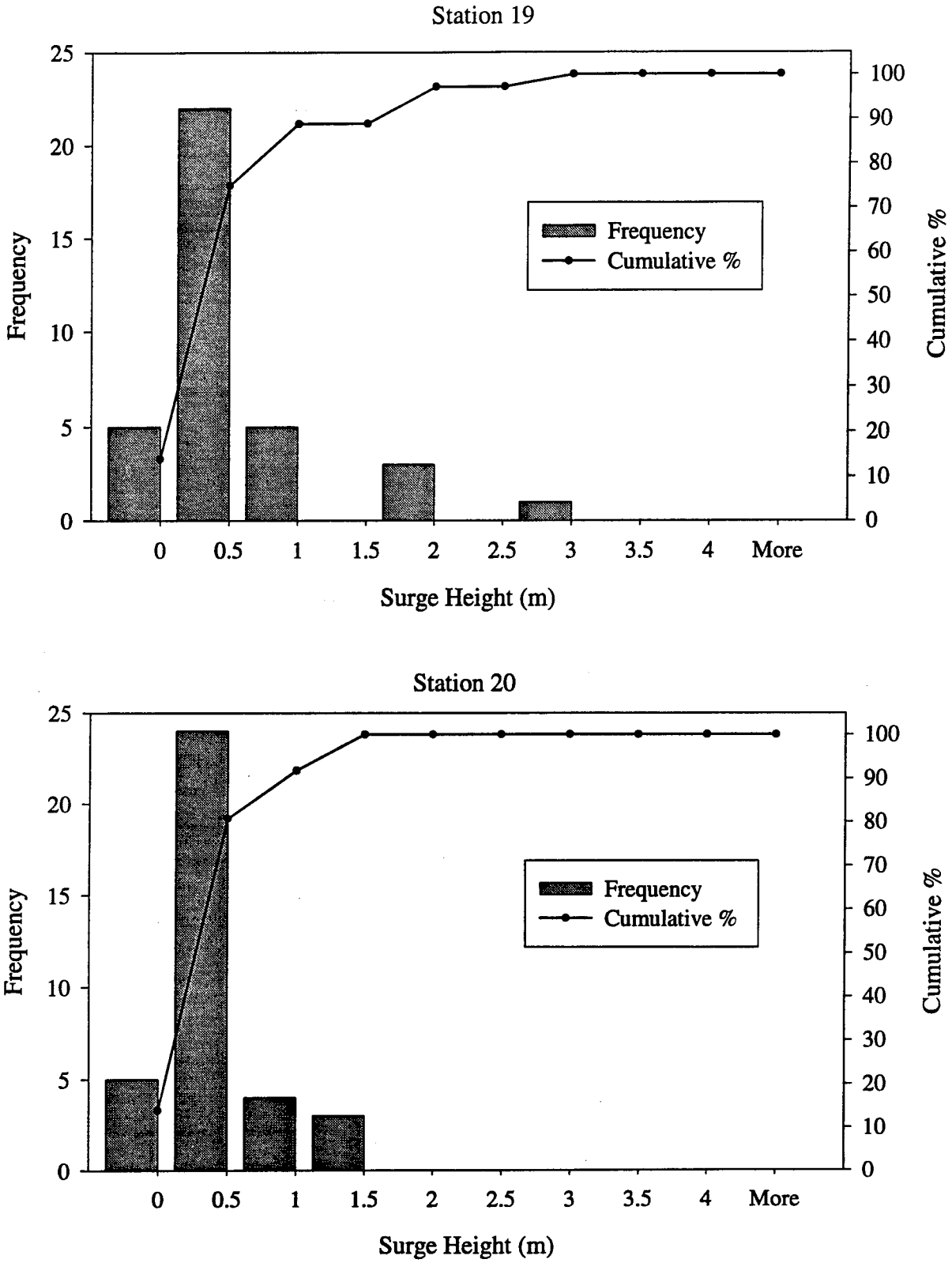

Figure A.10 Histograms of Surge Heights, Stations 19 and 20.

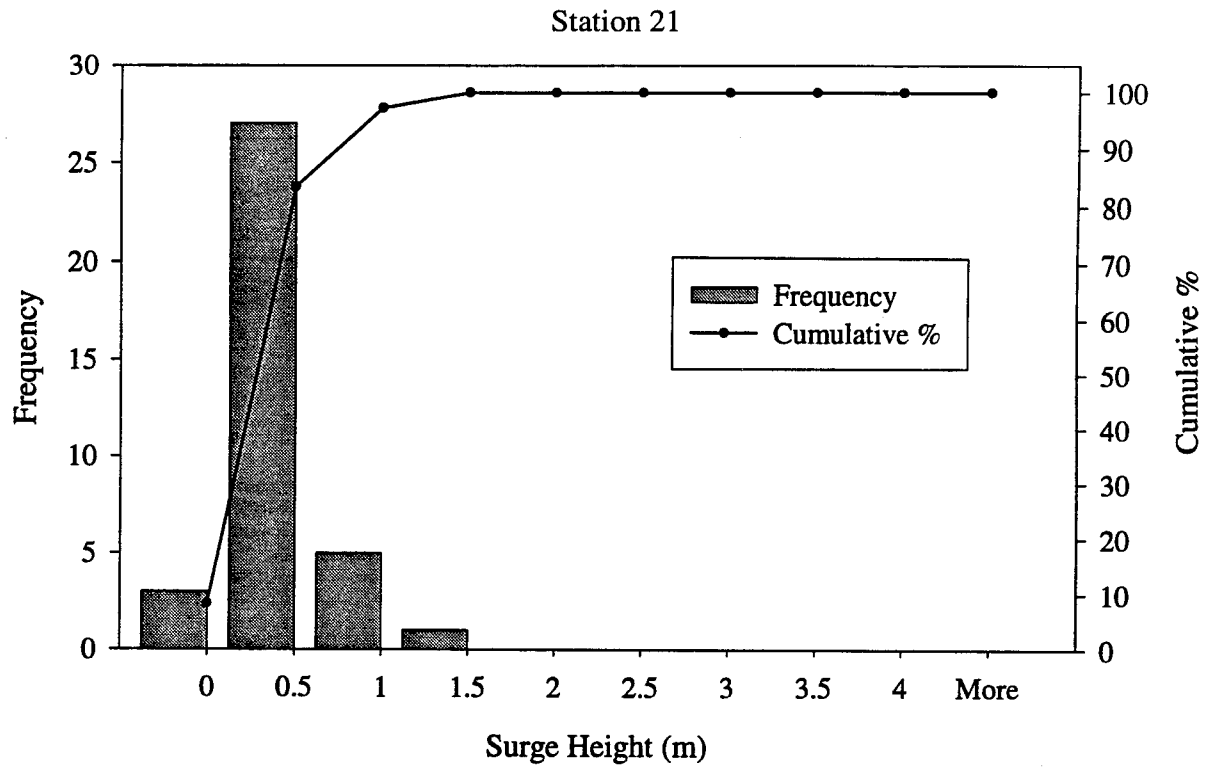

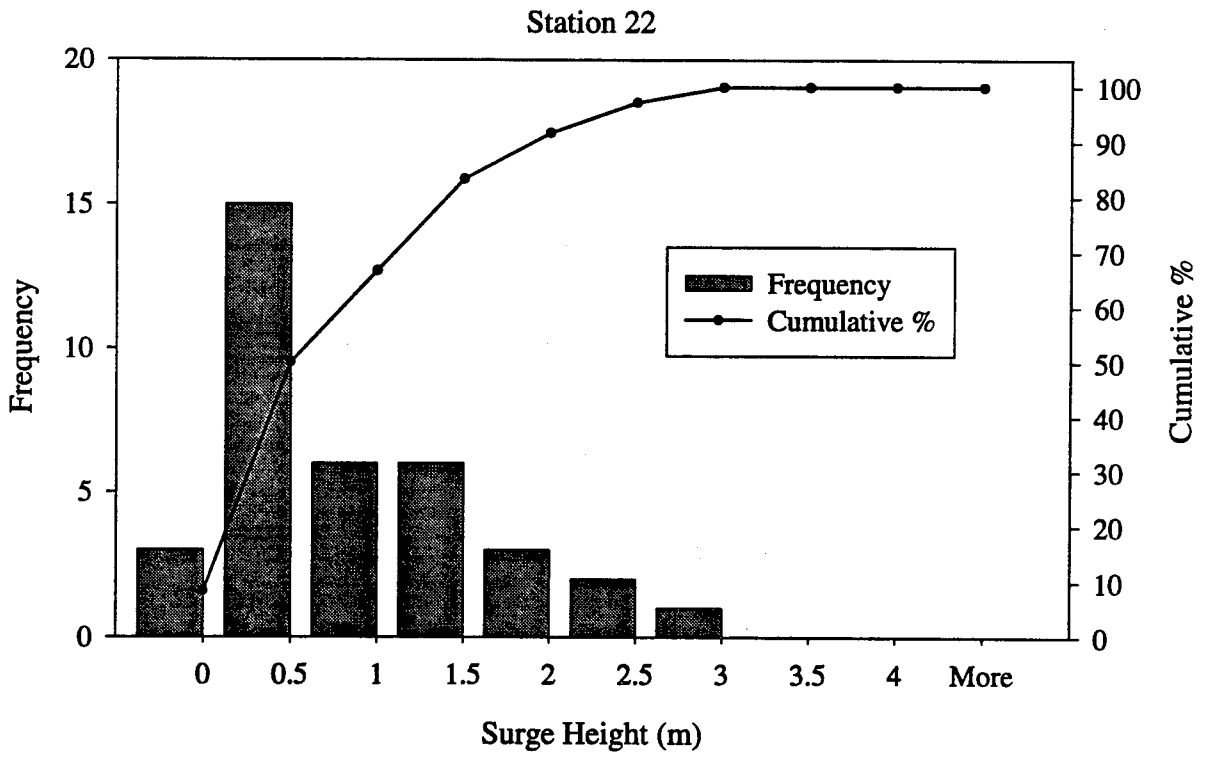

Figure A.11 Histograms of Surge Heights, Stations 21 and 22.

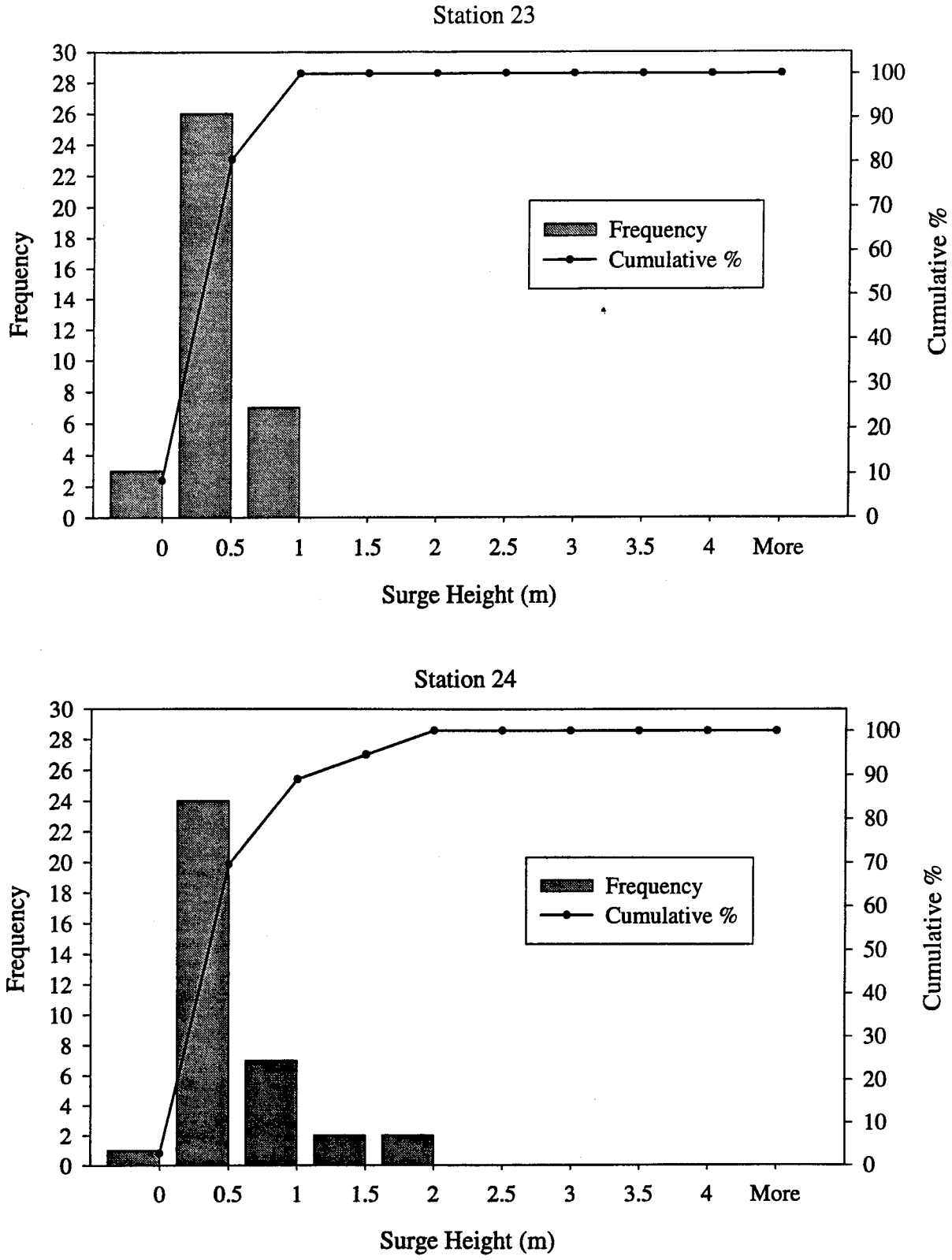

Figure A.12 Histograms of Surge Heights, Stations 23 and 24.

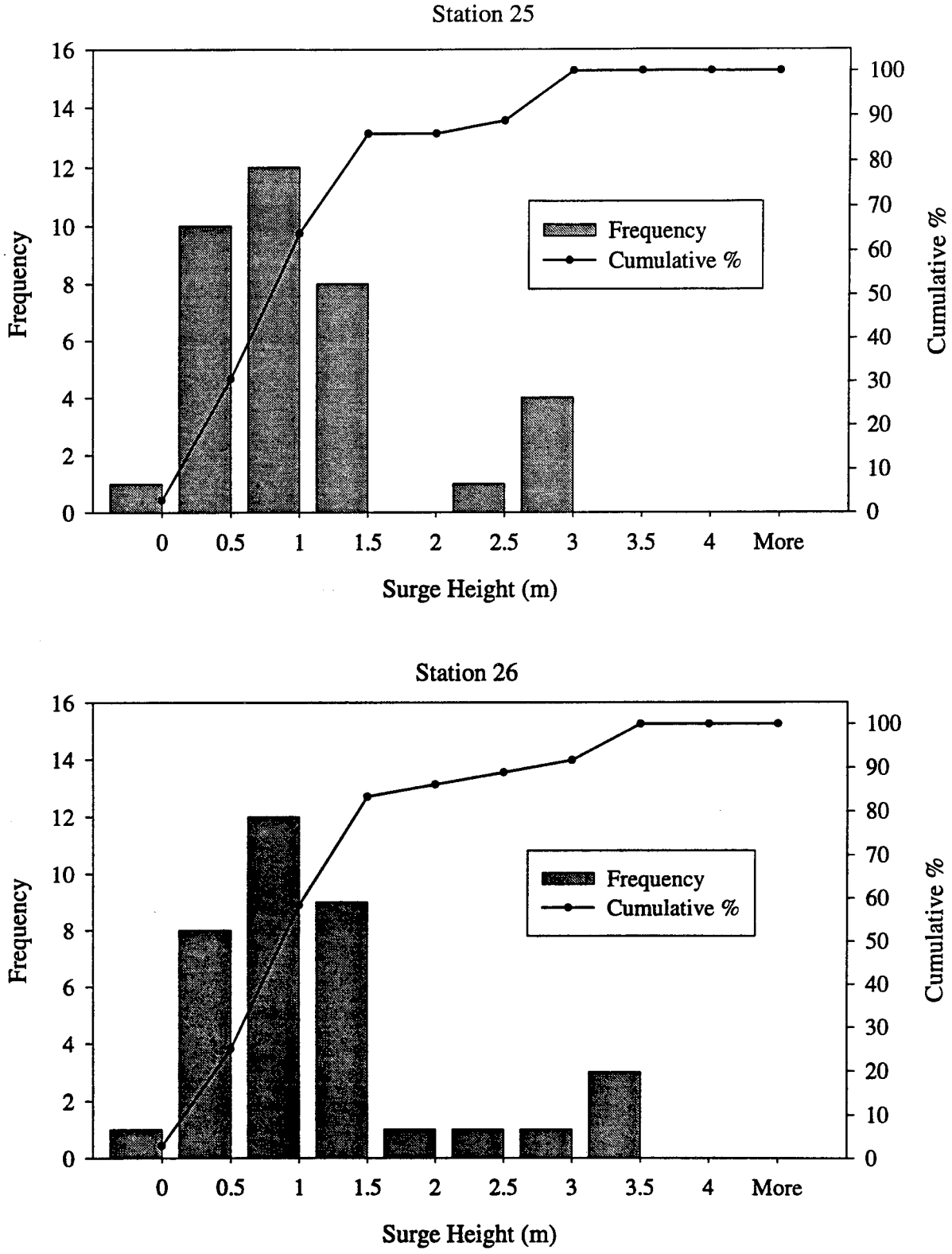

Figure A.13 Histograms of Surge Heights, Stations 25 and 26.

APPENDIX B

EST Results

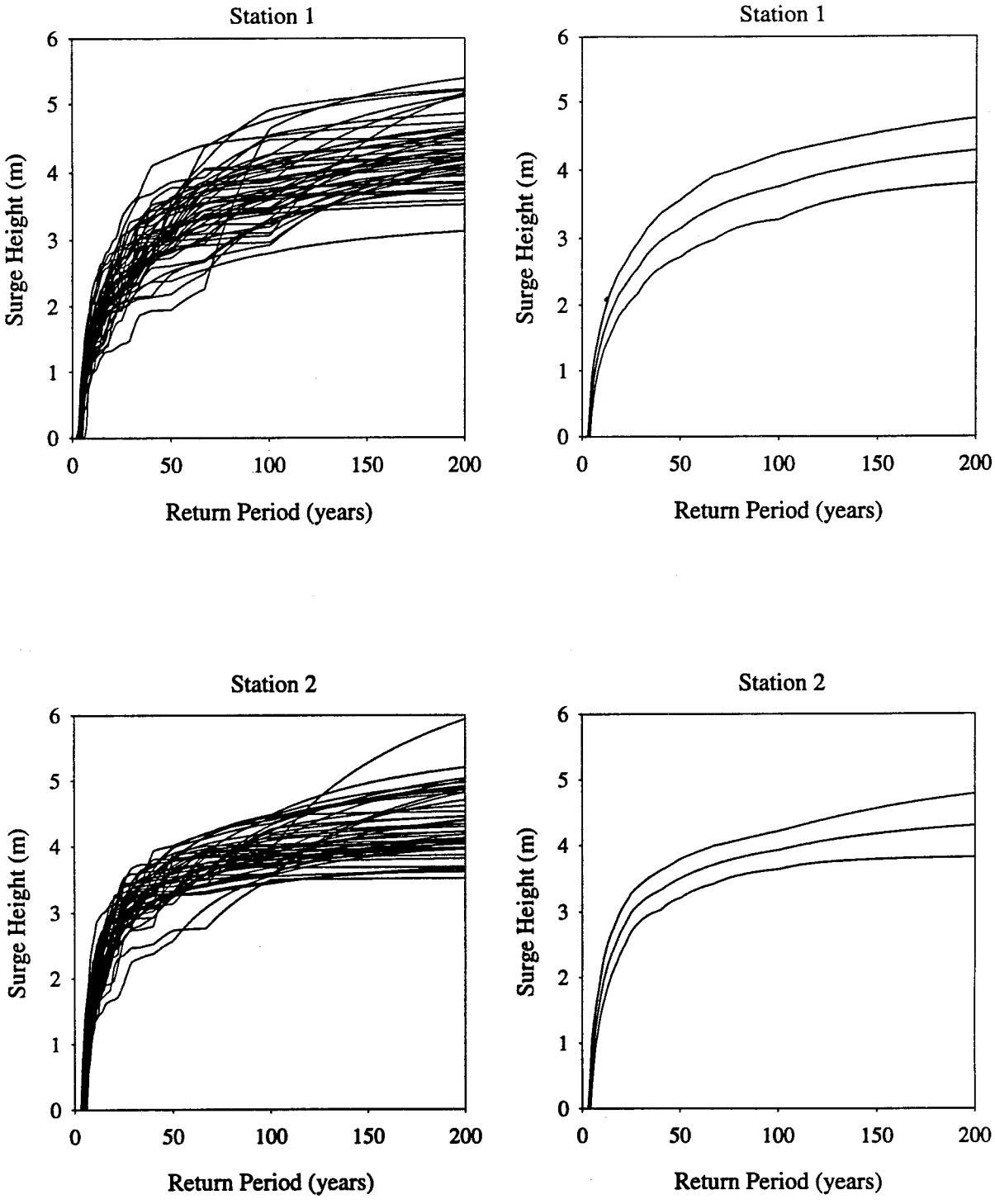

Figure B.1 EST results (left), with mean and plus/minus one standard deviation (right), Stations 1 and 2.

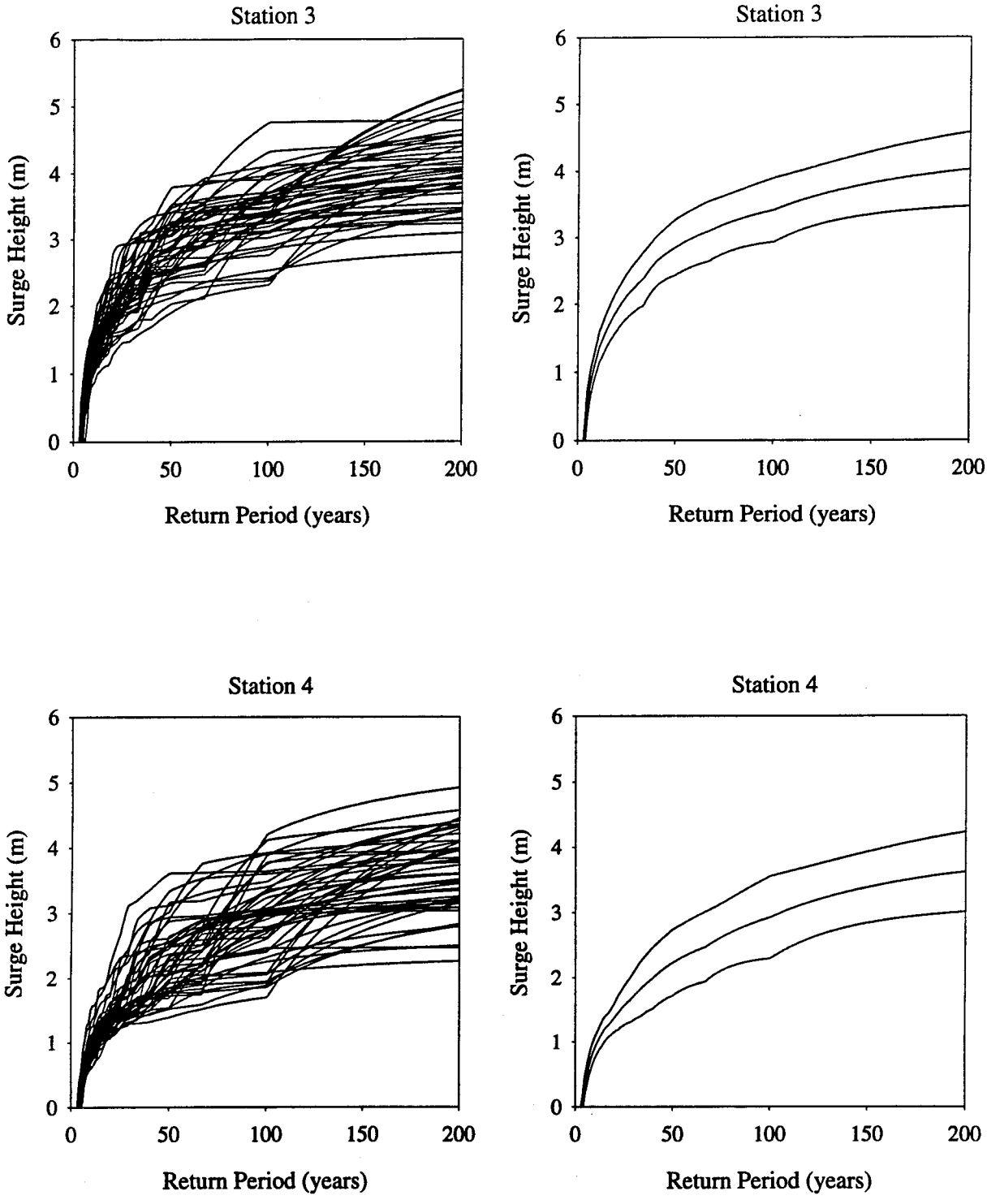

Figure B.2 EST results (left), with mean and plus/minus one standard deviation (right), Stations 3 and 4.

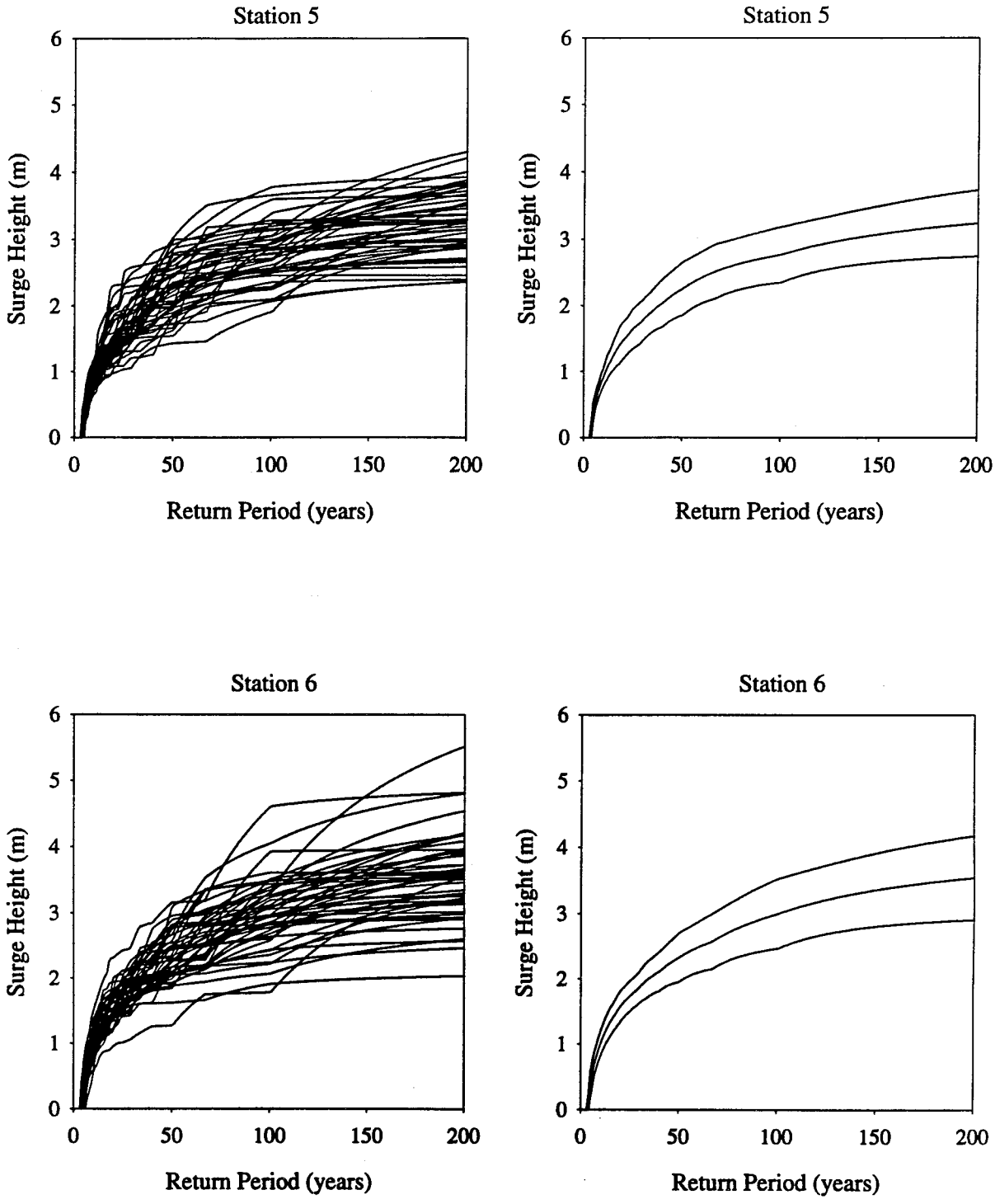

Figure B.3 EST results (left), with mean and plus/minus one standard deviation (right), Stations 5 and 6.

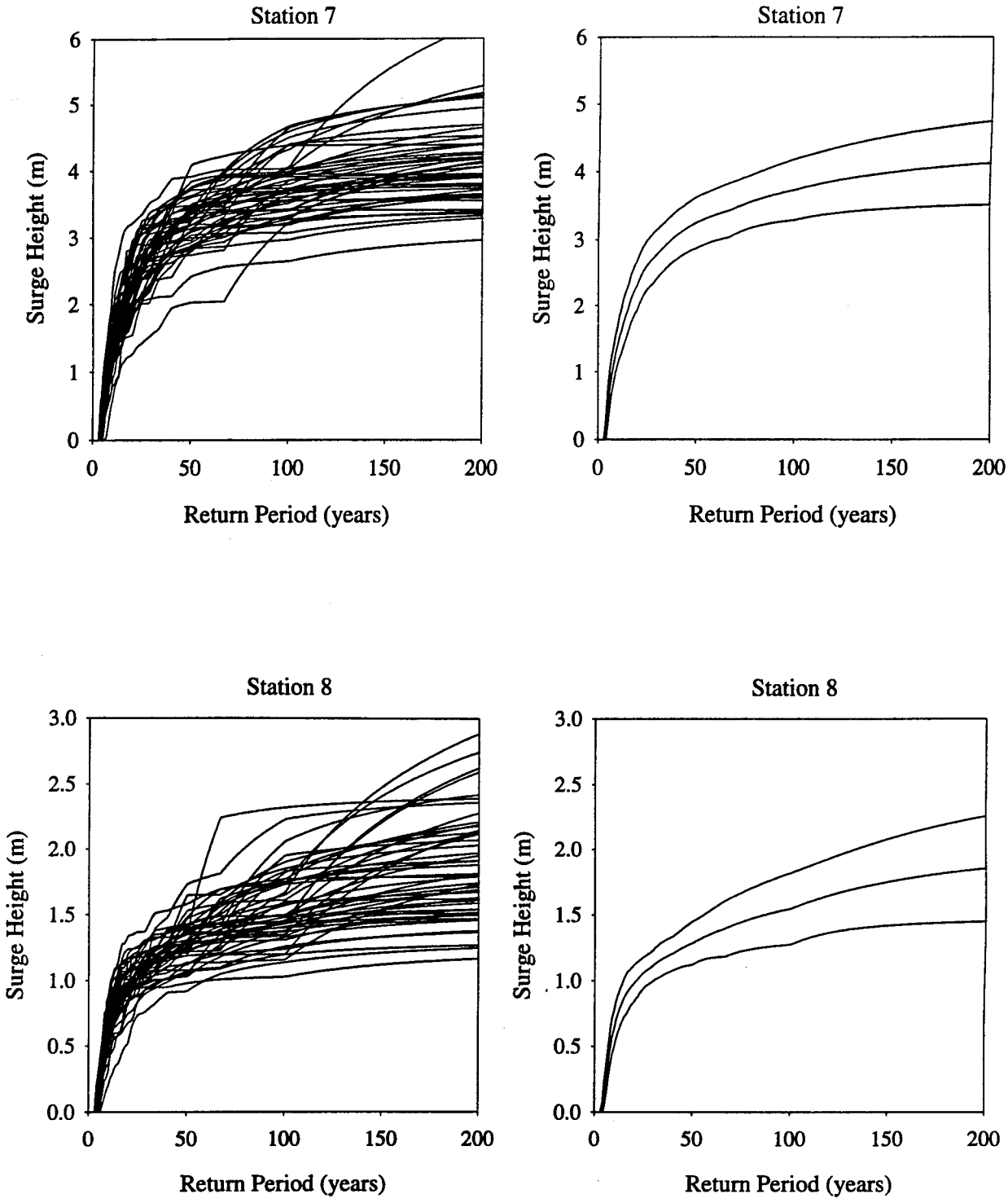

Figure B.4 EST results (left), with mean and plus/minus one standard deviation (right), Stations 7 and 8.

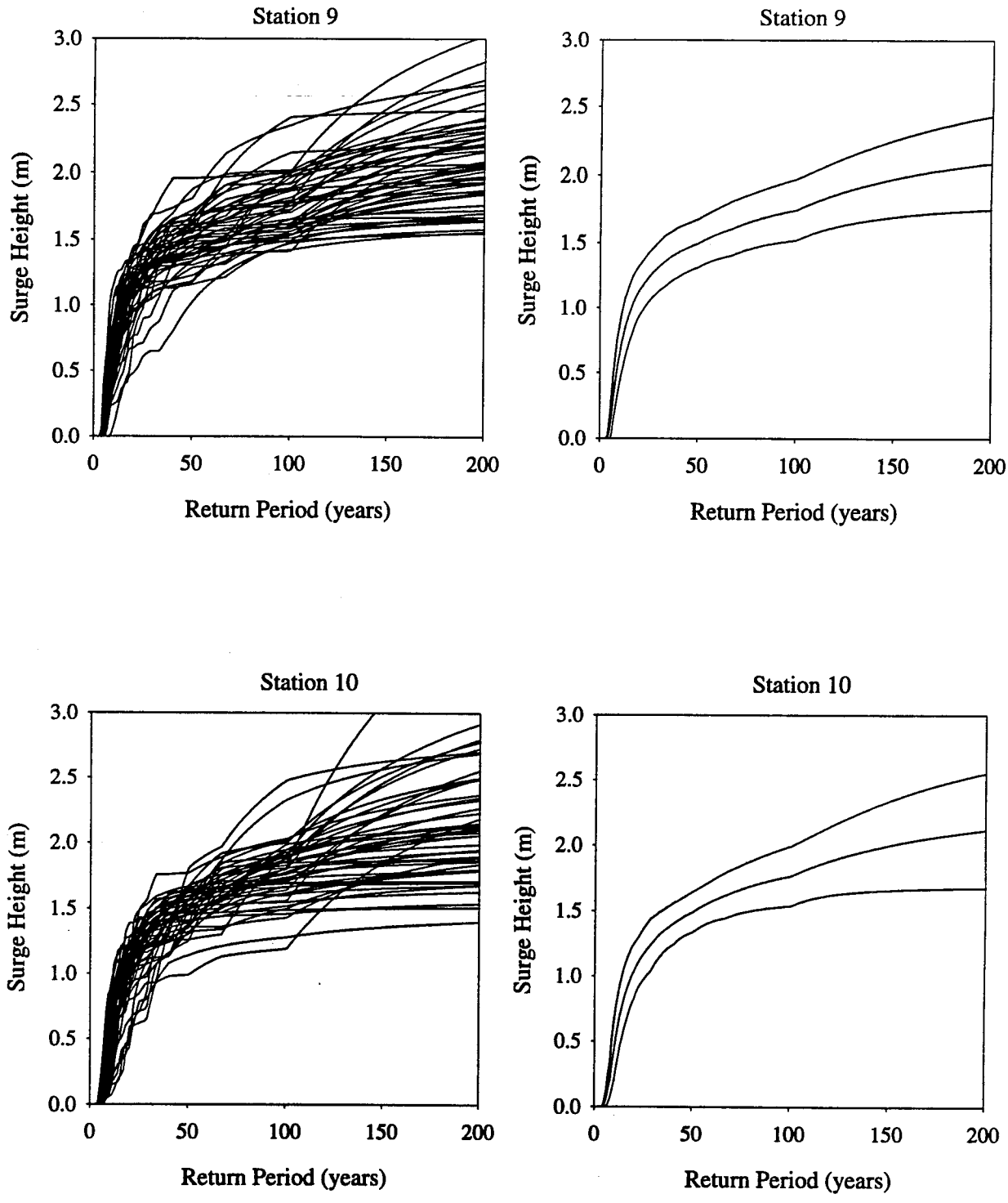

Figure B.5 EST results (left), with mean and plus/minus one standard deviation (right), Stations 9 and 10.

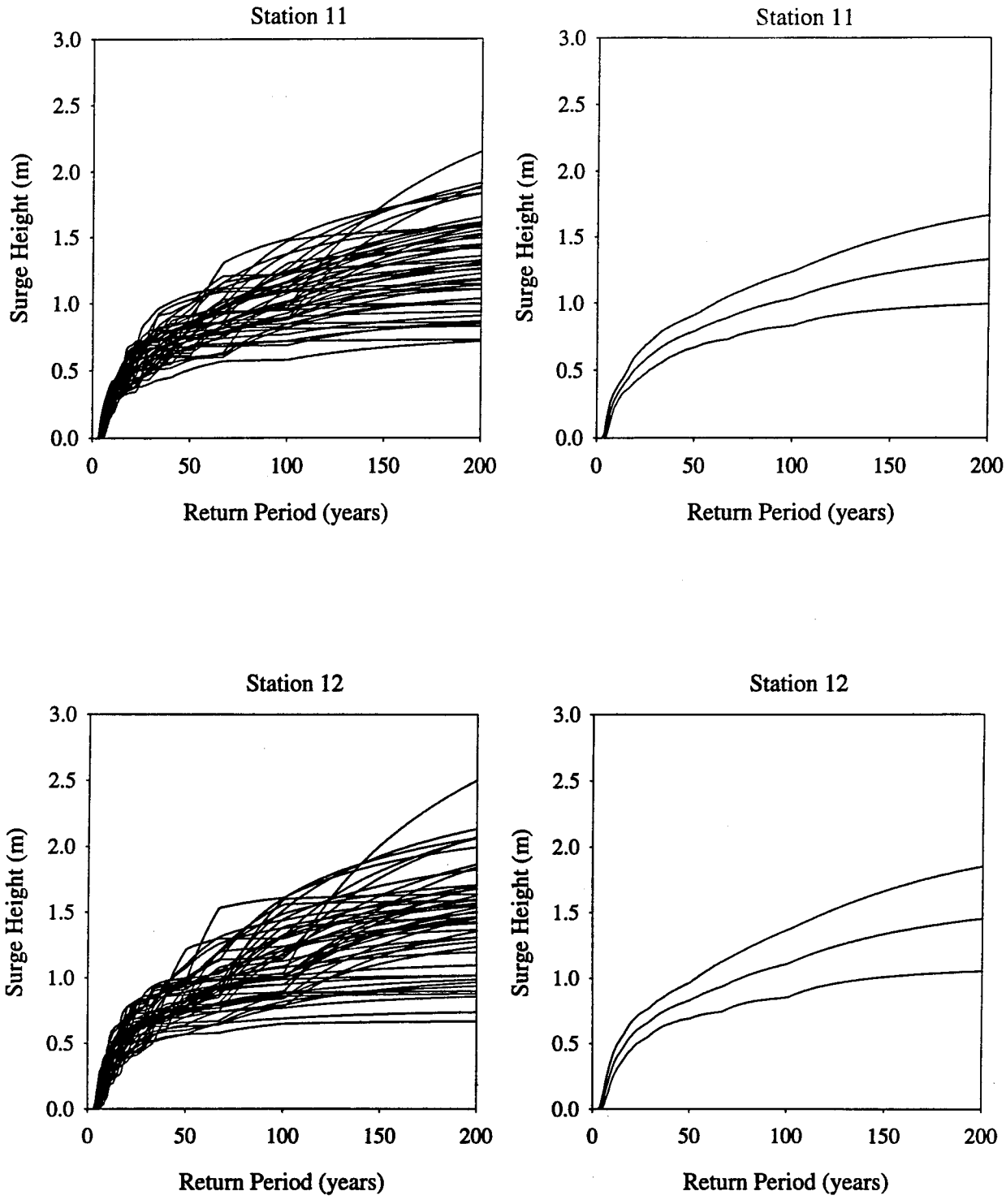

Figure B.6 EST results (left), with mean and plus/minus one standard deviation (right), Stations11 and 12.

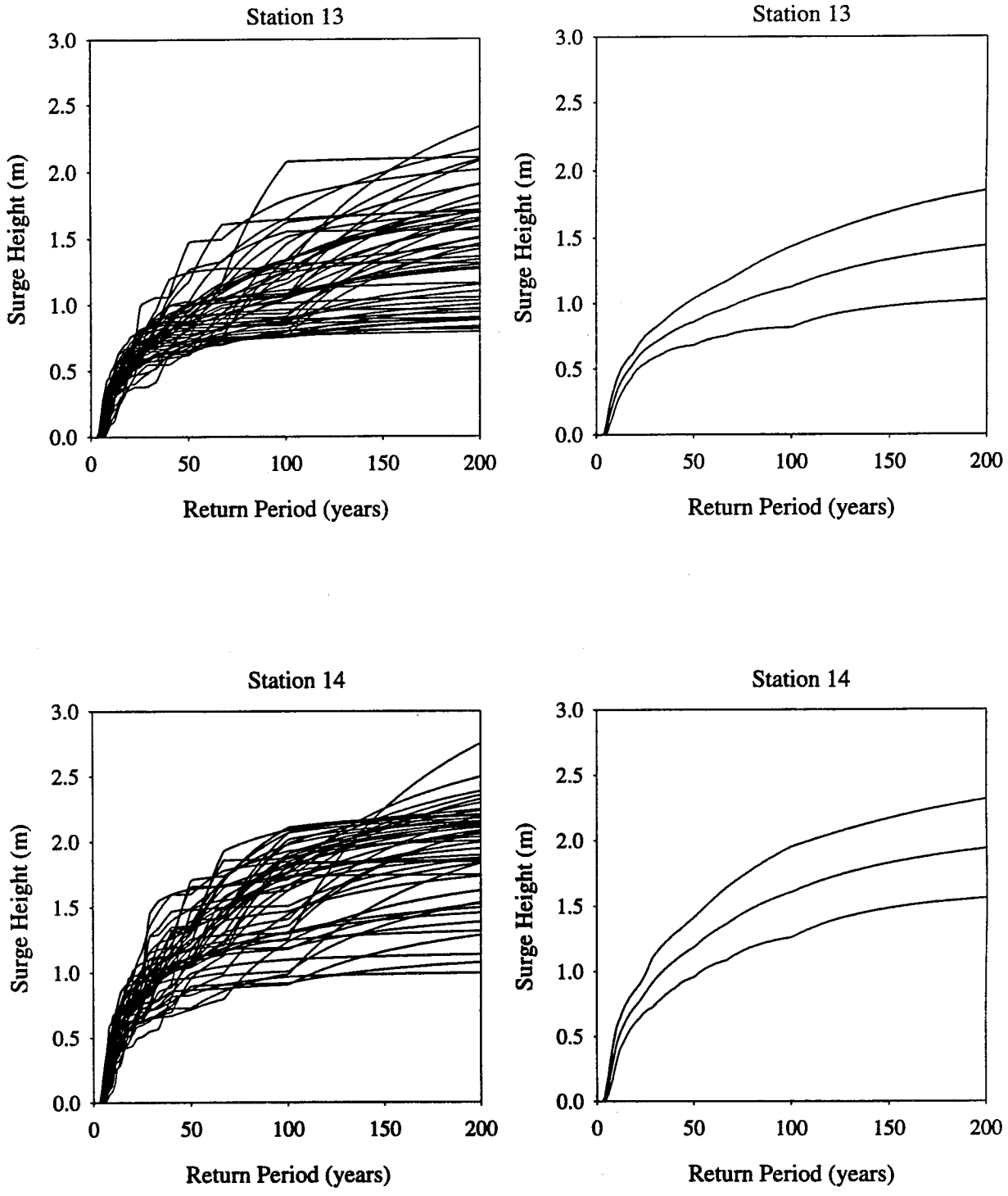

Figure B.7 EST results (left), with mean and plus/minus one standard deviation (right), Stations 13 and 14.

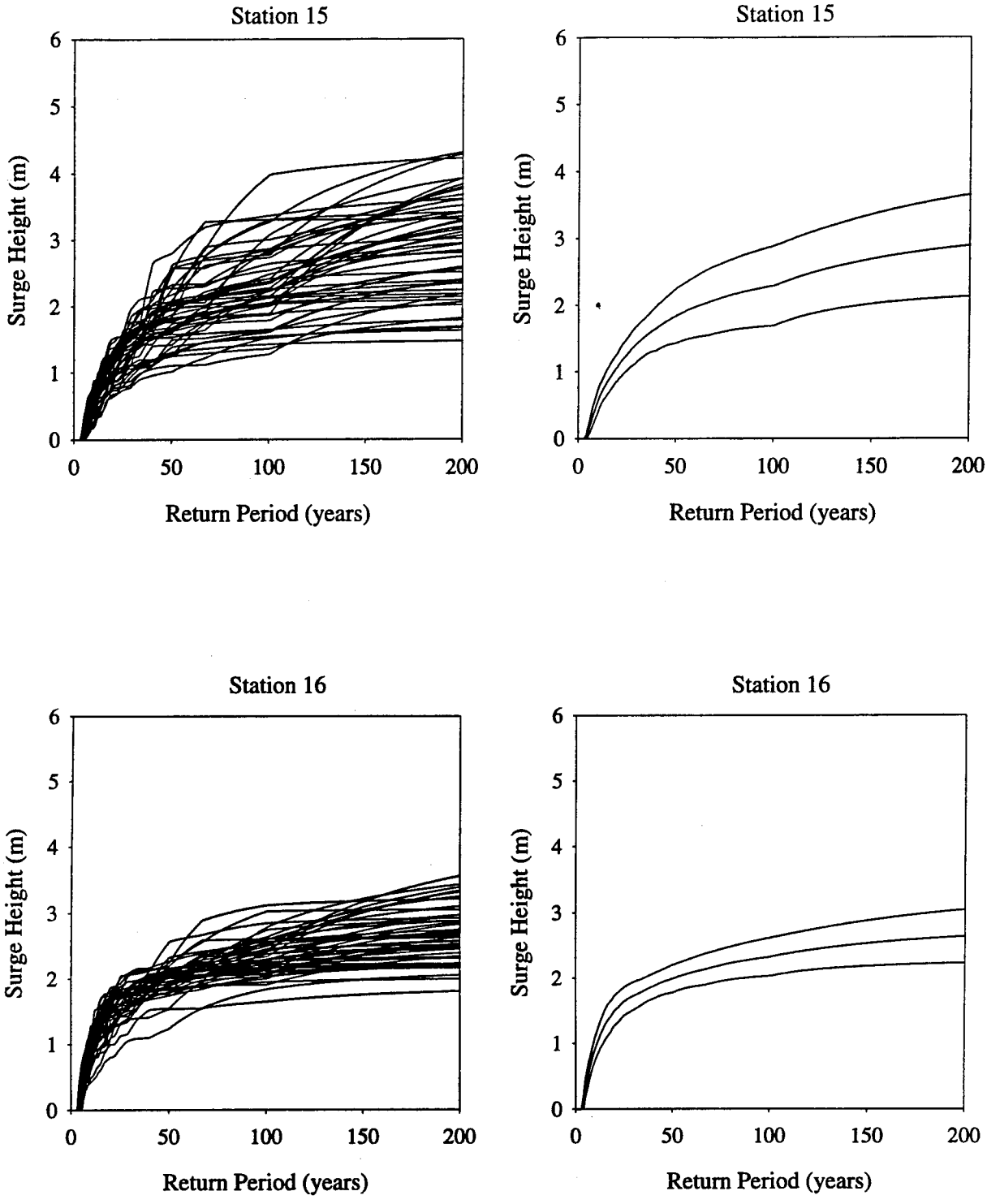

Figure B.8 EST results (left), with mean and plus/minus one standard deviation (right), Stations 15 and 16.

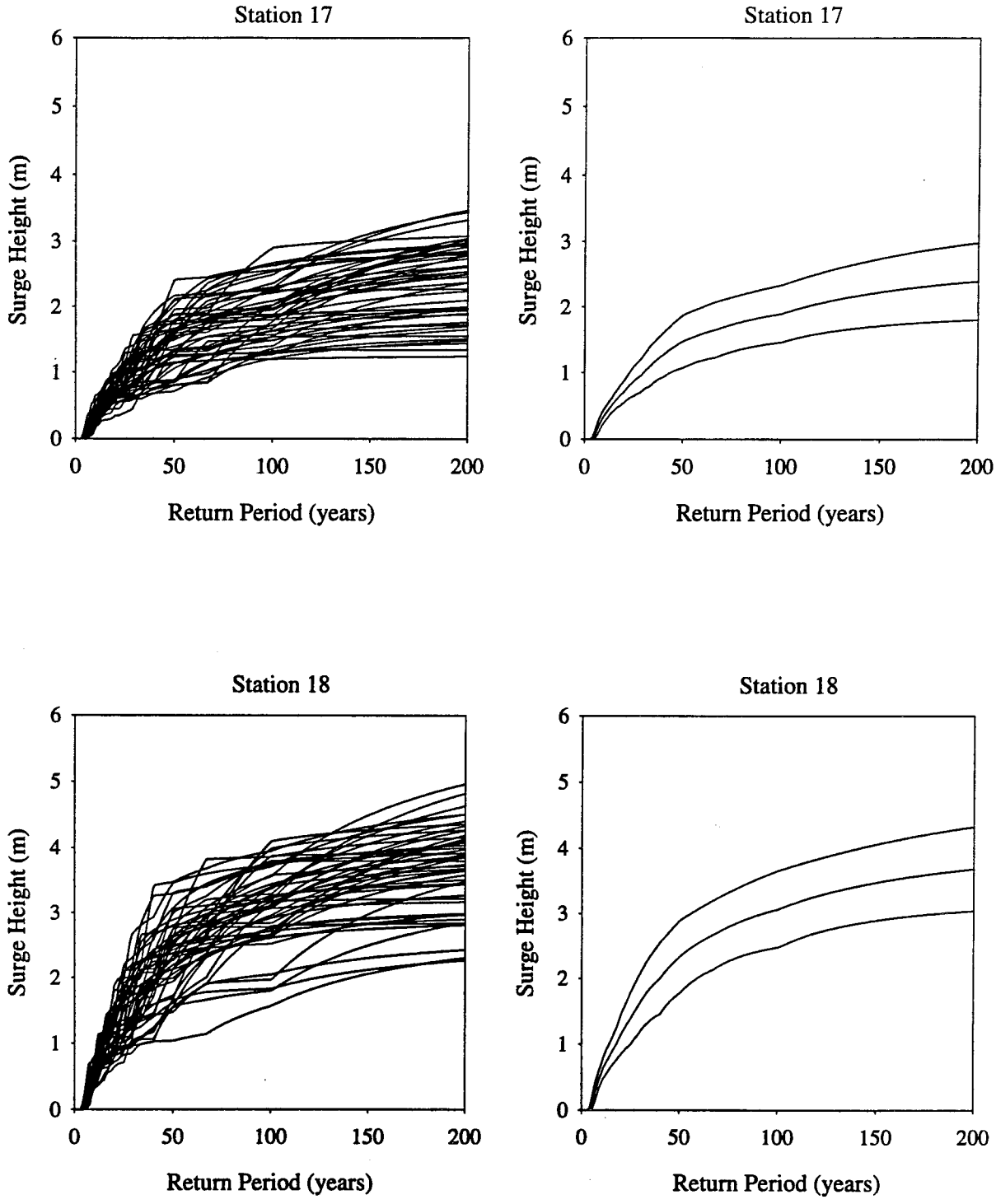

Figure B.9 EST results (left), with mean and plus/minus one standard deviation (right), Stations 17 and 18.

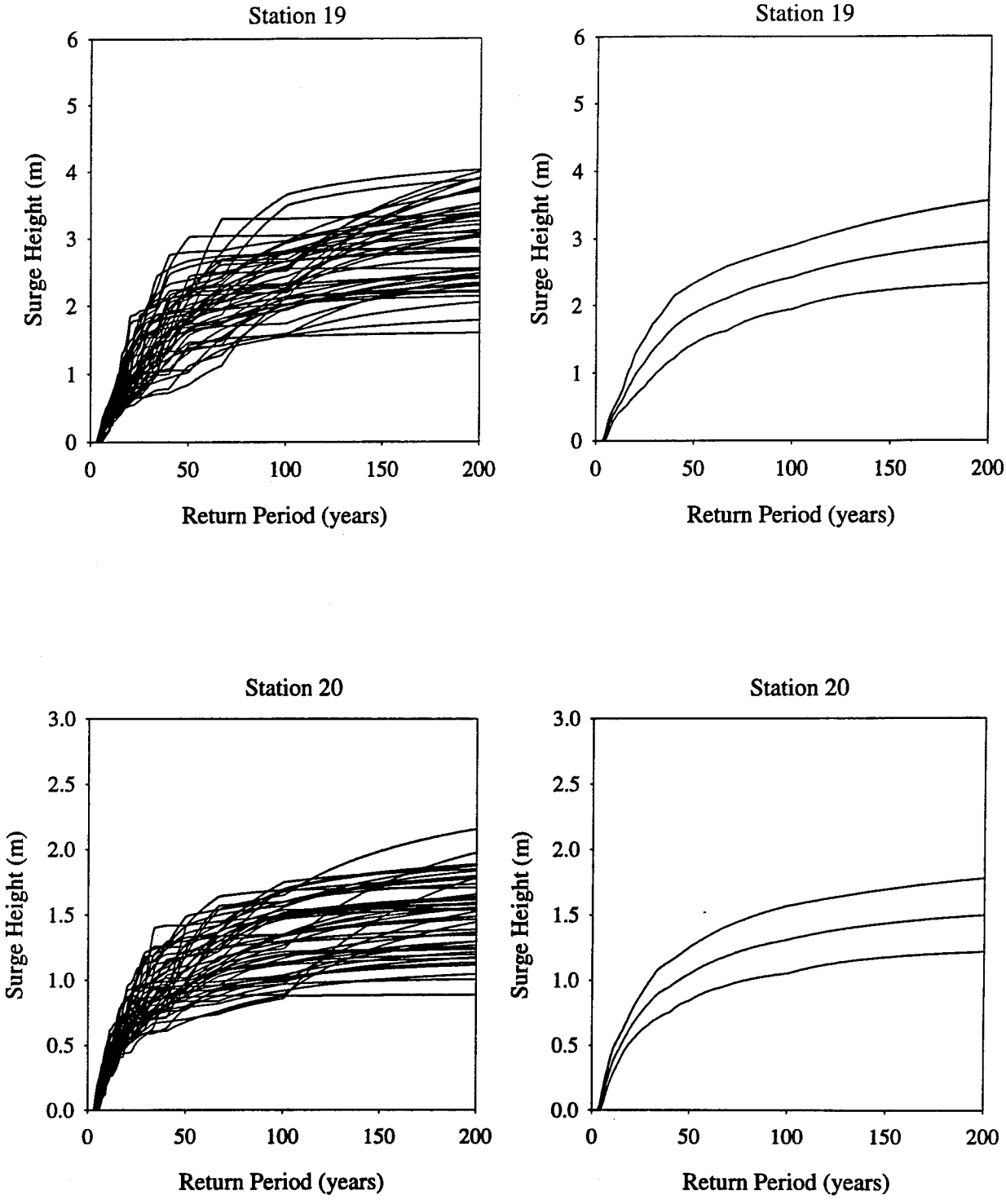

Figure B.10 EST results (left), with mean and plus/minus one standard deviation (right), Stations 19 and 20.

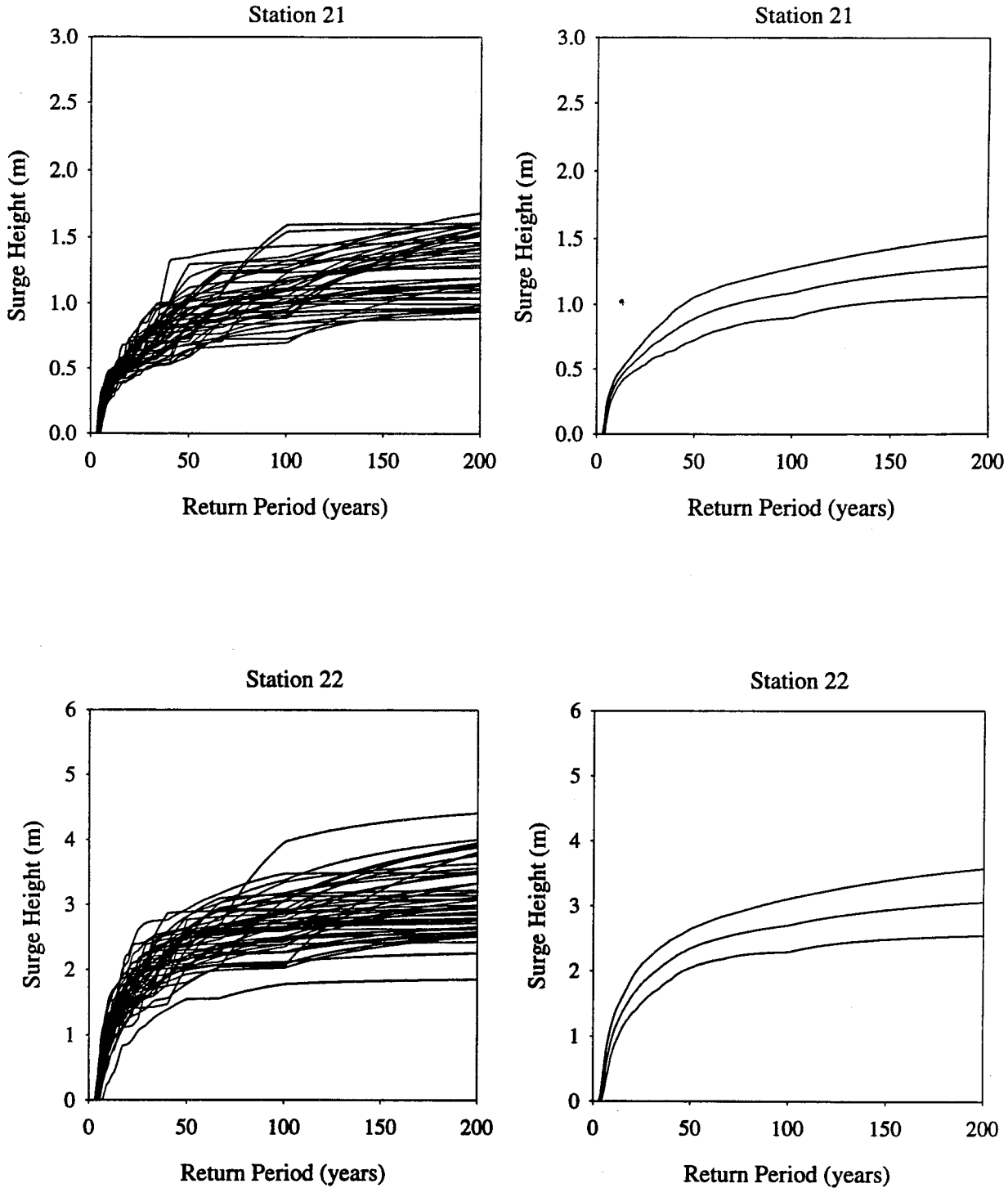

Figure B.11 EST results (left), with mean and plus/minus one standard deviation (right), Stations 21 and 22.

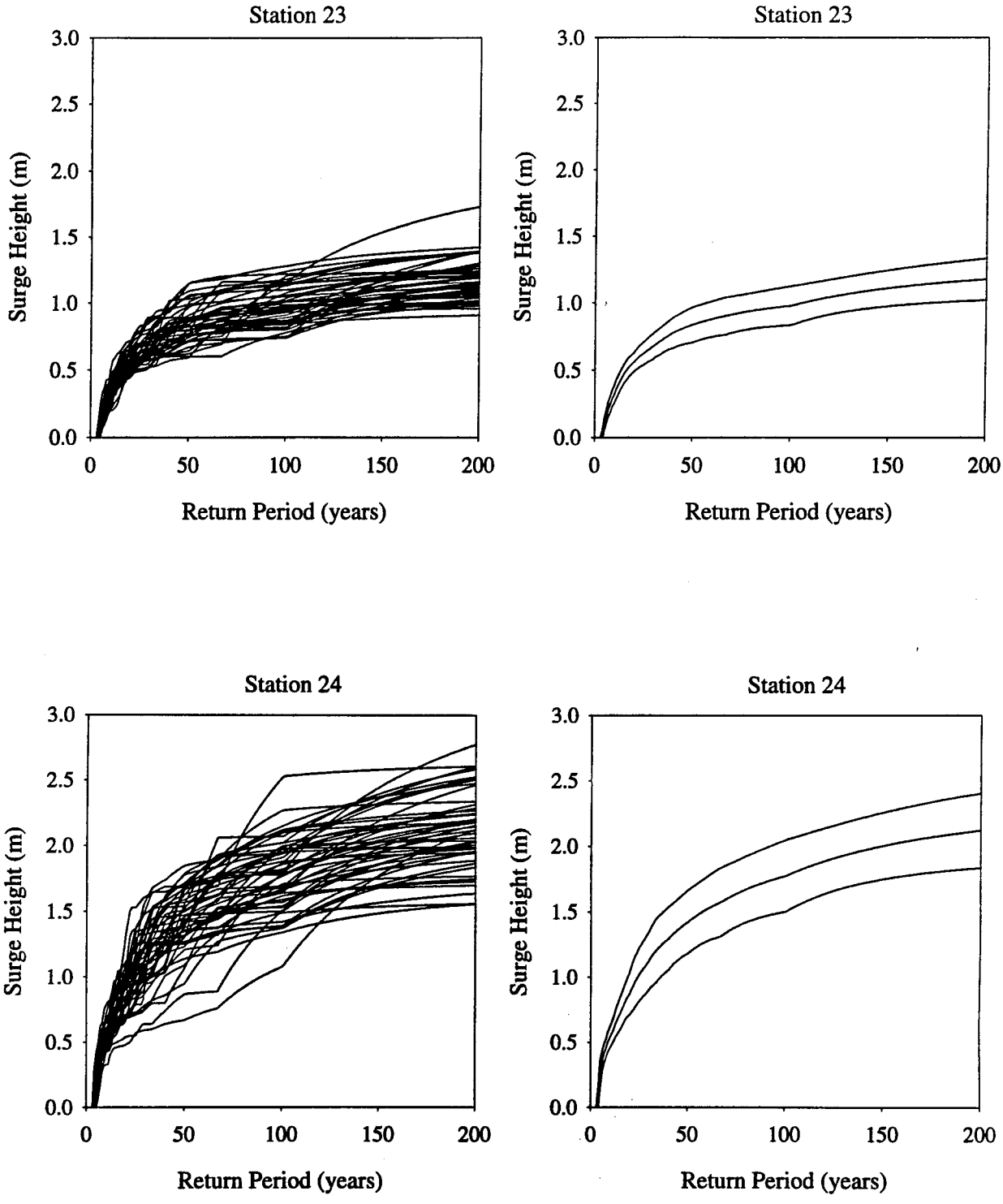

Figure B.12 EST results (left), with mean and plus/minus one standard deviation (right), Stations 23 and 24.

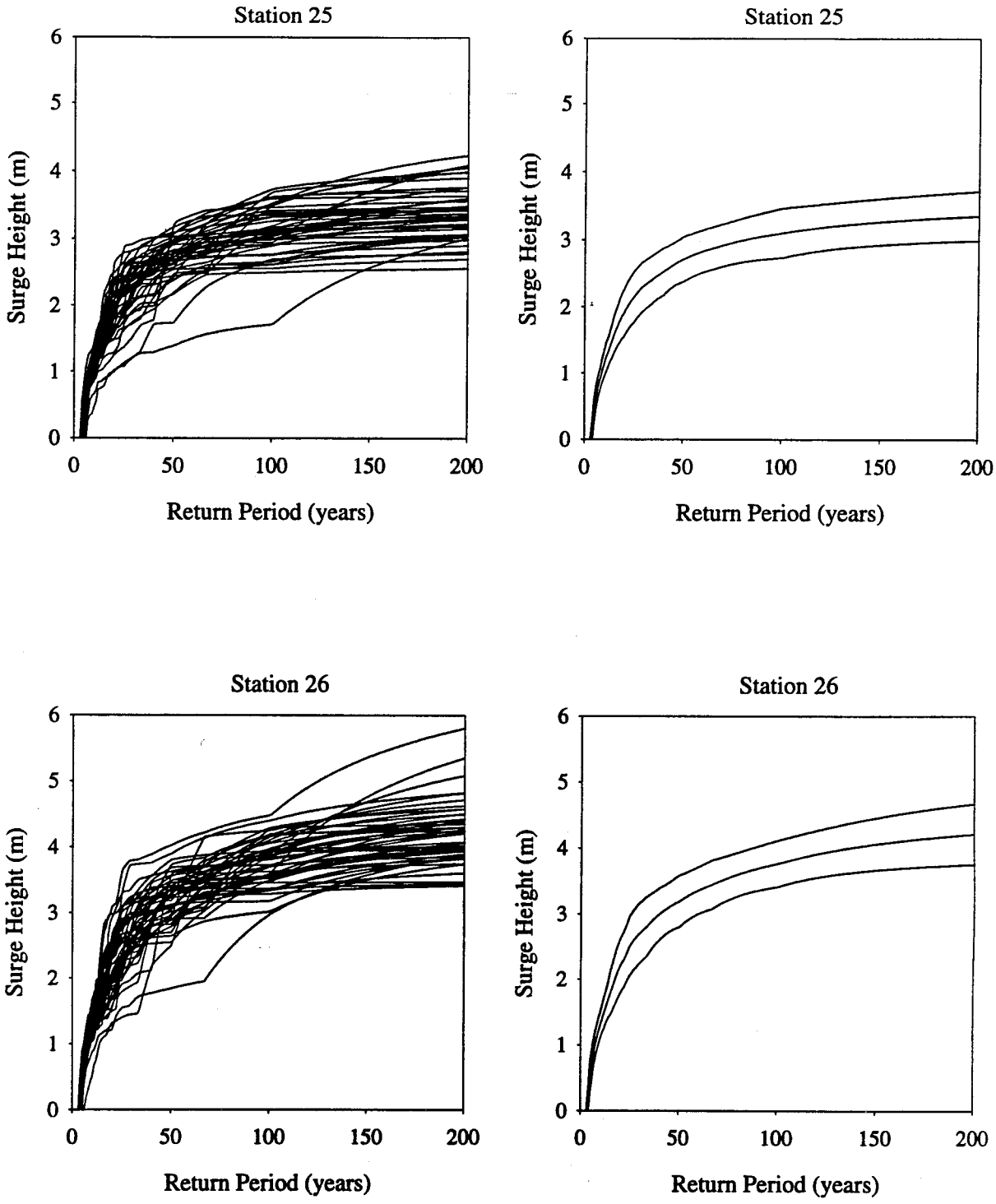

Figure B.13 EST results (left), with mean and plus/minus one standard deviation (right), Stations 25 and 26.